ENRIQUE IGNACIO SANCHEZ GONZALEZ

SPECIES OF *Calonectria* ASSOCIATED WITH *Eucalyptus* PLANTATIONS IN NORTHEASTERN BRAZIL

LAVRAS – MG
2023

ENRIQUE IGNACIO SANCHEZ GONZALEZ

SPECIES OF *Calonectria* ASSOCIATED WITH *Eucalyptus* PLANTATIONS IN NORTHEASTERN BRAZIL

Tese apresentada à Universidade Federal de Lavras, como parte das exigências do Programa de Pós-Graduação em Agronomia/Fitopatologia, área de concentração Fitopatologia, para a obtenção do título de Doutor.

Prof[a]. Dr[a]. Maria Alves Ferreira
Orientadora

LAVRAS – MG
2023

Ficha catalográfica elaborada pelo Sistema de Geração de Ficha Catalográfica da Biblioteca Universitária da UFLA, com dados informados pelo(a) próprio(a) autor(a).

Gonzalez, Enrique Ignacio Sanchez.
Species of *Calonectria* associated with *Eucalyptus* plantations in northeastern Brazil / Enrique Ignacio Sanchez Gonzalez. - 2023.
107 p. : il.

Orientador(a): Maria Alves Ferreira.

Tese (doutorado) - Universidade Federal de Lavras, 2023.
Bibliografia.

1. Cylindrocladium. 2. Multi-locus phylogeny. 3. Leaf blight disease. I. Ferreira, Maria Alves. II. Título.

ENRIQUE IGNACIO SANCHEZ GONZALEZ

SPECIES OF *Calonectria* ASSOCIATED WITH *Eucalyptus* PLANTATIONS IN NORTHEASTERN BRAZIL

ESPÉCIES DE *Calonectria* ASSOCIADAS A PLANTAÇÕES DE *Eucalyptus* NO NORDESTE DO BRASIL

Tese apresentada à Universidade Federal de Lavras, como parte das exigências do Programa de Pós-Graduação em Agronomia/Fitopatologia, área de concentração Fitopatologia, para a obtenção do título de Doutor.

APROVADA em 03 de março de 2023

Dr. Valter Cruz Magalhães	UFLA
Dr. Flavio Augusto de Oliveira Garcia	UNICENTRO
Dr. Leonardo Sarno Soares de Oliveira	BRACELL
Drª. Mara Elisa Soares de Oliveira	UFT

Profª. Drª. Maria Alves Ferreira
Orientadora

LAVRAS – MG
2023

Aos meus queridos pais, Juanita e Enrique,

À minha irmã Elizabeth.

Dedico

AGRADECIMENTOS

A minha família, por estar sempre presentes apesar de estar distantes.

À Universidade Federal de Lavras pela oportunidade concedida para cursar o doutorado.

Ao Departamento de Fitopatologia por toda a atenção e facilidades oferecidas durante o doutorado.

À Drª. Maria Alves Ferreira, pela confiança em me aceitar em seu grupo de pesquisa, orientação, e apoio durante todos esses anos.

Aos meus amigos e colegas do Laboratório de Patologia Florestal da UFLA: Gabrielle, Thaissa, Leticia, Eduarda, Géssica, Iêda, Aline, Teresa, Rodrigo, e Eduardo, pelo ensino, convívio, apoio e amizade.

Aos meus amigos Javier, Jéssica e Daniele, pela amizade, convivência e apoio quando mais precisei.

Aos professores do Programa de Pós-Graduação em Fitopatologia, pelo treinamento, apoio e orientação.

À Suzano Papel e Celulose S. A., pelo financiamento da pesquisa.

À Coordenação de Aperfeiçoamento de Pessoal de Nível Superior (CAPES) pela bolsa de doutorado concedida por meio do Programa de Bolsas PAEC OAS-GCUB no Brasil.

RESUMO

Nas últimas décadas, as plantações comerciais de *Eucalyptus* expandiram-se para regiões quentes e úmidas do norte e nordeste do Brasil, nas quais a mancha foliar por Calonectria (CLB) tornou-se a principal doença fúngica foliar dessa cultura. A CLB pode ser causada por diferentes espécies de *Calonectria*, e estudos prévios indicaram que *Calonectria* pode ter uma alta diversidade de espécies no Brasil. Portanto, este estudo teve como objetivos: 1) caracterizar as espécies de *Calonectria* associadas às plantações de *Eucalyptus* nos estados do Pará e Maranhão, através de análises morfológicas e filogenéticas e confirmar sua patogenicidade ao *Eucalyptus*, (2) determinar a diversidade genotípica dentro de cada espécie de *Calonectria* , (3) entender a estratégia reprodutiva de cada espécie de *Calonectria* e, (4) determinar a diversidade de espécies de *Calonectria* e sua distribuição em diferentes plantações de *Eucalyptus*. Durante levantamentos de doenças de campo realizados entre 2020 e 2021 em plantações comerciais de *Eucalyptus* no nordeste do Brasil, foram coletadas folhas doentes de *Eucalyptus* e amostras de solo, dos quais foram obtidos 206 isolados de *Calonectria*. Um total de oito espécies de *Calonectria* foram encontradas em associação com plantações de *Eucalyptus*, das quais duas são novas para a ciência, *C. paragominensis* sp. nov. e *C. imperata* sp. nov. Além disso, foi o primeiro relato de *C. quinqueramosa* e *C. amazonica* causando mancha foliar em árvores de *Eucalyptus urophylla* no nordeste do Brasil. A coleção completa de espécies foi *C. imperata* com 48,7% de todos os isolados, seguida por *C. amazonica* (24,9%), *C. ovata* (9,1%), *C. brasiliensis* (6,1%), *C. variabilis* (4,1%), *C. quinqueramosa* (3,6%), *C. paragominensis* (2%) e *C. maranhensis* (1,5%). A patogenicidade de *C. paragominensis*, *C. imperata* e *C. quinqueramosa* ao *Eucalyptus* foi confirmada pelo cumprimento dos postulados de Koch. Com relação à diversidade genética, *C. imperata* apresentou a maior diversidade genética, com 17 genótipos em 96 isolados, seguido por *C. brasiliensis* com 10 genótipos em 12 isolados. Em relação ao sistema de acasalamento, a amplificação dos genes MAT1-1-1 e MAT1-2-1 mostrou que *C. maranhensis* é possivelmente heterotálica, e que o ciclo assexual é o principal modo reprodutivo de *C. amazonica*. As espécies mais prevalentes foram *C. amazonica* e *C. imperata*, encontradas em sete e seis plantios, respectivamente. Com esse estudo foi possível compreender melhor as espécies, diversidade genética, distribuição, estratégia de acasalamento e características morfológicas de *Calonectria* em dez plantações comerciais de *Eucalyptus* no nordeste do Brasil aumentou como resultado deste estudo. Esse conhecimento pode ser usado para criar uma estratégia de manejo eficaz para CLB em plantações de *Eucalyptus* e na obtenção de clones de *Eucalyptus* resistentes.

Palavras-chave: *Cylindrocladium*. Multi-locus phylogeny. Leaf blight disease. Tree pathogen

ABSTRACT

In recent decades, commercial *Eucalyptus* plantations have expanded toward the warm and humid regions of northern and northeastern Brazil, where Calonectria leaf blight (CLB) has become the primary fungal leaf disease of this crop. CLB can be caused by different *Calonectria* species, and previous studies have indicated that *Calonectria* might have high species diversity in Brazil. Therefore, this study aimed: 1) to characterize the species of *Calonectria* associated with *Eucalyptus* plantations in the Pará and Maranhão states, trough morphological and phylogenetic analyses and to confirm their pathogenicity to *Eucalyptus*, (2) to determine the genotypic diversity within each *Calonectria* species, (3) to understand the mating strategy of each *Calonectria* species and, (4) to determine the species diversity of *Calonectria* and its distribution in different *Eucalyptus* plantations. During disease surveys conducted between 2020 and 2021 in commercial plantations of *Eucalyptus* in northeastern Brazil, diseased leaves from *Eucalyptus* trees and soil samples were collected, and 206 *Calonectria* isolates were obtained. A total of eight species of *Calonectria* were find in association with *Eucalyptus* plantations, of which two were new to science, *C. paragominensis* sp. nov. and *C. imperata* sp. nov. Also, was the first report of *C. quinqueramosa* and *C. amazonica* causing leaf blight on *E. urophylla* trees in northeastern Brazil. The complete species collection was *C. imperata* with 48.7% of all the isolates, followed by *C. amazonica* (24.9%), *C. ovata* (9.1%), *C. brasiliensis* (6.1%), *C. variabilis* (4.1%), *C. quinqueramosa* (3.6%), *C. paragominensis* (2%), and *C. maranhensis* (1.5%). The pathogenicity of *C. paragominensis*, *C. imperata* and *C. quinqueramosa* to *Eucalyptus* was confirmed by fulfilling the Koch's postulates. Concerning to genetic diversity, *C. imperata* presented the highest genetic diversity, with 17 genotypes in 96 isolates, followed by *C. brasiliensis* with 10 genotypes in 12 isolates. Regarding the mating system, MAT1-1-1 and MAT1-2-1 genes amplification showed that *C. maranhensis* is putative heterothallic, and that the asexual cycle is the main reproductive mode of *C. amazonica*. The most prevalent species were *C. amazonica* and *C. imperata*, found in seven and six plantations, respectively. Our understanding of the species, genetic diversity, distribution, mating strategy, and morphological characteristics of *Calonectria* in ten commercial *Eucalyptus* plantations in northeastern Brazil has increased as a result of this study. This knowledge could be used to create an effective management strategy for CLB in *Eucalyptus* plantations and the breeding of resistant *Eucalyptus* clones.

Keywords: *Cylindrocladium*. Multi-locus phylogeny. Leaf blight disease. Tree pathogen

TABLE OF CONTENTS

FIRST PART:

1 INTRODUCTION

Eucalyptus spp. is considered an important forest crop around the world and the most grown forest tree in Brazil (IBÁ, 2021). Brazil became one of the world's main producers of pulp, paper, and wood panels in 2021, with a total area of 7.53 million hectares planted with *Eucalyptus* trees, and a productivity of 38.9 $m^3 \cdot ha$ per year (IBÁ, 2022). Planted areas have expanded and considering climate change, fungal diseases such Calonectria Leaf Blight (CLB) have threatened the *Eucalyptus* spp. plantations, being *Calonectria pteridis* regarded as the most important causal agent of CLB in *Eucalyptus* spp. throughout Brazil (ALFENAS *et al*., 2015). CLB can be caused by different *Calonectria* species, is widely distributed throughout the country, and affects *Eucalyptus* spp. plants most severely from six months to 2–3 years after planting (GRAÇA *et al*., 2009). This disease is currently controlled by integrated cultivation and chemical methods, also by the selection and multiplication of resistant genotypes, which is a much more effective approach (SOARES *et al*., 2018).

The demand for strategies to control this disease requires a proper identification of the pathogen species. Therefore, this study aimed: 1) to characterize the species of *Calonectria* associated with *Eucalyptus* plantations in the Pará and Maranhão states, trough morphological and phylogenetic analyses and to confirm their pathogenicity to *Eucalyptus*, (2) to determine the genotypic diversity within each *Calonectria* species, (3) to understand the mating strategy of each *Calonectria* species and, (4) to determine the species diversity of *Calonectria* and its distribution in different *Eucalyptus* plantations.

This thesis is organized in three original articles, the first article contemplates the description of two new *Calonectria* species causing leaf blight, both isolated from diseased *Eucalyptus* leaves from commercial plantations localized in a tropical zone. The second article consists of the first report of *Calonectria quinqueramosa* causing leaf blight on *Eucalyptus urophylla* in Brazil, supported by molecular and morphological characterization. The third article entitled "*Calonectria* species associated with *Eucalyptus* plantations in northeastern Brazil: phylogeny, morphology, and mating strategy" describes the species diversity of *Calonectria* in different *Eucalyptus* plantations, the genotypic diversity within each *Calonectria* species, and the mating strategy of each *Calonectria* species.

REFERENCES

ALFENAS, R. F., LOMBARD, L., PEREIRA, O. L., ALFENAS, A. C., CROUS, P. W. Diversity and potential impact of *Calonectria* species in *Eucalyptus* plantations in Brazil. Studies in Mycology, v.80, p.89–130, 2015.

GRAÇA, R. N., ALFENAS, A. C., MAFFIA, L. A., TITON, M., ALFENAS, R. F., LAU, D., ROCABADO, J. M. A. Factors influencing infection of eucalypts by *Cylindrocladium pteridis*. Plant Pathology, v.58, n.5, p.971–981, 2009.

IBÁ (2021) IBÁ–Indústria Brasileira de Árvores. Relatório 2020. Available at: https://iba.org/datafiles/publicacoes/relatorios/relatorio-iba-2020.pdf Accessed 30 may 2022

IBÁ (2022) IBÁ–Indústria Brasileira de Árvores. Relatório 2021. https://iba.org/datafiles/publicacoes/relatorios/relatorio-anual-iba2022-compactado.pdf Accessed jan 2023

SOARES, T. P., POZZA, E. A., POZZA, A. A., MAFIA. R. G., FERREIRA, M. A. Calcium and potassium imbalance favours leaf blight and defoliation caused by *Calonectria pteridis* in *Eucalyptus* plants. Forests, v.9, n.12, p.782, 2018.

SECOND PART–ARTICLES:

ARTICLE 1 – TWO NEW SPECIES OF *Calonectria* (HYPOCREALES, NECTRIACEAE) CAUSING EUCALYPTUS LEAF BLIGHT IN BRAZIL

Enrique I. Sanchez-Gonzalez[1], Thaissa de Paula Farias Soares[2], Talyta Galafassi Zarpelon[2], Edival Angelo Valverde Zauza[2], Reginaldo Gonçalves Mafia[2], Maria Alves Ferreira[1]

[1] Universidade Federal de Lavras, Departamento de Fitopatologia, Lavras, MG, 37200-900, Brasil

[2] Suzano Papel e Celulose S. A. Centro de Tecnologia, Aracruz, ES, 29197-900, Brasil

*Corresponding author: M. A. Ferreira; mariaferreira@ufla.br

Article published in *MycoKeys* 2022, presented according to journal guidelines.

Two new species of *Calonectria* (Hypocreales, Nectriaceae) causing *Eucalyptus* leaf blight in Brazil

Enrique I. Sanchez-Gonzalez[1], Thaissa de Paula Farias Soares[2], Talyta Galafassi Zarpelon[2], Edival Angelo Valverde Zauza[2], Reginaldo Gonçalves Mafia[2], Maria Alves Ferreira[1]

1 Universidade Federal de Lavras, Departamento de Fitopatologia, Lavras, MG, 37200-900, Brasil **2** Suzano Papel e Celulose S. A. Centro de Tecnologia, Aracruz, ES, 29197-900, Brasil

Corresponding author: Maria A. Ferreira (mariaferreira@ufla.br)

Abstract

In recent decades, commercial *Eucalyptus* plantations have expanded toward the warm and humid regions of northern and northeastern Brazil, where *Calonectria* leaf blight (CLB) has become the primary fungal leaf disease of this crop. CLB can be caused by different *Calonectria* species, and previous studies have indicated that *Calonectria* might have high species diversity in Brazil. During a disease survey conducted in three commercial plantations of *Eucalyptus* in northeastern Brazil, diseased leaves from *Eucalyptus* trees with typical symptoms of CLB were collected, and *Calonectria* fungi were isolated. Based on phylogenetic analyses of six gene regions (*ac*t, *cmdA*, *his3*, *rpb2*, *tef1*, and *tub2*) and morphological characteristics, two new species of *Calonectria* were identified. Five isolates were named as *C. paragominensis* sp. nov. and four were named as *C. imperata* sp. nov. The pathogenicity to *Eucalyptus* of both species was confirmed by fulfilling the Koch's postulates.

.

Keywords

Cylindrocladium, GCPSR, phylogenetic network analysis, phylogeny

Introduction

Calonectria species are widely distributed around the world and cause diseases in more than 335 plant species, distributed among nearly 100 plant families, including forestry, agricultural and horticultural crops (Crous 2002; Lombard et al. 2010c; Vitale et al. 2013; Lombard et al. 2016; Li et al. 2021). Most reports of *Calonectria* from Brazil are focused on forestry crops, such as *Acacia*, *Eucalyptus*, and *Pinus* trees (Alfenas et al. 2015), and mainly evaluate the epidemiology and disease control of *Calonectria*-associated diseases such as *Calonectria* leaf blight (CLB), damping-off, cutting rot and root rot in commercial plantations and nurseries of *Eucalyptus* (Soares et al. 2018).

Currently, 130 *Calonectria* species have been identified based on DNA phylogenetic analyses and morphological comparisons (Crous et al. 2018, 2019, 2021a, 2021b; Wang et al. 2019; Liu et al. 2020; Mohali and Stewart 2021; Pham et al. 2022). These species are accommodated in eleven species complexes, which are divided into two main phylogenetic groups based on their morphological features: the Prolate Group (*C. brassicae*, *C. candelabrum*, *C. colhounii*, *C. cylindrospora*, *C. gracilipes*, *C. mexicana*, *C. pteridis*, *C.*

reteaudii and *C. spathiphylli* species complexes), and the Sphaero-Naviculate Group (*C. kyotensis* and *C. naviculata* species complexes) (Lombard et al. 2016; Liu et al. 2020).

In Brazil, a total of 35 species have been described: eleven species isolated from diseased tissues of *Eucalyptus*, ten species isolated from soil samples of *Eucalyptus* plantations, seven species isolated from different plant species, six species isolated from soil samples of tropical rainforests, and one mycoparasite species (Crous et al. 2018, 2019; Liu et al. 2020); they belong in the species complexes of *C. candelabrum*, *C. brassicae*, *C. cylindrospora*, *C. pteridis*, *C. gracilipes*, and *C. naviculata* (Crous 2018, 2019; Liu et al. 2020). The results from a previous study indicated high species diversity of *Calonectria* in Brazil (Alfenas et al. 2015).

Brazil is one of the main producers of pulp, paper, and wood panels in the world, mainly due to the genus *Eucalyptus*; its hybrids are the most grown trees in the country for these purposes (IBÁ, 2021). In 2020, the total area of *Eucalyptus* plantations was 7.47 million hectares, with an average productivity of 36.8 m^3/ha per year (IBÁ, 2021). However, in recent decades, commercial *Eucalyptus* plantations have expanded toward the warm and humid regions of northern and northeastern Brazil, where CLB has become the primary fungal leaf disease of this crop (Alfenas et al. 2015). CLB can be caused by different *Calonectria* species, is widely distributed throughout the country, and affects *Eucalyptus* plants most severely from six months to 2–3 years after planting (Graça et al. 2009). This disease starts from spores or microsclerotia present in soil or diseased plant debris on the ground and disseminates to lower branches of the tree canopy; lesions start at the base, apex or margins of leaves and can reach a large area of the leaf blade, resulting in leaf drop and, in some cases, severe defoliation in the basal, middle, and apical thirds of the canopy (Alfenas et al. 2009). The defoliation may decrease timber volume as a result of the reduced photosynthetic area and facilitates weed growth due to the increased entrance of light through the subcanopy, leading to competition for nutrients between *Eucalyptus* and understory plants (Graça et al. 2009; Alfenas et al. 2015).

CLB can be controlled by integrated cultivation and chemical methods as well as by the selection and cultivation of resistant genotypes, which is a much more effective approach (Soares et al. 2018). The demand for new strategies to control this disease requires proper identification of the pathogen species. Additionally, this information may be useful for breeding programs, leading to the development of *Eucalyptus* genotypes resistant to CLB. Recently, during a disease survey conducted in three commercial plantations of *Eucalyptus* in northeastern Brazil, diseased leaves from *Eucalyptus* trees with typical symptoms of CLB were collected, and *Calonectria* fungi were isolated. Thus, the aims of this study were to identify these isolates based on phylogenetic analyses and morphological characteristics and to confirm their pathogenicity to *Eucalyptus*.

Materials and methods

Sample collection and fungal isolation

In February 2020, during a disease survey conducted in three commercial plantations of *Eucalyptus* on six-month-old to one-year-old trees, diseased leaves with typical symptoms

of CLB (small, circular or elongated pale grey to pale brown to dark brown spots, that extend throughout the leaf blade), were observed and collected for fungal isolation and species characterization. On average, 50 diseased leaves were sampled from each *Eucalyptus* genotype, one leaf per tree, depending on the planted areas. The sampled *Eucalyptus* genotypes corresponded to *E. urophylla*, localized in the municipalities of Cidelândia (5°09'24"S; 47°46'26"W) and Itinga do Maranhão (4°34'43"S; 47°29'48"W), in the state of Maranhão, and to the *E. grandis* × *E. brassiana* hybrid genotype, in the microregion of Paragominas (3°10'51"S; 47°18'49"W), in the state of Pará, Brazil.

Samples were stored in paper bags and transported to the Laboratory of Forest Pathology at the Universidade Federal de Lavras. From each leaf, small segments of 1 cm^2 from the transition section between healthy and diseased tissue were cut and the surface was disinfected by washing with 1% sodium hypochlorite for 1 min, with 70% ethanol for 30 s and with sterilized water three times before culture on 2% malt extract agar (MEA; malt extract 20 $g \cdot L^{-1}$, agar 20 $g \cdot L^{-1}$, yeast extract 2 $g \cdot L^{-1}$, sucrose 5 $g \cdot L^{-1}$) plates at 25 °C. After 48 h of incubation, *Calonectria*-like mycelial plugs, 5 mm in diameter, were transferred to a fresh MEA plate and incubated at 25 °C until the fungus covered the plate completely. Induction of sporulation on MEA plates and single spore cultures was obtained following the procedures described by Alfenas et al. (2013). Each single spore culture was stored and maintained in a metabolically inactive state in dry culture and sterile water following Castellani's method (Castellani 1939). Holotypes were deposited as herbaria in the Coleção Micológica do Herbário da Universidade de Brasília (UB). Ex-types were deposited as pure cultures in the Coleção de Culturas de Microrganismos do Departamento de Ciência dos Alimentos/UFLA (CCDCA) at Universidade Federal de Lavras (UFLA), Minas Gerais, Brazil. Ex-paratypes were deposited as pure cultures in the Laboratory of Forest Pathology (PFC) at UFLA.

DNA extraction, PCR amplification, and sequencing

Total genomic DNA was extracted from fresh mycelia of single spore cultures grown on malt extract broth (MEB; malt extract 20 $g \cdot L^{-1}$, yeast extract 2 $g \cdot L^{-1}$, sucrose 5 $g \cdot L^{-1}$) for ten days at 25 °C in the dark. The protocol described by Lee and Taylor (1990) was followed with slight modifications; by adding 1.5 M NaCl and 2% polyvinylpyrrolidone (MW: 40000) to the lysis buffer; the DNA was precipitated directly with isopropanol without the use of 3 M NaOAc, and the DNA pellet was dried at room temperature overnight. A NanoDrop 1,000 spectrometer (Thermo Fisher Scientific, Waltham, MA, USA) was used to quantify its concentration.

Based on a previous study (Liu et al. 2020), actine (*act*), calmodulin (*cmdA*), histone H3 (*his3*), RNA polymerase II (*rpb2*), translation elongation factor 1-alpha (*tef1*), and β-tubulin (*tub2*) genes were used as DNA barcodes due to provide a stable and reliable resolution to distinguish all *Calonectria* species. The primers ACT-512F and ACT-783R (Carbone and Kohn 1999) were used to amplify the *act* gene region; CAL-228F and CAL-2Rd (Carbone and Kohn 1999; Quaedvlieg et al. 2011) for the *cmdA* gene region; CYLH3F and CYLH3R (Crous et al. 2004) for the *his3* gene region; fRpb2-5F and fRpb2-7cR (Liu et al. 1999; Reeb et al. 2004) for the *rpb2* gene region; EF1-728F (Carbone and Kohn 1999) and EF2

(O'Donnell et al. 1998) for the *tef1* gene region and the primer pairs T1 (O'Donnell and Cigelnik 1997) and CYLTUB1R (Crous et al. 2004) for the *tub2* gene region.

The PCRs were carried out in a 25 µL final volume containing molecular biology-grade water (Sigma–Aldrich, St. Louis, MO, USA) 1X PCR buffer (Promega, Madison, WI, USA), 2.5 mM $MgCl_2$, 0.2 mM deoxyribonucleotide triphosphate (dNTP) mix (Promega, Madison, WI, USA), 1 U GoTaq® Flexi DNA Polymerase (Promega, Madison, WI, USA), 0.2 mM each primer, and 30 ng DNA template. DNA amplifications were conducted in a thermal cycler (5 PRIME G gradient Thermal Cycler, Techne, Staffordshire, UK). The PCR conditions for the *act*, *cmdA*, *his3*, *tef1*, and *tub2* gene regions were as follows: an initial denaturation step at 95 °C for 5 min; then 35 amplification cycles at [94 °C for 30 s; 52 °C for 1 min; 72 °C for 2 min], and a final extension step at 72 °C for 5 min. For the *rpb2* gene region, a touchdown PCR protocol was used: an initial denaturation step at 95 °C for 5 min, then (95 °C for 30 s, 57 °C for 30 s, 72 °C for 90 s) × 10 cycles, (95 °C for 30 s, 57 °C for 45 s, 72 °C for 90 s + 5 s/cycle increase) × 30 cycles, and a final extension step at 72 °C for 10 min.

PCR products were separated by electrophoresis at 120 V for 1 h in a 1.2% agarose gel, stained with Diamond™ Nucleic Acid Dye (Promega, Madison, WI, USA), and visualized using an ultraviolet light transilluminator. Successful PCR products were purified and sequenced in both directions using the same primer pairs used for amplification by Macrogen Inc. (Macrogen, Seoul, Korea). Raw sequences from each gene region were edited, consensus sequences were generated using SeqAssem software ver. 07/2008 (Hepperle 2004), and the sequences generated in this study were deposited in the NCBI/GenBank database (http://www.ncbi.nlm.nih.gov).

Phylogenetic analyses

The generated sequences were aligned with other sequences of closely related *Calonectria* spp. obtained from GenBank (Table 1), using the online interface of MAFFT v. 7.0 (Katoh et al. 2019, http://mafft.cbrc.jp/alignment/server) with the alignment strategy FFT-NS-i (Slow; interactive refinement method). Alignments were manually corrected using MEGA7 (Kumar et al. 2016).

The partition homogeneity test (PHT) described by Farris et al. (1995) was conducted to determine if data for on six genes could be combined using PAUP 4.0b10 (Swofford 2003). To determine the phylogenetic relationships among species, phylogenetic analyses based on maximum parsimony (MP), maximum likelihood (ML), and bayesian inference (BI) were conducted on the individual gene regions and their concatenated dataset, depending on the sequence availability.

Maximum parsimony analysis was performed using PAUP 4.0b10 (Swofford 2003), with phylogenetic relationships estimated by heuristic searches, random stepwise addition sequences, and tree bisection and reconnection (TBR) branch swapping. Gaps were treated as missing data, and all characters were unordered and weighted equally. The measures calculated for parsimony included the tree length (TL), consistency index (CI), homoplasy index (HI), retention index (RI), and rescaled consistency index (RC). Statistical support for branch nodes was assessed with 1,000 bootstrap replicates.

The best evolutionary model of nucleotide substitution for each gene region was selected according to the Akaike Information Criterion (AIC) using MODELTEST v. 3.4 (Posada and Crandall 1998) for ML analyses and MRMODELTEST v. 2 (Nylander 2004) for BI analyses. ML analyses for individual gene regions were performed using PAUP 4.0b10 (Swofford 2003). The ML models used were K80 + G (*act*), TVM + G (*cmdA*), TrN + G (*his3*), SYM + G (*rpb2*), TVM + I + G (*tef1*) and HKY + I (*tub2*). Statistical support for branch nodes was assessed with 1,000 bootstrap replicates. A partitioned ML analysis was performed using IQ-TREE (Nguyen et al. 2015) as implemented in the IQ-TREE web server (http://iqtree.cibiv.univie.ac.at, Trifinopoulos et al. 2016) by using partition models (Chernomor et al. 2016). Branch support values were evaluated based on 10,000 replicates for ultrafast bootstrapping (UFBoot2) (Hoang et al. 2018).

Individual and partitioned BI analyses were performed using MRBAYES v.3.2.7a (Ronquist et al. 2012) on XSEDE at the CIPRES Science Gateway v.3.3 (http://www.phylo.org/). The BI models used were K80 + G (*act*), GTR + G (*cmdA* and *his3*), SYM + G (*rpb2*), GTR + I + G (*tef1*) and HKY + I (*tub2*). A Markov Chain Monte Carlo (MCMC) algorithm was employed, and two independent runs of four MCMC chains (three hot and one cold) were run in parallel simultaneously starting from random trees for 10^7 generations (individual gene regions) and 30^7 generations (concatenated dataset), sampling trees every 1,000 generations. The distribution of log-likelihood scores was examined with TRACER v.1.5 (Rambaut and Drummond 2007) to determine the whether the stationary phase of each search was reached and whether chains had achieved convergence. The convergence of the chains was also assessed by the convergent diagnostics of the effective sampling site (ESS), the potential scale reduction factor (PSRF), and the average standard deviation of split frequencies (ASDSF) (Ronquist et al. 2019). The first 25% of saved trees were discarded as the "burn-in" phase, and posterior probabilities (PP) were computed using the remaining trees. Trees were visualized in FIGTREE v. 1.4.4 (Rambaut 2009) and edited in INKSCAPE v. 1.0 (https://inkscape.org).

Pairwise homoplasy index (PHI) test and phylogenetic network analysis

Phylogenetically closely related species were analyzed using the Genealogical Concordance Phylogenetic Species Recognition (GCPSR) model (as described by Taylor et al. 2000) by performing a pairwise homoplasy index (Φw) test (PHI) (Bruen et al. 2006). The PHI test was performed in SPLIT TREE4 v.4.16.1. (https://uni-tuebingen.de) (Huson and Bryant 2006) to determine the recombination level within phylogenetically closely related species. Only the gene regions that were available for all compared individuals were used. Gaps sites were excluded. Significant recombination was considered at a PHI index below 0.05 ($\Phi w < 0.05$). The relationships between closely related taxa were visualized by constructing a phylogenetic network from the concatenated datasets using the LogDet transformation and the NeighborNet method; the resultant networks were displayed with the EqualAngle algorithm (Dress and Huson 2004). Bootstrap analysis was then conducted with 1,000 replicates.

Mating type and sexual compatibility test

The mating-type idiomorph of each *Calonectria* species isolate was determined through PCR by using the primer pairs Cal_MAT111_F/Cal_MAT111_R and Cal_MAT121_F/Cal_MAT121_R, which amplify the MAT1-1-1 and MAT1-2-1 genes using the protocol described by Li et al. (2020). Additionally, sexual compatibility tests were performed for all the single-spore isolates of both species on minimal salt agar (MSA; Guerber and Correll 2001) by crossing them in all possible combinations, following the procedure described by Lombard et al. (2010a). The plates were stacked in plastic bags and incubated at 25 °C for 12 weeks.

Morphology

Morphological characterization of representative isolates of each *Calonectria* species identified by phylogenetic analyses was performed as described by Liu and Chen (2017). Optimal growth temperatures were determined by incubating the representative isolate at temperatures ranging from 5 °C to 30 °C at 5 °C intervals in the dark on MEA plates (three replicates per isolate were used). Colonial characteristics (diameter, color, and texture of colonies) were determined by inoculating the isolates on MEA plates at 25 °C in the dark after seven days of incubation.

Pathogenicity tests

One representative isolate of each *Calonectria* species was selected for inoculation. Healthy leaves of three short cut branches from an approximately eleven-month-old *Eucalyptus* plants were inoculated with suspensions of 1×10^4 conidia·mL^{-1} obtained from single spore cultures. The conidia suspensions for each isolate were prepared using the method described by Graça et al. (2009). *Calonectria paragominensis* was inoculated on *E. grandis* × *E. brassiana* hybrid genotype and *C. imperata* on *E. urophylla* genotype. The inoculation consisted of spraying the conidia suspension until the suspension run off the leaves. Sterile water was sprayed onto healthy leaves as the negative control. The branches with inoculated leaves were covered with plastic bags to maintain high humidity and kept at 25 °C under a photoperiod of 12 h for 72 h. After that time, the plastic bags were removed, and necrotic symptoms were observed.

Results

Fungal isolates

A total of 34 isolates with the typical morphology of *Calonectria* species were obtained from infected leaves of the *Eucalyptus* genotypes sampled. Based on preliminary phylogenetic analyses of the *tef1* and *tub2* gene regions (data not shown), nine isolates were selected for further studies (Table 1).

Phylogenetic analyses

Sequences from 50 isolates corresponding to 25 *Calonectria* species closely related to the isolates obtained in this study were downloaded from GenBank (Table 1). For the nine isolates selected in this study, five resided in the *Calonectria spathiphylli* species complex (CSSC), and four resided in the *Calonectria candelabrum* species complex (CCSC). Both *Calonectria* complexes belong to the Prolate Group, whose species are characterized by their clavate to pyriform to ellipsoidal vesicles (Liu et al. 2020). Therefore, both complexes were combined into a single sequence dataset for phylogenetic analyses, including two strains of *Calonectria gracilipes* as the outgroup taxa.

Alignments for each gene region and the concatenated dataset were as follows: *act* (36 isolates, 267 characters), *cmdA* (58 isolates, 485 characters), *his3* (59 isolates, 439 characters), *rpb2* (28 isolates, 863 characters), *tef1* (58 isolates, 496 characters), *tub2* (59 isolates, 511 characters) and concatenated (59 isolates, 3061 characters). The PHT generated a *p* value of 0.01 for the concatenated dataset, suggesting some incongruence in the datasets for the six regions and the accuracy of the combined data could have suffered relative to the individual partitions (Cunningham 1997). Although the *p* value was low, the different gene regions were combined because the significance threshold of 0.05 may be too conservative and it has been shown that combining incongruent datasets improves phylogenetic accuracy (Sullivan 1996; Cunningham 1997); moreover, this approach was followed by several previous studies (Lombard et al. 2016; Pham et al. 2019; Liu et al. 2020, 2021).

Tree topologies derived from the MP, ML, and BI analyses of the individual gene regions were similar overall, but the relative positions of some *Calonectria* species slightly differed. Moreover, the concatenated dataset formed well-supported lineages in the MP, ML, and BI analyses. Only the ML trees are presented in this study (Fig. 1, Supplementary Figures S1-S6). The concatenated dataset had 466 parsimony-informative characters, 67 parsimony-uninformative characters, and 2,528 constant characters. Analysis of the 466 parsimony-informative characters yielded 2 equally parsimonious trees, with TL = 862, CI = 0.7042, HI = 0.2958, RI = 0.9192, RC = 0.6472. For the partitioned BI analysis, the convergence of the chains was confirmed by an ESS > 200, a PSRF approaching 1, and an ASDSF equal to 0.000793. The aligned sequences were deposited in TreeBASE (http://treebase.org ;No. 29573).

Phylogenetic analyses of the six individual gene regions showed that the five isolates from the CSSC were clustered in an independent clade（Suppl. Figs S1–S6). Based on the concatenated dataset of the six genes, the five isolates formed a new, strongly defined phylogenetic clade that was distinct from the other *Calonectria* species of the CSSC and was supported by high bootstrap values (MP = 100%, ML = 100%) and high values of posterior probability (1.0) (Fig. 1). A total of 41 fixed unique single nucleotide polymorphisms (SNPs) were identified in the new phylogenetic clade of the five isolates in comparison with their phylogenetically closely related *Calonectria* species in the six-gene concatenated dataset (Table 2). The results of these phylogenetic and SNP analyses indicate that the five isolates in the CSSC represent a distinct, undescribed species, which we named *C. paragominesis*.

Phylogenetic analyses of the individual gene regions of *act*, *cmdA*, *his3*, *rpb2*, and *tub2* showed that the four isolates that resided in the CCSC were clustered in an independent clade (Suppl. Figs 1–4 and 6). However, the phylogenetic tree based on *tef1* showed that three of those isolates formed an independent clade, while one isolate was closely related to *C. metrosideri*, *C. pseudometrosideri*, and *C. candelabrum* (Suppl. Fig. 5). Based on the concatenated dataset of the six genes, the four isolates formed a new, strongly defined phylogenetic clade that was distinct from other *Calonectria* species in the CSSC and was supported by high bootstrap values (MP = 91%, ML = 99%) and high values of posterior probability (1.0) (Fig. 1). The four isolates of the new phylogenetic clade were distinguished from their phylogenetically closely related *Calonectria* species using SNP analyses for the six-gene concatenated dataset, by presenting eight unique SNPs from a total of 78 SNPs (Table 3). The results of these phylogenetic and SNP analyses indicate that the four isolates in the CCSC represent a distinct, undescribed species, which we named *C. imperata*.

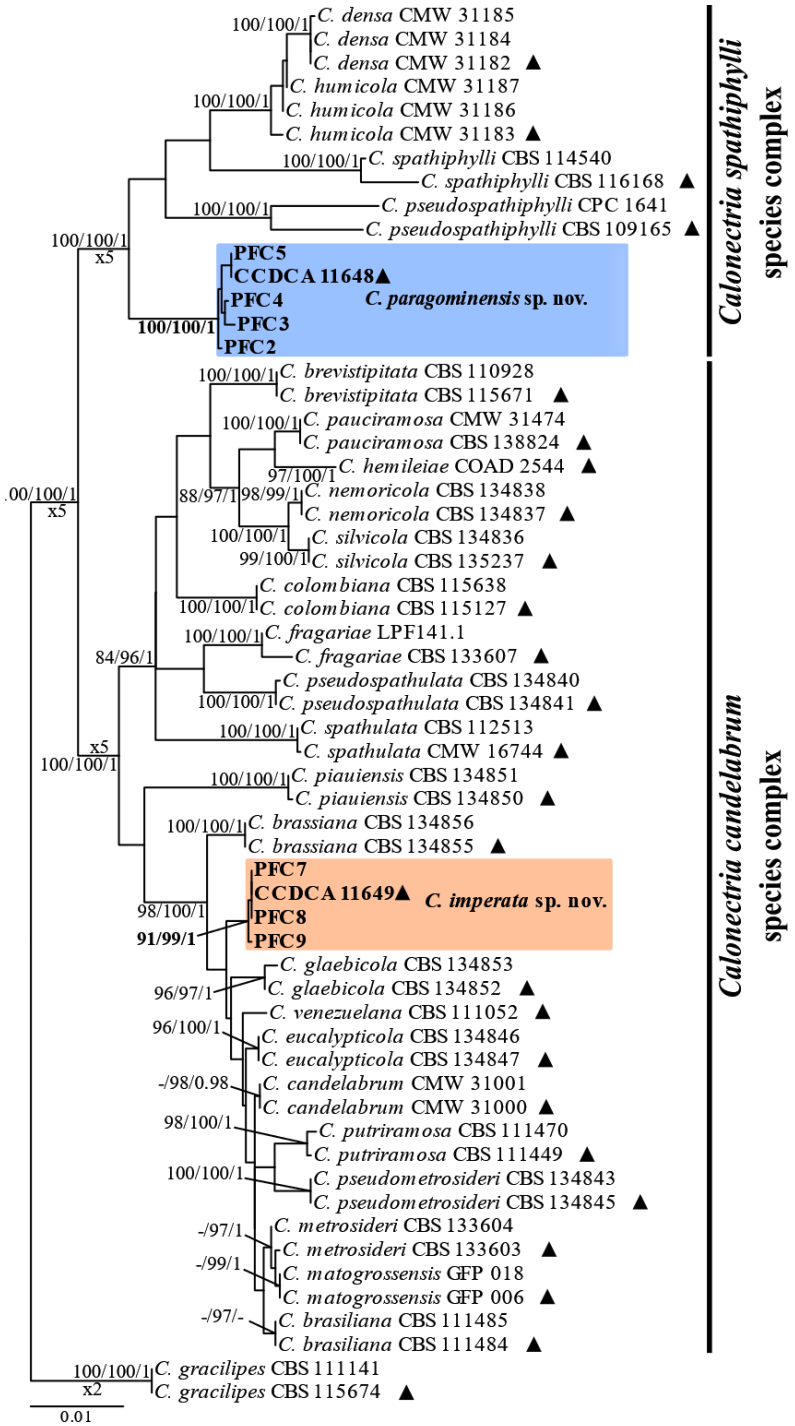

Figure 1. Phylogenetic tree based on maximum likelihood analysis of concatenated *act*, *cmdA*, *his3*, *rpb2*, *tef1* and *tub2* gene regions. Bootstrap support values ≥ 80% for maximum parsimony (MP), Ultrafast bootstrap support values ≥ 95% for maximum likelihood (ML), and posterior probability (PP) values ≥ 0.95 from BI analyses are presented at the nodes (MP/ML/PP). Bootstrap values below 80% (MP), 95% (ML) and posterior probabilities below 0.80 are marked with "-". Ex-type isolates are indicated by "▲", isolates highlighted in bold were sequenced in this study, and novel species are in blue and orange. *C. gracilipes* was used as outgroup. The scale bar indicates the number of nucleotide substitutions per site.

Species delimitation by GCPSR analysis

A PHI test using a five-locus concatenated dataset (*act*, *cmdA*, *his3*, *tef1*, *tub2*) was performed to determine the recombination level among *C. paragominensis* and its phylogenetically closely related species, *C. densa*, *C. humicola*, *C. spathiphylli* and *C. pseudospathiphylli*. A value of Φw = 0.2879 revealed no significant genetic recombination events, and this relationship was supported with a high bootstrap value (100%) in the phylogenetic network analysis, indicating that they are different species (Fig. 2A).

A PHI test using a four-locus concatenated dataset (*cmdA*, *his3*, *tef1*, *tub2*) was performed to determine the recombination level among *C. imperata* and its phylogenetically closely related species, *C. brassiana*, *C. glabeicola*, *C. piauiensis*, and *C. venezuelana*. A value of Φw = 0.1587 revealed no significant genetic recombination events, and this relationship was supported with a high bootstrap value (94%) in the phylogenetic network analysis, indicating that they are different species (Fig. 2B).

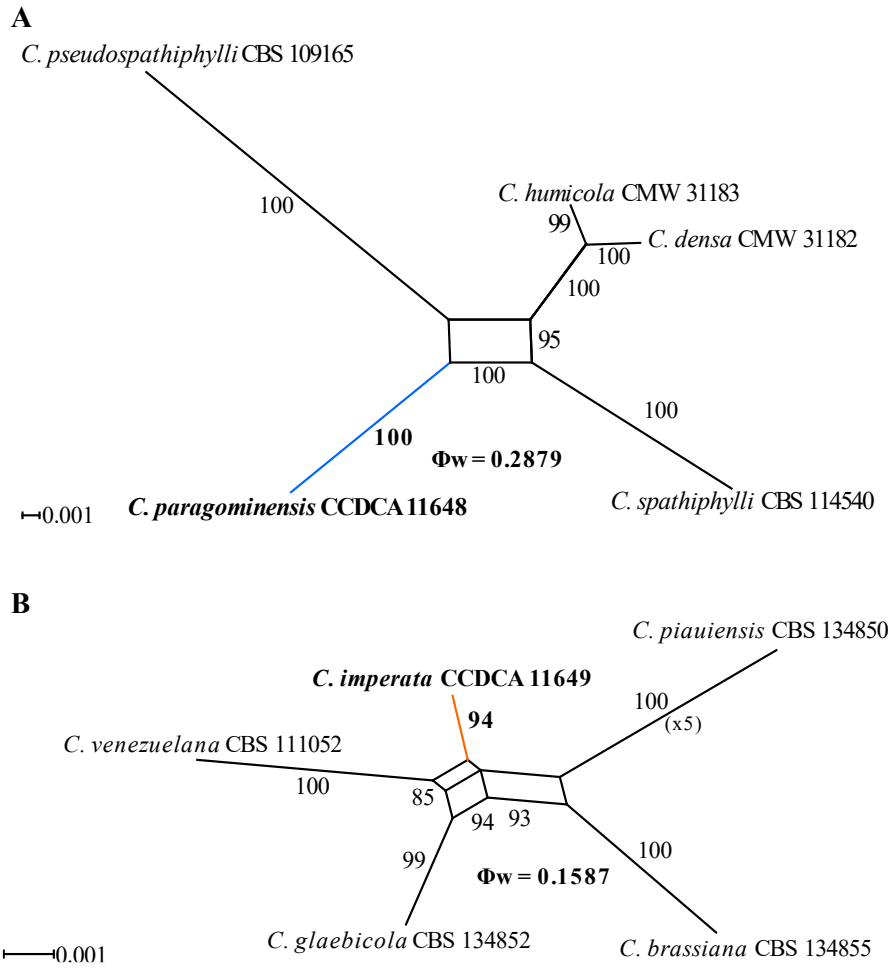

Figure 2. Results of the pairwise homoplasy index (PHI) test for *C. paragominensis* and *C. imperata*. Phylogenetic networks constructed using the LogDet transformation and the NeighborNet method and displayed with the EqualAngle algorithm. Bootstrap support values > 80% are shown. Φw < 0.05 indicate significant recombination. New species described in this study are highlighted in bold, with blue (A) and orange (B) lines.

Mating-type and sexual compatibility test

MAT1-1-1 and MAT1-2-1 genes were amplified in all isolates of each identified species, indicating that they are putatively homothallic. However, after a twelve-week mating test on MSA, all isolates failed to yield sexual structures, indicating that they have lost the ability to be self-fertile or have retained the ability to favor outcrossing rather than selfing.

Taxonomy

Based on phylogenetic analyses, GCPSR, and network analyses, the nine isolates presented two strongly defined phylogenetic clades in both the *Calonectria spathiphylli* species complex and the *Calonectria candelabrum* species complex. Morphological differences, especially in the macroconidia and stipe dimensions, were observed between each phylogenetic clade and its phylogenetically closely related species (Table 4). Thus, the fungi isolated in this study represent two new species of *Calonectria* and are described as follows:

Calonectria paragominensis **E.I.Sanchez, T.P.F.Soares & M.A.Ferreira, sp. nov.**
MycoBank No: 843460
Fig. 3

Etymology. The term "*paragominensis*" refers to the microregion of Paragominas, Brazil, which is the place where the fungus was collected.
Diagnosis. *Calonectria paragominensis* differs from the phylogenetically closely related species *C. densa*, *C. humicola*, *C. spathiphylli* and *C. pseudospathiphylli* with respect to its macroconidia dimensions.
Type. BRAZIL,• Pará state, Paragominas microregion; 3°10'51"S, 47°18'49"W; From infected leaves of *E. grandis* × *E. brassiana*; 20 Feb. 2020; M.A. Ferreira; **holotype**: UB24349, **ex-type**: CCDCA 11648 = PFC1. GenBank: *act* = ON009346; *cmdA* = OM974325; *his3* = OM974334; *rpb2* = OM974343; *tef1* = OM974352; *tub2* = OM974361.
Description. Sexual morph unknown. Macroconidiophores consisted of a stipe, a suite of penicillate arrangements of fertile branches, a stipe extension, and a terminal vesicle; stipe septate, hyaline, smooth, (112–)135–207(–281) × (2–)2.6–3.5(–4) µm; stipe extension septate, straight to flexuous, (123–)147–220(–295) µm long, (1.5–)1.9–2.4(–3) µm wide at the apical septum, terminating in a globose to sphaeropedunculate vesicle, (8–)8.5–10.5(–12) µm diam; lateral stipe extensions (90° to the axis) also present. Conidiogenous apparatus was (40–)56–88(–113) µm long, (45–)67–107(–129) µm wide; primary branches aseptate or 1-septate, (15.7–)18.4–25.9(–30.6) × (3.3–)4–6(–6.5) µm; secondary branches aseptate, (12.7–)14.3–19.6(–22.1) × (3–)3.5–5(–6) µm; tertiary branches aseptate, (9.9–)11.6–15.3(–17.9) × (2.8–)3.6–5.3(–6.4) µm; additional branches (–4), aseptate, (10.3–)11–13.2(–14) × (3–)3.2–4.4(–5) µm; each terminal branch produced 2–4 phialides; phialides doliiform to reniform, hyaline, aseptate, (8–)9.1–11.8(–14) × (2–)2.7–4.1(–6) µm, apex with minute periclinal thickening and inconspicuous collarette. Macroconidia were cylindrical, rounded at both ends, straight, (47–)56–66(–71) × (4–)4.8–5.9(–7) µm (av. = 61 × 5 µm), (1–3) septate, lacking a visible abscission scar, held in parallel cylindrical clusters by colorless slime. Megaconidia and microconidia were not observed.
Culture characteristics. Colonies formed abundant white aerial mycelium on MEA at 25 °C after seven days, with irregular margins and moderate sporulation. The surface had white

to buff outer margins, and sienna to amber in reverse with abundant chlamydospores throughout the medium, forming microsclerotia. The optimal growth temperature was 23.8 °C, with no growth at 5 °C; after seven days, colonies at 10 °C, 15 °C, 20 °C, 25 °C, and 30 °C reached 7 mm, 23 mm, 38.3 mm, 36.1 mm, and 31.8 mm, respectively.

Substratum. Leaves of *E. grandis* × *E. brassiana*.

Distribution. Northeast Brazil.

Other specimens examined. BRAZIL,• Pará state, Paragominas microregion; From infected leaves of *E. grandis* × *E. brassiana*; 20 Feb. 2020; M.A. Ferreira; cultures PFC2, PFC3, PFC4, PFC5.

Notes. *C. paragominensis* is a new species in the *C. spathiphylli* species complex (Liu et al., 2020). Morphologically, *C. paragominensis* is very similar to *C. densa*, since both form lateral stipe extensions, which have not been reported for the other three species in the complex. However, the macroconidia of *C. paragominensis* (av. 61 × 5 μm) are longer than those of *C. densa* (av. 54 × 6 μm), *C. humicola* (av. 51 × 5 μm) and *C. pseudospathiphylli* (av. 52 × 4 μm) but smaller than those of *C. spathiphylli* (av. 70 × 6 μm).

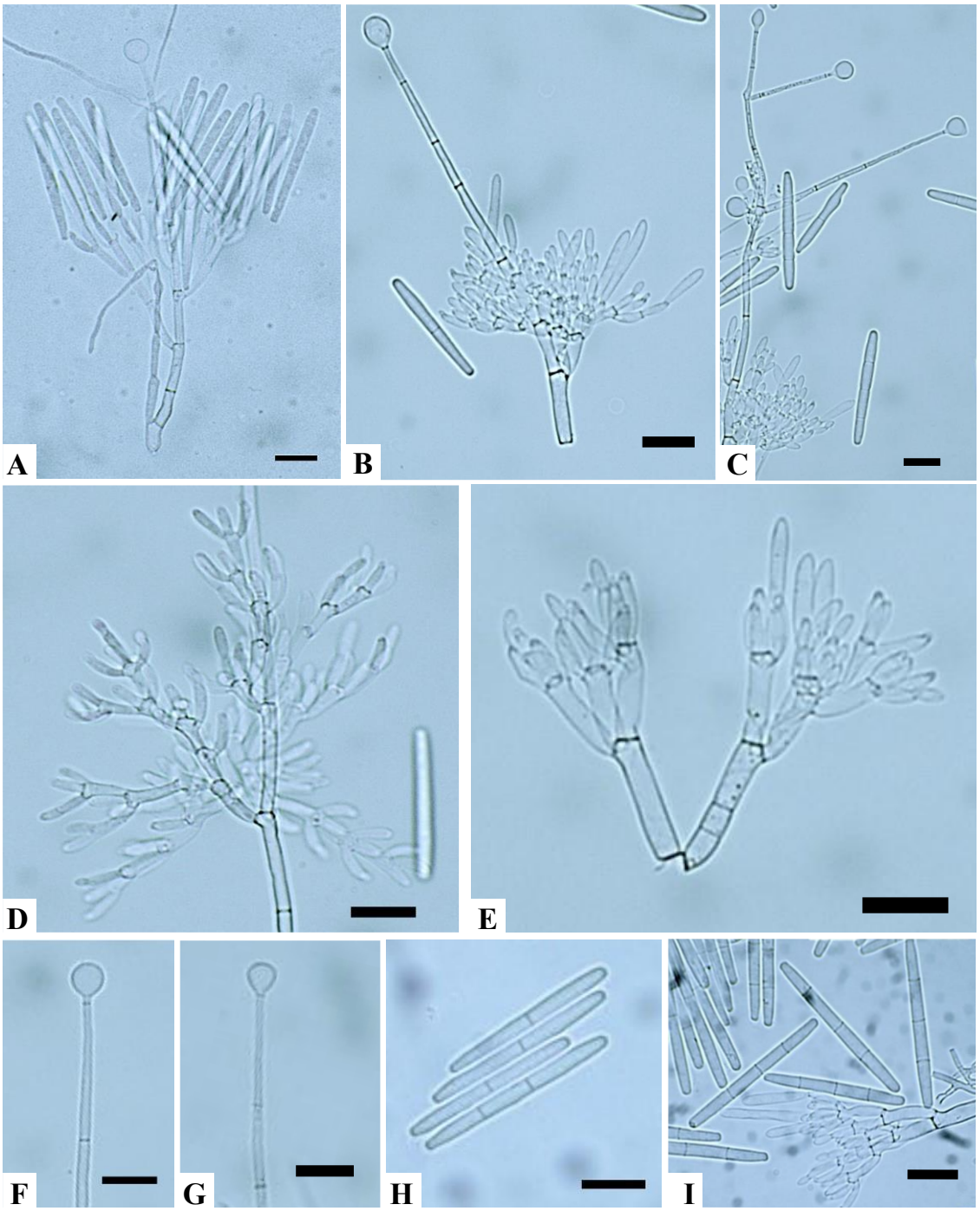

Figure 3. *Calonectria paragominensis*. **A–B** Macroconidiophore **C** Lateral stipe extensions **D–E** Conidiogenous apparatus with conidiophore branches and doliiform to reniform phialides **F–G** Globose to sphaeropedunculate vesicles **H–I** One, two, and three-septate macroconidia. Scale bars = 20 µm.

Calonectria imperata **E.I.Sanchez, T.P.F.Soares & M.A.Ferreira, sp. nov.**
MycoBank No: 843461
Fig. 4

Etymology. The term "*imperata"* is in honor of the city of Imperatriz, Brazil, which was close to the place where the fungus was collected.
Diagnosis. *Calonectria imperata* differs from the phylogenetically closely related species *C. brassiana, C. glaebicola, C. piauiensis* and *C. venezuelana* with respect to the number of unique alleles and stipe dimensions.
Type. BRAZIL,• Maranhão state, Cidelândia municipality; 5°09'24"S, 47°46'26"W; From infected leaves of *E. urophylla*; 20 Feb. 2020; M.A. Ferreira; **holotype**: UB24350, **ex-type**: CCDCA 11649 = PFC6. GenBank: *act* = ON009351; *cmdA* = OM974330; *his3* = OM974339; *rpb2* = OM974348; *tef1* = OM974357; *tub2* = OM974366.
Description. Sexual morph unknown. Macroconidiophores consisted of a stipe, a suite of penicillate arrangements of fertile branches, a stipe extension, and a terminal vesicle; stipe septate, hyaline, smooth, (135–)151–198(–227) × (2–)2.6–3.4(–4) μm; stipe extension septate, straight to flexuous, (151–)169–220(–254) μm long, (1.5–)1.9–2.7(–3) μm wide at the apical septum, terminating in an ellipsoidal to narrowly obpyriform vesicle (3–)3.1–4.6(–6) μm diam. Conidiogenous apparatus was (50–)66–100(–127) μm long, (41–)62–89(–110) μm wide; primary branches aseptate, (14.6–)19–24.8(–28.5) × (2.5–)3.2–4(–4.5) μm; secondary branches aseptate, (12.1–)13.5–18.2(–24.2) × (2.3–)2.8–3.7(–4) μm; tertiary branches aseptate, (10.1–)11–15(–18.1) × (1.9–)2.3–3.2(–4.1) μm; each terminal branch producing 2–4 phialides; phialides doliiform to reniform, hyaline, aseptate, (8–)9.1–13(–15) × (2–)2.7–3.3(–4) μm, apex with minute periclinal thickening and inconspicuous collarette. Macroconidia were cylindrical, rounded at both ends, straight, (38–)43–49(–52) × (2–)2.7–3.2(–4) μm (av. = 46 × 3 μm), (–1) septate, lacking a visible abscission scar, held in parallel cylindrical clusters by colorless slime. Megaconidia and microconidia were not observed.
Culture characteristics: Colonies formed moderate aerial mycelium on MEA at 25 °C after seven days, with moderate sporulation. The surface had white to buff outer margins, and sepia to umber in reverse with abundant chlamydospores throughout the medium, forming microsclerotia. The optimal growth temperature was 25 °C, with no growth at 5 °C; after seven days, colonies at 10 °C, 15 °C, 20 °C, 25 °C, and 30 °C reached 10.1 mm, 25.5 mm, 29.1 mm, 44.5 mm, and 40.6 mm, respectively.
Substratum. Leaves of *E. urophylla*.
Distribution. Northeast Brazil.
Other specimens examined. BRAZIL,• Maranhão state, Cidelândia municipality; 5°09'24"S, 47°46'26"W; From infected leaves of *E. urophylla*; 20 Feb. 2020; M.A. Ferreira; cultures PFC7, PFC8. BRAZIL• Maranhão state, Itinga do Maranhão; 4°34'43"S, 47°29'48"W; From infected leaves of *E. urophylla*; 20 Feb. 2020; M.A. Ferreira; culture PFC9.
Notes. *C. imperata* is a new species in the *C. candelabrum* species complex (Liu et al., 2020). Morphologically, *C. imperata* is very similar to its closest relatives, from which it can be distinguished based on stipe dimensions and phylogenetic inference. Stipe of *C. imperata* (135–227 × 2–4 μm) is larger than those of *C. piauiensis* (50–110 × 4–6 μm), *C. glaebicola* (50–130 × 5–7 μm), and *C. venezuelana* (35–100 × 4–8 μm) but narrower than those of *C.*

brassiana (55–155 × 5–8 µm). Additionally, *C. imperata* lacks lateral stipe extensions, which are present in *C. piauiensis*.

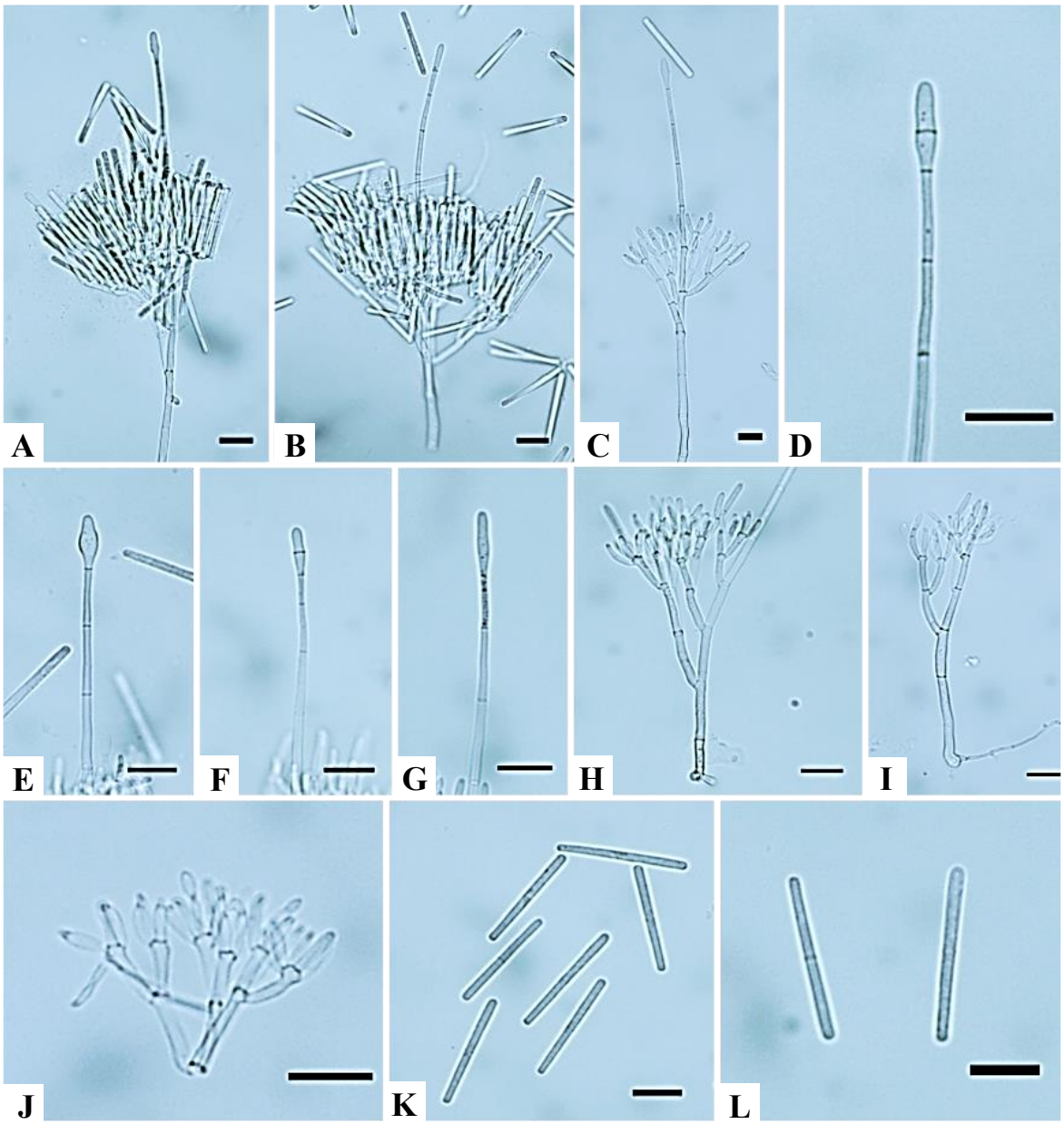

Figure 4. *Calonectria imperata*. **A–C** Macroconidiophore **D–G** Ellipsoidal to narrowly obpyriform vesicles **H–J** Conidiogenous apparatus with conidiophore branches and doliiform to reniform phialides **K–L** Macroconidia. Scale bars = 20 µm.

Pathogenicity tests

The conidia suspensions of the representative isolates of *C. paragominensis* and *C. imperata* produced lesion symptoms on leaves (Fig. 5E, F, H, I), but no lesions were observed on the negative control inoculations (Fig. 5G, J). The pathogens were reisolated from inoculated

leaves but not from the negative controls and identified by the same morphological characteristics as the originally inoculated species, thus, fulfilling the requirements of Koch's postulates.

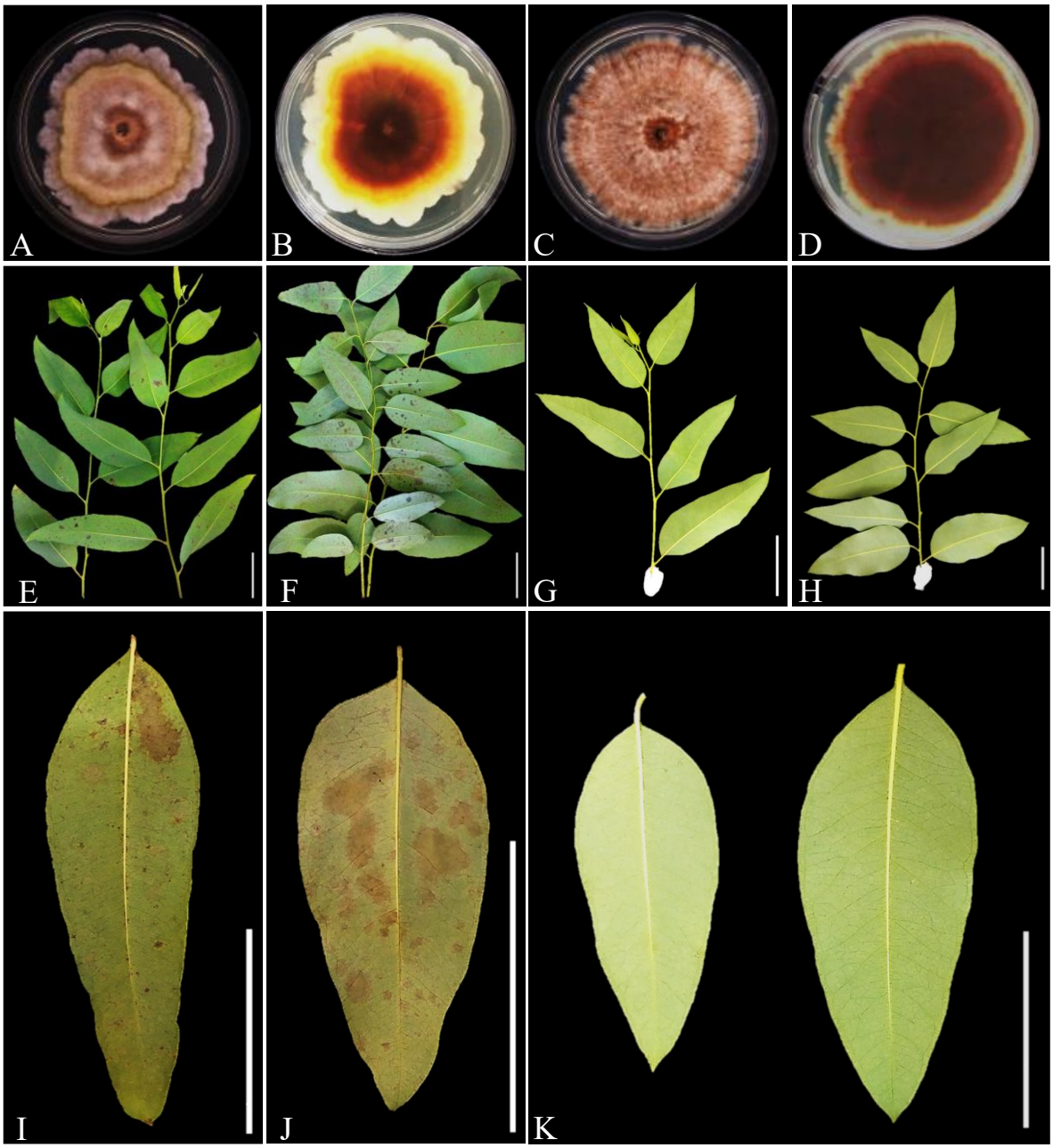

Figure 5. Pathogenicity tests on leaves of *Eucalyptus* genotypes. **A–B** Surface and reverse of *C. paragominensis* on MEA plates after 14 days grown at 25 °C **C–D** Surface and reverse of *C. imperata* on MEA plates after 14 days grown at 25 °C **E–I** Lesions on leaves of *E. grandis* × *E. brassiana* induced by *C. paragominensis* 72 h after inoculation **F–J** Lesions on leaves of *E. urophylla* induced by *C. imperata* 72 h after inoculation **G–H–K** No disease symptoms on leaves inoculated with sterile water **(**negative controls). Scale bars: 5 cm (**E–K**).

Discussion

Two new species of *Calonectria* isolated from diseased *Eucalyptus* leaves were identified based on phylogenetic analyses of six gene regions and on morphological comparisons. These two species were named *C. paragominensis* and *C. imperata*.

Calonectria paragominensis is a new species in the *C. spathiphylli* complex. The five species identified and described in *C. spathiphylli* complex are *C. densa*, *C. humicola*, *C. spathiphylli*, *C. pseudospathiphylli*, and *C. paragominensis*, where *C. paragominensis* can be differentiated morphologically with respect to the macroconidia dimensions (El-Gholl et al. 1992; Kang et al. 2001; Crous 2002; Lombard et al. 2010b). These species are characterized by presenting globoid to ovoid to sphaeropedunculate terminal vesicles (Kang et al. 2001; Crous 2002; Lombard et al. 2010b). *Calonectria spathiphylli* is described as heterothallic (El-Gholl et al. 1992), *C. densa* as putatively heterothallic (Li et al. 2020) and *C. pseudospatiphilly* as homothallic (Kang et al. 2001). The *C. humicola* mating type has not been indicated (Lombard et al. 2010b). Here, *C. paragominensis* is described as putatively homothallic based on PCR amplification of the mating-type genes. Regarding pathogenicity, *C. paragominensis* is pathogenic to *Eucalyptus* sp., *C. spathiphylli* is pathogenic to *Sapthiphyllum* sp. *Heliconia* sp. *Ludwigia* sp. *Strelitzia* sp. and *Eugenia* sp. (El-Gholl et al. 1992; Poltronieri et al. 2011). *Calonectria densa*, *C. humicola*, and *C. pesudospathiphylli* were isolated from soil, and their pathogenicity has not been indicated (Kang et al. 2001; Lombard et al. 2010b). In addition to *C. paragominensis*, only *C. spathiphylli* has been indicated to be present in Brazil (Reis et al. 2004; Poltronieri et al. 2011).

Calonectria imperata is a new species in the *C. candelabrum* complex. Species in this complex are characterized by presenting ellipsoidal to obpyriform terminal vesicles, in both heterothallic and homothallic species, and occur in Africa, Asia, Europe, North and South America, and Oceania (Liu et al. 2020). Of the 21 species in the *C. candelabrum* complex (Crous et al. 2018, 2019; Liu et al. 2020), 17 have been found in Brazil (Schoch et al. 1999; Crous et al. 2018, 2019; Liu et al. 2020). *Calonectria imperata* is phylogenetically closely related to *C. brassiana, C. glaebicola, C. piauiensis* and *C. venezuelana*, which can be differentiated with respect to the number of unique alleles and stipe dimensions (Alfenas et al. 2015; Lombard et al. 2016). *Calonectria brassiana, C. glaebicola,* and *C. piauiensis* were found in Brazil, isolated from soil samples of *Eucalyptus* plantations, but only *C. glaebicola* has been confirmed to be pathogenic to *Eucalyptus* sp. (Alfenas et al. 2015). *Calonectria venezuelana* was reported in Venezuela, similarly, isolated from soil samples, but its pathogenicity has not been indicated (Lombard et al. 2016). The mating-type for *C. brassiana, C. glaebicola, C. piauiensis* and *C. venezuelana* has not been determined (Liu et al. 2020).

Pathogenicity tests showed that *C. paragominensis* and *C. imperata* are pathogenic to *E. grandis* × *E. brassiana* hybrid genotype and *E. urophylla* genotype, respectively. Although the death of *Eucalyptus* trees due to CLB is not common, it affects *Eucalyptus* plants most severely from six months to 2–3 years after planting (Graça et al. 2009). Although the economic loss due to defoliation caused by CLB has not been quantified directly, according to artificial pruning studies conducted by Pulrolnik et al. (2005) and Pires (2000), when the

loss of branches is equal to or greater than 75% of *E. grandis* seedlings of one year of age, the volumetric productivity has decreased by 45% by the time they reach seven years old. Therefore, it has been inferred that in susceptible clones, the pathogen can cause economic losses, since under favorable conditions, infection by *Calonectria* can result in severe defoliation (Soares et al. 2018). Additionally, Miranda et al. (2021) indicated a potential growth loss of 19.8 to 39.6% due to CLB, and by using the estimates of growth reduction from Pires (2000) as a baseline, concluded that a reduction in the volumetric increment on the order of 39.6% may result in an economic loss of R$ 4291.00 per ha, considering a price of *Eucalyptus* wood as R$ 38.70 per m^3 (IEA, 2020) and a production of 280 $m^3 \cdot ha^{-1}$ in the first 7-year rotation. Therefore, accurate diagnoses of plant diseases and identification of their casual agents are fundamental in promoting the development of effective disease management strategies (Wingfield et al. 2015; Liu and Chen 2017).

In this study, we described two new *Calonectria* species, both isolated from diseased *Eucalyptus* leaves from commercial plantations localized in a tropical zone. These results suggest that there are still more *Calonectria* species to be discovered in Brazil, and that they require careful monitoring, since this knowledge could facilitate the development of resistant *Eucalyptus* clones.

Acknowledgments

We thank Heitor S. Dallapiccola and Francisco J. A. Gomes for their help during sample collection. We thank the laboratories of Molecular Biology, Plant Virology, and Nematology at Universidade Federal de Lavras (UFLA) for the facilities granted during the completion of this study. The first author thanks the “Coordenação de Aperfeiçoamento de Pessoal de Nível Superior (CAPES)” for the doctorate scholarship assigned through Brazil’s PAEC OAS-GCUB Scholarships Program.

Author contribution

Conceptualization: M.A.F. and E.I.S.G.; Methodology: E.I.S.G. and M.A.F.; Software: E.I.S.G.; Validation: E.I.S.G., T.P.F.S., T.G.Z., E.A.V.Z., R.G.M., and M.A.F.; Formal analysis: E.I.S.G.; Investigation: E.I.S.G.; Resources: T.G.Z., E.A.V.Z., R.G.M., and M.A.F.; Data Curation: E.I.S.G.; Writing - Original draft: E.I.S.G.; Writing - Review and Editing: E.I.S.G., T.P.F.S., T.G.Z., E.A.V.Z., R.G.M., and M.A.F.; Visualization: E.I.S.G., T.P.F.S., T.G.Z., E.A.V.Z., R.G.M., and M.A.F.; Supervision: M.A.F.; Project administration: M.A.F.; Funding Acquisition: M.A.F. All authors read and approved the final manuscript.

Funding
This research was financed by Suzano Papel e Celulose S. A.

Competing interests

The authors have declared that no competing interests exist.

References

Alfenas AC, Zauza EAV, Mafia RG, de Assis TF (2009) Clonagem e doenças do eucalipto. 2nd ed, Editora UFV, Viçosa, MG, Brazil, 500 pp.

Alfenas RF, Lombard L, Pereira OL, Alfenas AC, Crous PW (2015) Diversity and potential impact of *Calonectria* species in *Eucalyptus* plantations in Brazil. Studies in Mycology 80:89–130. https://doi.org/10.1016/j.simyco.2014.11.002

Alfenas RF, Pereira OL, Freitas RG, Freitas CS, Dita MA, Alfenas AC (2013) Mass spore production and inoculation of *Calonectria pteridis* on *Eucalyptus* spp. under different environmental conditions. Tropical Plant Pathology 38:406–413. https://doi.org/10.1590/S1982-56762013000500005

Bruen TC, Philippe H, Bryant D (2006) A simple and robust statistical test for detecting the presence of recombination. Genetics 172(4):2665–2681. https://doi.org/10.1534/genetics.105.048975

Carbone I, Kohn LM (1999) A method for designing primer sets for speciation studies in filamentous ascomycetes. Mycologia 91(3):553–556. https://doi.org/10.1080/00275514.1999.12061051

Castellani A (1939) Viability of some pathogenic fungi in distilled water. Journal of Tropical Medicine and Hygiene 42:225–226.

Chernomor O, Von Haeseler A, Minh BQ (2016) Terrace aware data structure for phylogenomic inference from supermatrices. Systematic biology 65(6):997–1008. https://doi.org/10.1093/sysbio/syw037

Crous PW (2002) Taxonomy and pathology of *Cylindrocladium* (*Calonectria*) and allied genera. APS Press, St. Paul, Minnesota, USA, 278 pp.

Crous PW, Groenewald JZ, Risède JM, Simoneau P, Hywel-Jones NL (2004) *Calonectria* species and their *Cylindrocladium* anamorphs: species with sphaeropedunculate vesicles. Studies in mycology 50:415–430. https://doi.org/10.3114/sim.55.1.213

Crous PW, Hernández-Restrepo M, Schumacher RK, Cowan DA, Maggs-Kölling G, Marais E, Wingfield MJ, Yilmaz N, Adan OCG, Akulov A, Duarte E Álvarez, Berraf-Tebbal A, Bulgakov TS, Carnegie AJ, de Beer ZW, Decock C, Dijksterhuis J, Duong TA, Eichmeier A, Hien LT, Houbraken JAMP, Khanh TN, Liem NV, Lombard L, Lutzoni FM, Miadlikowska JM, Nel WJ, Pascoe IG, Roets F, Roux J, Samson RA, Shen M, Spetik M, Thangavel R, Thanh HM, Thao LD, van Nieuwenhuijzen EJ, Zhang JQ, Zhang Y, Zhao LL, Groenewald JZ (2021a) New and Interesting Fungi 4. Fungal systematics and evolution 7:255–343. https://doi.org/10.3114/fuse.2021.07.13

Crous PW, Luangsa-ard JJ, Wingfield MJ, Carnegie AJ, Hernández-Restrepo M, Lombard L, Roux J, Barreto RW, Baseia IG, Cano-Lira JF, Martín MP, Morozova OV, Stchigel AM, Summerell BA, Brandrud TE, Dima B, García D, Giraldo A, Guarro J, Gusmão LFP, Khamsuntorn P, Noordeloos ME, Nuankaew S, Pinruan U, Rodríguez-Andrade E, Souza-Motta CM, Thangavel R, van Iperen AL, Abreu VP, Accioly T, Alves JL, Andrade JP, Bahram M, Baral H-O, Barbier E, Barnes CW, Bendiksen E, Bernard E, Bezerra JDP, Bezerra JL, Bizio E, Blair JE, Bulyonkova TM, Cabral TS, Caiafa MV, Cantillo T, Colmán AA, Conceição LB, Cruz S, Cunha AOB, Darveaux BA, da Silva AL, da Silva GA, da Silva GM, da Silva RMF, de Oliveira RJV, Oliveira RL, De Souza JT, Dueñas M, Evans HC, Epifani F, Felipe MTC, Fernández-López J, Ferreira BW, Figueiredo CN, Filippova NV, Flores JA, Gené J, Ghorbani G, Gibertoni TB, Glushakova AM, Healy R, Huhndorf SM, Iturrieta-González I, Javan-Nikkhah M, Juciano RF, Jurjević Ž, Kachalkin AV,

Keochanpheng K, Krisai-Greilhuber I, Li Y-C, Lima AA, Machado AR, Madrid H, Magalhães OMC, Marbach PAS, Melanda GCS, Miller AN, Mongkolsamrit S, Nascimento RP, Oliveira TGL, Ordoñez ME, Orzes R, Palma MA, Pearce CJ, Pereira OL, Perrone G, Peterson SW, Pham THG, Piontelli E, Pordel A, Quijada L, Raja HA, Rosas de Paz E, Ryvarden L, Saitta A, Salcedo SS, Sandoval-Denis M, Santos TAB, Seifert KA, Silva BDB, Smith ME, Soares AM, Sommai S, Sousa JO, Suetrong S, Susca A, Tedersoo L, Telleria MT, Thanakitpipattana D, Valenzuela-Lopez N, Visagie CM, Zapata M, Groenewald JZ et al (2018) Fungal Planet description sheets: 785–867. Persoonia: Molecular Phylogeny and Evolution of Fungi 41:238–417. https://doi.org/10.3767/persoonia.2018.41.12

Crous PW, Cowan DA, Maggs-Kölling G, Yilmaz N, Thangavel R, Wingfield MJ, Noordeloos ME, Dima B, Brandrud TE, Jansen GM, Morozova OV, Vila J, Shivas RG, Tan YP, Bishop-Hurley S, Lacey E, Marney TS, Larsson E, Le Floch G, Lombard L, Nodet P, Hubka V, Alvarado P, Berraf-Tebbal A, Reyes JD, Delgado G, Eichmeier A, Jordal JB, Kachalkin AV, Kubátová A, Maciá-Vicente JG, Malysheva EF, Papp V, Rajeshkumar KC, Sharma A, Spetik M, Szabóová D, Tomashevskaya MA, Abad JA, Abad ZG, Alexandrova AV, Anand G, Arenas F, Ashtekar N, Balashov S, Bañares Á, Baroncelli R, Bera I, Biketova AYu, Blomquist CL, Boekhout T, Boertmann D, Bulyonkova TM, Burgess TI, Carnegie AJ, Cobo-Diaz JF, Corriol G, Cunnington JH, da Cruz MO, Damm U, Davoodian N, de A Santiago ALCM, Dearnaley J, de Freitas LWS, Dhileepan K, Dimitrov R, Di Piazza S, Fatima S, Fuljer F, Galera H, Ghosh A, Giraldo A, Glushakova AM, Gorczak M, Gouliamova DE, Gramaje D, Groenewald M, Gunsch CK, Gutiérrez A, Holdom D, Houbraken J, Ismailov AB, Istel Ł, Iturriaga T, Jeppson M, Jurjević Ž, Kalinina LB, Kapitonov VI, Kautmanova I, Khalid AN, Kiran M, Kiss L, Kovács Á, Kurose D, Kusan I, Lad S, Læssøe T, Lee HB, Luangsa-ard JJ, Lynch M, Mahamedi AE, Malysheva VF, Mateos A, Matočec N, Mešić A, Miller AN, Mongkolsamrit S, Moreno G, Morte A, Mostowfizadeh-Ghalamfarsa R, Naseer A, Navarro-Ródenas A, Nguyen TTT, Noisripoom W, Ntandu JE, Nuytinck J, Ostrý V, Pankratov TA, Pawłowska J, Pecenka J, Pham THG, Polhorský A, Posta A, Raudabaugh DB, Reschke K, Rodríguez A, Romero M, Rooney-Latham S, Roux J, Sandoval-Denis M, Smith MTh, Steinrucken TV, Svetasheva TY, Tkalčec Z, van der Linde EJ, vd Vegte M, Vauras J, Verbeken A, Visagie CM, Vitelli JS, Volobuev SV, Weill A, Wrzosek M, Zmitrovich IV, Zvyagina EA, Groenewald JZ (2021b) Fungal planet description sheets: 1182–1283. Persoonia: Molecular Phylogeny and Evolution of Fungi, 46:313–528. https://doi.org/10.3767/persoonia.2021.46.11

Crous PW, Carnegie AJ, Wingfield MJ, Sharma R, Mughini G, Noordeloos ME, Santini A, Shouche YS, Bezerra JDP, Dima B, Guarnaccia V, Imrefi I, Jurjević Ž, Knapp DG, Kovács GM, Magistà D, Perrone G, Rämä T, Rebriev YA, Shivas RG, Singh SM, Souza-Motta CM, Thangavel R, Adhapure NN, Alexandrova AV, Alfenas AC, Alfenas RF, Alvarado P, Alves AL, Andrade DA, Andrade JP, Barbosa RN, Barili A, Barnes CW, Baseia IG, Bellanger J-M, Berlanas C, Bessette AE, Bessette AR, Biketova AYu, Bomfim FS, Brandrud TE, Bransgrove K, Brito ACQ, Cano-Lira JF, Cantillo T, Cavalcanti AD, Cheewangkoon R, Chikowski RS, Conforto C, Cordeiro TRL, Craine JD, Cruz R, Damm U, de Oliveira RJV, de Souza JT, de Souza HG, Dearnaley JDW, Dimitrov RA, Dovana F, Erhard A, Esteve-Raventós F, Félix CR, Ferisin G, Fernandes RA, Ferreira RJ, Ferro LO, Figueiredo CN, Frank JL, Freire KTLS, García D, Gené J, Gęsiorska A, Gibertoni TB, Gondra RAG, Gouliamova DE, Gramaje D, Guard F, Gusmão LFP, Haitook S, Hirooka Y, Houbraken J, Hubka V, Inamdar A, Iturriaga T, Iturrieta-González I, Jadan M, Jiang N, Justo A, Kachalkin AV, Kapitonov VI, Karadelev M, Karakehian J, Kasuya T, Kautmanová I, Kruse J, Kušan I,

Kuznetsova TA, Landell MF, Larsson K-H, Lee HB, Lima DX, Lira CRS, Machado AR, Madrid H, Magalhães OMC, Majerova H, Malysheva EF, Mapperson RR, Marbach PAS, Martín MP, Martín-Sanz A, Matočec N, McTaggart AR, Mello JF, Melo RFR, Mešič A, Michereff SJ, Miller AN, Minoshima A, Molinero-Ruiz L, Morozova OV, Mosoh D, Nabe M, Naik R, Nara K, Nascimento SS, Neves RP, Olariaga I, Oliveira RL, Oliveira TGL, Ono T, Ordoñez ME, de M Ottoni A, Paiva LM, Pancorbo F, Pant B, Pawłowska J, Peterson SW, Raudabaugh DB, Rodríguez-Andrade E, Rubio E, Rusevska K, Santiago ALCMA, Santos ACS, Santos C, Sazanova NA, Shah S, Sharma J, Silva BDB, Siquier JL, Sonawane MS, Stchigel AM, Svetasheva T, Tamakeaw N, Telleria MT, Tiago PV, Tian CM, Tkalčec Z, Tomashevskaya MA, Truong HH, Vecherskii MV, Visagie CM, Vizzini A, Yilmaz N, Zmitrovich IV, Zvyagina EA, Boekhout T, Kehlet T, Læssøe T, Groenewald JZ (2019) Fungal Planet description sheets: 868–950. Persoonia: Molecular Phylogeny and Evolution of Fungi 42:291–473. https://doi.org/10.3767/persoonia.2019.42.11

Cunningham CW (1997) Can three incongruence tests predict when data should be combined? Molecular Biology and Evolution 14(7):733–740. https://doi.org/10.1093/oxfordjournals.molbev.a025813

Dress AW, Huson DH (2004) Constructing splits graphs. IEEE/ACM transactions on Computational Biology and Bioinformatics 1(3):109–115. https://doi.org/10.1109/TCBB.2004.27

El-Gholl NE, Uchida JY, Alfenas AC, Schubert TS, Alfieri SA (1992) Induction and description of perithecia of *Calonectria spathiphylli* sp. nov. Mycotaxon 45:285-300.

Farris JS, Kallersjo M, Kluge AG, Bult C, (1995) Testing significance of incongruence. Cladistics 10:315–319. https://doi.org/10.1111/j.1096-0031.1994.tb00181.x

Graça RN, Alfenas AC, Maffia LA, Titon M, Alfenas RF, Lau D, Rocabado JMA (2009) Factors influencing infection of eucalypts by *Cylindrocladium pteridis*. Plant Pathology 58(5):971–981.
https://doi.org/10.1111/j.1365-3059.2009.02094.x

Guerber JC, Correll JC (2001) Characterization of *Glomerella acutata*, the teleomorph of *Colletotrichum acutatum*. Mycologia 93(1):216–229. https://doi.org/10.1080/00275514.2001.12063151

Hepperle D (2004) SeqAssem©. Win32–Version. A sequence analysis tool contig assembler and trace data visualization tool for molecular sequences. Win32-Version. Distributed by the author via: http://www.sequentix.de

Hoang DT, Chernomor O, Von Haeseler A, Minh BQ, Vinh LS (2018) UFBoot2: improving the ultrafast bootstrap approximation. Molecular biology and evolution 35(2):518–522. https://doi.org/10.1093/molbev/msx281

Huson DH, Bryant D (2006) Application of phylogenetic networks in evolutionary studies. Molecular biology and evolution 23(2):254–267. https://doi.org/10.1093/molbev/msj030

IBÁ (2021) IBÁ–Indústria Brasileira de Árvores. Relatório 2020. https://iba.org/datafiles/publicacoes/relatorios/relatorio-iba-2020.pdf

IEA. IEA–Instituto de Economia Agrícola. Available at: https://www.noticiasagricolas.com.br/cotacoes/silvicultura/preco-eucalipto. Accessed 20 November 2020

Kang JC, Crous PW, Schoch CL (2001) Species concepts in the *Cylindrocladium floridanum* and *Cy. spathiphylli* complexes (Hypocreaceae) based on multi-allelic sequence data, sexual

compatibility and morphology. Systematic and Applied Microbiology 24(2):206–217. https://doi.org/10.1078/0723-2020-00026
Katoh K, Rozewicki J, Yamada KD (2019) MAFFT online service: multiple sequence alignment, interactive sequence choice and visualization. Briefings in bioinformatics 20(4):1160–1166. https://doi.org/10.1093/bib/bbx108
Kumar S, Stecher G, Tamura K (2016) MEGA7: molecular evolutionary genetics analysis version 7.0 for bigger datasets. Molecular Biology and Evolution 33(7):1870–1874. https://doi.org/10.1093/molbev/msw054
Lee SB, Taylor JW (1990) Isolation of DNA from fungal mycelia and single spores. In: Innis MA, Gelfand DV, Sninsky JJ, White TJ (Eds) PCR protocols: a guide to methods and applications. Academic Press, New York, 282–287. http://dx.doi.org/10.1016/b978-0-12-372180-8.50038-x
Li JQ, Barnes I, Liu FF, Wingfield MJ, Chen SF (2021) Global genetic diversity and mating type distribution of *Calonectria pauciramosa*: an important wide host-range plant pathogen. Plant Disease PDIS-05. https://doi.org/10.1094/PDIS-05-20-1050-RE
Li JQ, Wingfield BD, Wingfield MJ, Barnes I, Fourie A, Crous PW, Chen SF (2020) Mating genes in *Calonectria* and evidence for a heterothallic ancestral state. Persoonia: Molecular Phylogeny and Evolution of Fungi 45(1):163–176. https://doi.org/10.3767/persoonia.2020.45.06
Liu Q, Chen S (2017) Two novel species of *Calonectria* isolated from soil in a natural forest in China. MycoKeys 26:25–60. https://doi.org/10.3897/mycokeys.26.14688
Liu YJ, Whelen S, Hall BD (1999) Phylogenetic relationships among ascomycetes: evidence from an RNA polymerse II subunit. Molecular Biology and Evolution 16(12):1799–1808. https://doi.org/10.1093/oxfordjournals.molbev.a026092
Liu L, Wu W, Chen S (2021) Species diversity and distribution characteristics of *Calonectria* in five soil layers in a eucalyptus plantation. Journal of Fungi 7(10):857. https://doi.org/10.3390/jof7100857
Liu QL, Li JQ, Wingfield MJ, Duong TA, Wingfield BD, Crous PW, Chen SF (2020) Reconsideration of species boundaries and proposed DNA barcodes for *Calonectria*. Studies in Mycology 97:100106. https://doi.org/10.1016/j.simyco.2020.08.001
Lombard L, Crous PW, Wingfield BD, Wingfield MJ (2010a) Multigene phylogeny and mating tests reveal three cryptic species related to *Calonectria pauciramosa*. Studies in Mycology 66:15–30. https://doi.org/10.3114/sim.2010.66.02
Lombard L, Crous PW, Wingfield BD, Wingfield MJ (2010b). Phylogeny and systematics of the genus *Calonectria*. Studies in Mycology 66:31–69. https://doi.org/10.3114/sim.2010.66.03
Lombard L, Crous PW, Wingfield BD, Wingfield MJ (2010c) Species concepts in *Calonectria* (*Cylindrocladium*). Studies in Mycology 66:1–13. https://doi.org/10.3114/sim.2010.66.01
Lombard L, Wingfield MJ, Alfenas AC, Crous PW (2016) The forgotten *Calonectria* collection: pouring old wine into new bags. Studies in Mycology 85:159–198. https://doi.org/10.1016/j.simyco.2016.11.004
Miranda IDS, Auer CG, dos Santos ÁF, Ferreira MA, Tambarussi EV, da Silva RAF, Rezende EH (2021) Occurrence of *Calonectria* leaf blight in *Eucalyptus benthamii* progenies and potential for disease resistance. Tropical Plant Pathology 46(3):254–264. https://doi.org/10.1007/s40858-021-00426-4

Mohali SR, Stewart JE (2021) *Calonectria vigiensis* sp. nov. (Hypocreales, Nectriaceae) associated with dieback and sudden-death symptoms of *Theobroma cacao* from Mérida state, Venezuela. Botany 99(11):683–693. https://doi.org/10.1139/cjb-2021-0050

Nguyen LT, Schmidt HA, Von Haeseler A, Minh BQ (2015) IQ-TREE: a fast and effective stochastic algorithm for estimating maximum-likelihood phylogenies. Molecular Biology and Evolution 32(1):268–274. https://doi.org/10.1093/molbev/msu300

Nylander JAA (2004) MrModeltest v2. Program distributed by the author. Evolutionary Biology Centre, Uppsala University.

O'Donnell K, Cigelnik E (1997) Two divergent intragenomic rDNA ITS2 types within a monophyletic lineage of the fungus *Fusarium* are nonorthologous. Molecular phylogenetics and evolution 7(1):103–116. https://doi.org/10.1006/mpev.1996.0376

O'Donnell K, Kistler HC, Cigelnik E, Ploetz RC (1998) Multiple evolutionary origins of the fungus causing Panama disease of banana: concordant evidence from nuclear and mitochondrial gene genealogies. Proceedings of the National Academy of Sciences 95(5):2044–2049. https://doi.org/10.1073/pnas.95.5.2044

Pham, NQ, Marincowitz S, Chen S, Yaparudin Y, Wingfield MJ (2022) *Calonectria* species, including four novel taxa, associated with *Eucalyptus* in Malaysia. Mycological Progress 21(1):181-197. https://doi.org/10.1007/s11557-021-01768-8Pham NQ, Barnes I, Chen S, Liu F, Dang QN, Pham TQ, Lombard L, Crous PW, Wingfield MJ (2019) Ten new species of *Calonectria* from Indonesia and Vietnam. Mycologia 111(1):78–102. https://doi.org/10.1080/00275514.2018.1522179

Pires BM (2000) Efeito da desrama artificial no crescimento e qualidade da madeira de *Eucalyptus grandis* para serraria. MSc Dissertation, Universidade Federal de Viçosa, Viçosa, Brasil. https://locus.ufv.br//handle/123456789/11170

Poltronieri LS, Alfenas RF, Verzignassi JR, Alfenas AC, Benchimol RL, Poltronieri, TPDS (2011) Leaf blight and defoliation of *Eugenia* spp. caused by *Cylindrocladium candelabrum* and *C. spathiphylli* in Brazil. Summa Phytopathologica 37:147–149. https://doi.org/10.1590/S0100-54052011000200011

Posada D, Crandall KA (1998) Modeltest: testing the model of DNA substitution. Bioinformatics 14(9):817–818. https://doi.org/10.1093/bioinformatics/14.9.817

Pulrolnik K, Reis GGD, Reis MDGF, Monte MA, Fontan IDCI (2005) Crescimento de plantas de clones de *Eucalyptus grandis* [Hill ex Maiden] submetidas a diferentes tratamentos de desrama artificial, na região do cerrado. Revista Árvore 29(4):495–505. https://doi.org/10.1590/S0100-67622005000400001

Quaedvlieg W, Kema GHJ, Groenewald JZ, Verkley GJM, Seifbarghi S, Razavi M, Gohari AM, Mehrabi R, Crous PW (2011) *Zymoseptoria* gen. nov.: a new genus to accommodate *Septoria*-like species occurring on graminicolous hosts. Persoonia: Molecular Phylogeny and Evolution of Fungi 26:57–69. https://doi.org/10.3767/003158511X571841

Rambaut, A (2009) FigTree, a graphical viewer of phylogenetic trees. http://tree.bio.ed.ac.uk/software/figtree/

Rambaut A, Drummond AJ (2007) Tracer v1.5. http://tree.bio.ed.ac.uk/software/tracer/

Reeb V, Lutzoni F, Roux C (2004) Contribution of RPB2 to multilocus phylogenetic studies of the euascomycetes (Pezizomycotina, Fungi) with special emphasis on the lichen-forming Acarosporaceae and evolution of polyspory. Molecular phylogenetics and evolution 32(3):1036–1060. https://doi.org/10.1016/j.ympev.2004.04.012

Reis A, Mafia RG, Silva PP, Lopes CA, Alfenas AC (2004) *Cylindrocladium spathiphylli*, causal agent of *Spathiphyllum* root and collar rot in the Federal District-Brazil. Fitopatologia Brasileira 29(1):102–102. https://doi.org/10.1590/S0100-41582004000100017

Ronquist F, Huelsenbeck J, Teslenko M, Nylander JAA (2019) MrBayes version 3.2 manual: tutorials and model summaries. https://nbisweden.github.io/MrBayes/manual.html.

Ronquist F, Teslenko M, Van Der Mark P, Ayres DL, Darling A, Höhna S, Larget B, Liu L, Suchard MA, Huelsenbeck JP (2012) MrBayes 3.2: efficient Bayesian phylogenetic inference and model choice across a large model space. Systematic biology 61(3):539–542. https://doi.org/10.1093/sysbio/sys029

Schoch CL, Crous PW, Wingfield BD, Wingfield MJ (1999) The *Cylindrocladium candelabrum* species complex includes four distinct mating populations. Mycologia 91(2):286–298. https://doi.org/10.1080/00275514.1999.12061019

Soares TP, Pozza EA, Pozza AA, Mafia RG, Ferreira MA (2018) Calcium and potassium imbalance favours leaf blight and defoliation caused by *Calonectria pteridis* in *Eucalyptus* plants. Forests 9(12):782. https://doi.org/10.3390/f9120782

Sullivan J (1996) Combining data with different distributions of among-site rate variation. Systematic Biology 45(3):375–380. https://doi.org/10.2307/2413571

Swofford DL (2003) PAUP*. Phylogenetic analysis using parsimony (*and other methods). V. 4.0b10. Sinauer Associates, Sunderland, Massachusetts, USA.

Taylor JW, Jacobson DJ, Kroken S, Kasuga T, Geiser DM, Hibbett DS, Fisher MC (2000) Phylogenetic species recognition and species concepts in fungi. Fungal genetics and biology 31(1):21–32. https://doi.org/10.1006/fgbi.2000.1228

Trifinopoulos J, Nguyen LT, von Haeseler A, Minh BQ (2016) W-IQ-TREE: a fast online phylogenetic tool for maximum likelihood analysis. Nucleic acids research 44(W1):W232–W235. https://doi.org/10.1093/nar/gkw256

Vitale A, Crous PW, Lombard L, Polizzi G (2013) *Calonectria* diseases on ornamental plants in Europe and the Mediterranean basin: an overview. Journal of Plant Pathology 95(3):463–476. http://dx.doi.org/10.4454/JPP.V95I3.007

Wang QC, Liu QL, Chen SF (2019) Novel species of *Calonectria* isolated from soil near *Eucalyptus* plantations in southern China. Mycologia 111(6):1028–1040. https://doi.org/10.1080/00275514.2019.1666597

Wingfield MJ, Brockerhoff EG, Wingfield BD, Slippers B (2015) Planted forest health: the need for a global strategy. Science 349: 832–836. https://doi.org/10.1126/science.aac6674

Supplementary material

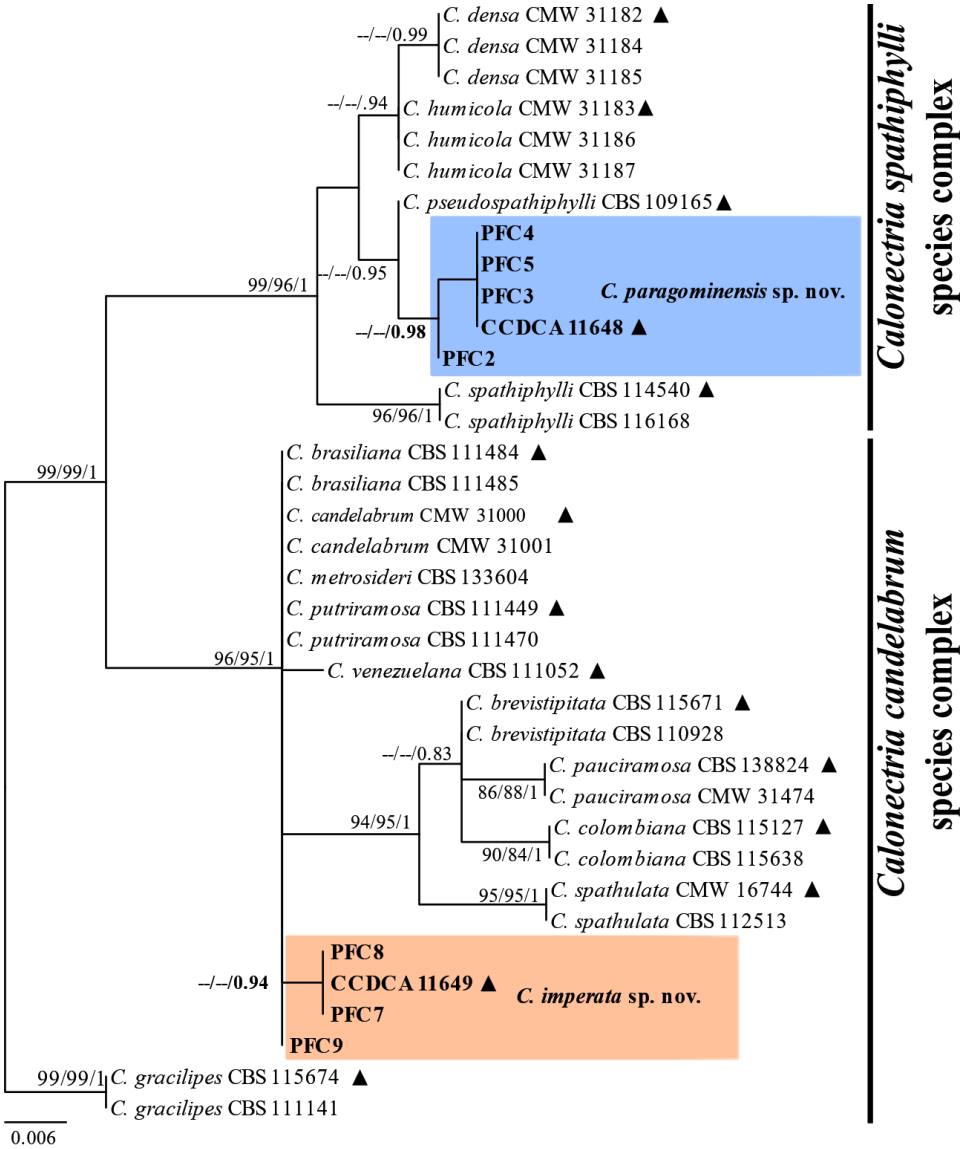

Figure 1S. Phylogenetic tree based on maximum likelihood analysis of *act* gene region. Bootstrap support values ≥ 80% for maximum parsimony (MP), Ultrafast bootstrap support values ≥ 95% for maximum likelihood (ML), and posterior probability (PP) values ≥ 0.95 from BI analyses are presented at the nodes (MP/ML/PP). Bootstrap values below 80% (MP), 95% (ML) and posterior probabilities below 0.80 are marked with "-". Ex-type isolates are indicated by "▲", isolates highlighted in bold were sequenced in this study, and novel species are in blue and orange. *C. gracilipes* was used as outgroup. The scale bar indicates the number of nucleotide substitutions per site.

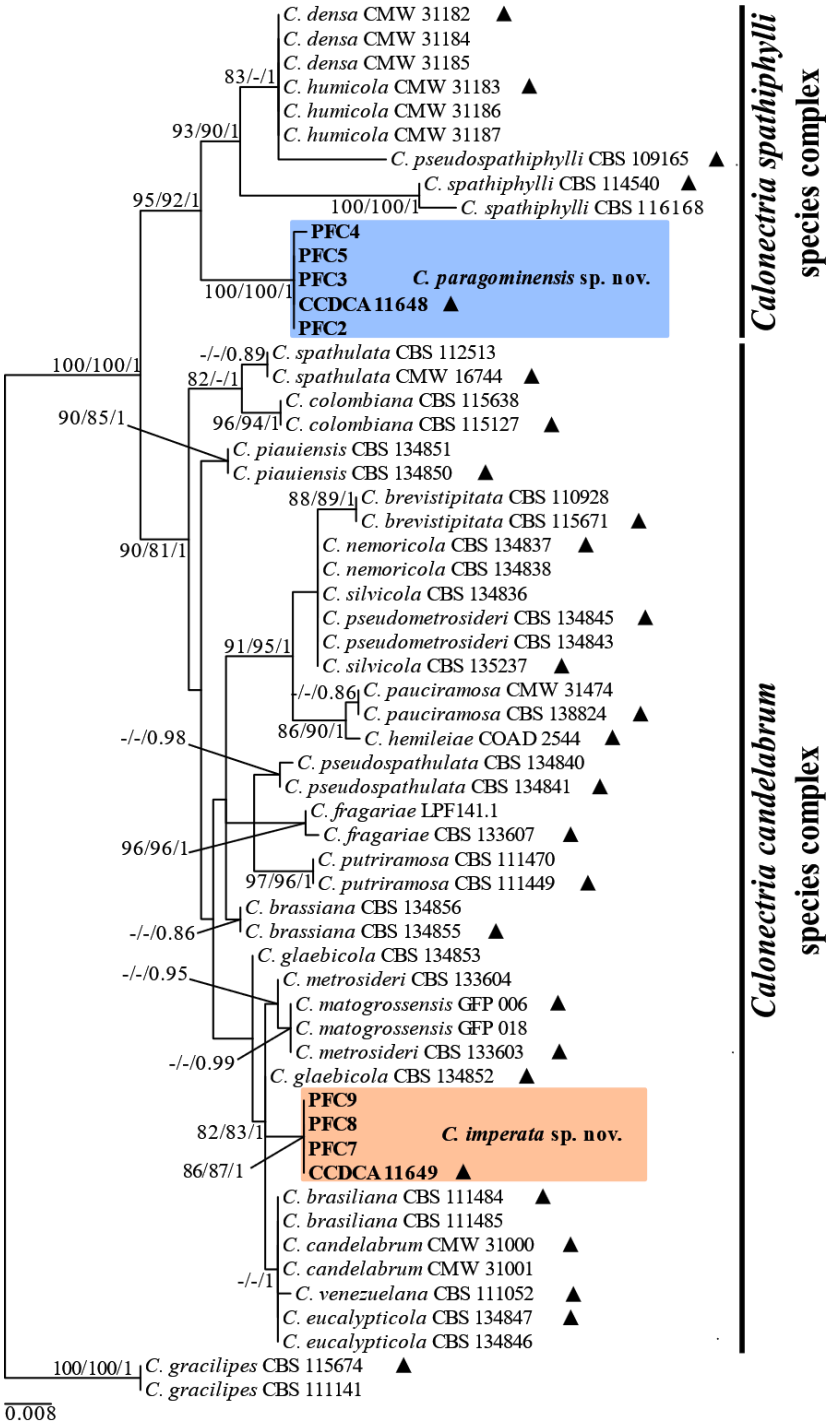

Figure 2S. Phylogenetic tree based on maximum likelihood analysis of *cmdA* gene region. Bootstrap support values ≥ 80% for maximum parsimony (MP), Ultrafast bootstrap support values ≥ 95% for maximum likelihood (ML), and posterior probability (PP) values ≥ 0.95 from BI analyses are presented at the nodes (MP/ML/PP). Bootstrap values below 80% (MP), 95% (ML) and posterior probabilities below 0.80 are marked with "-". Ex-type isolates are indicated by "▲", isolates highlighted in bold were sequenced in this study, and novel species are in blue and orange. *C. gracilipes* was used as outgroup. The scale bar indicates the number of nucleotide substitutions per site.

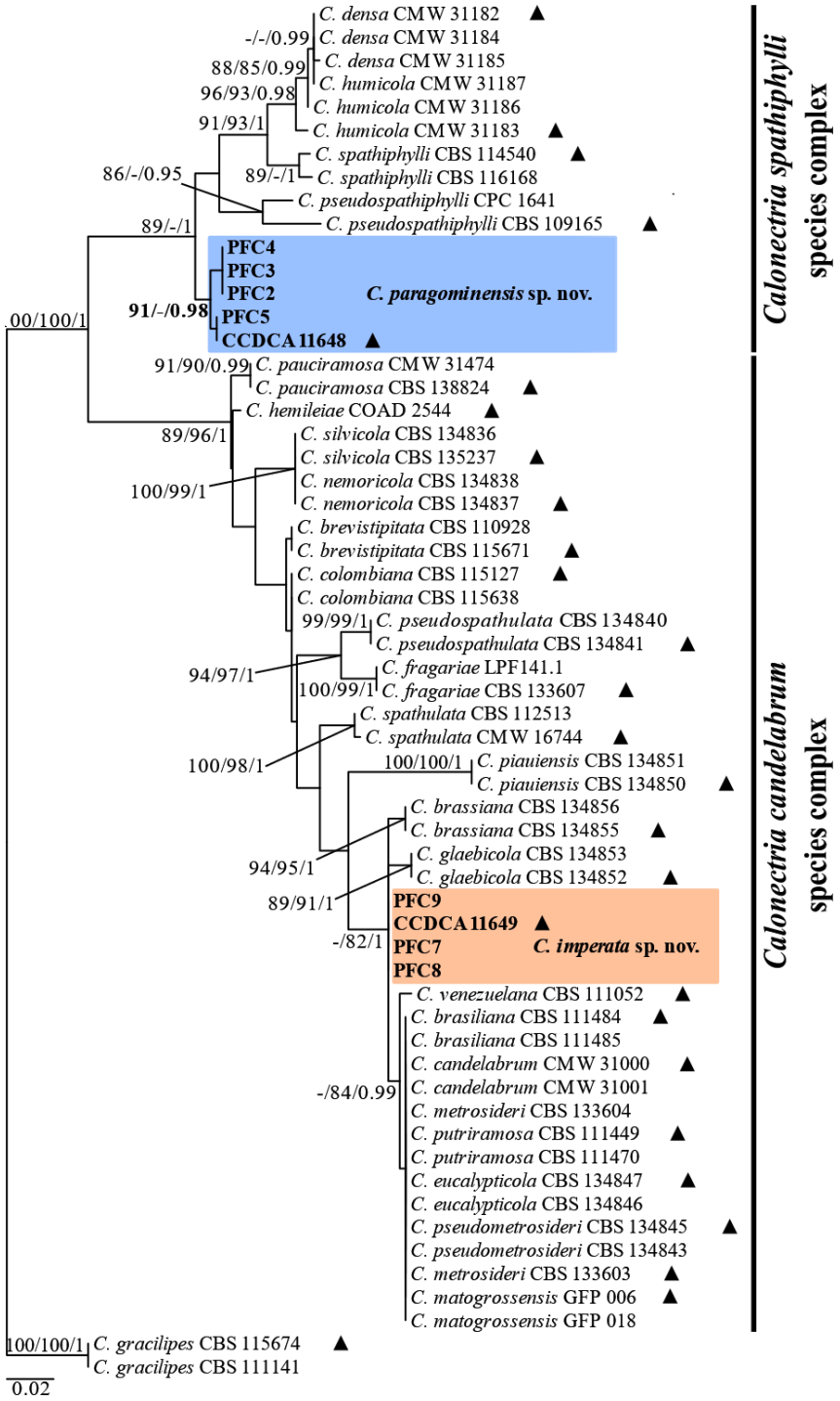

Figure 3S. Phylogenetic tree based on maximum likelihood analysis of *his3* gene region. Bootstrap support values ≥ 80% for maximum parsimony (MP), Ultrafast bootstrap support values ≥ 95% for maximum likelihood (ML), and posterior probability (PP) values ≥ 0.95 from BI analyses are presented at the nodes (MP/ML/PP). Bootstrap values below 80% (MP), 95% (ML) and posterior probabilities below 0.80 are marked with "-". Ex-type isolates are indicated by "▲", isolates highlighted in bold were sequenced in this study, and novel species are in blue and orange. *C. gracilipes* was used as outgroup. The scale bar indicates the number of nucleotide substitutions per site.

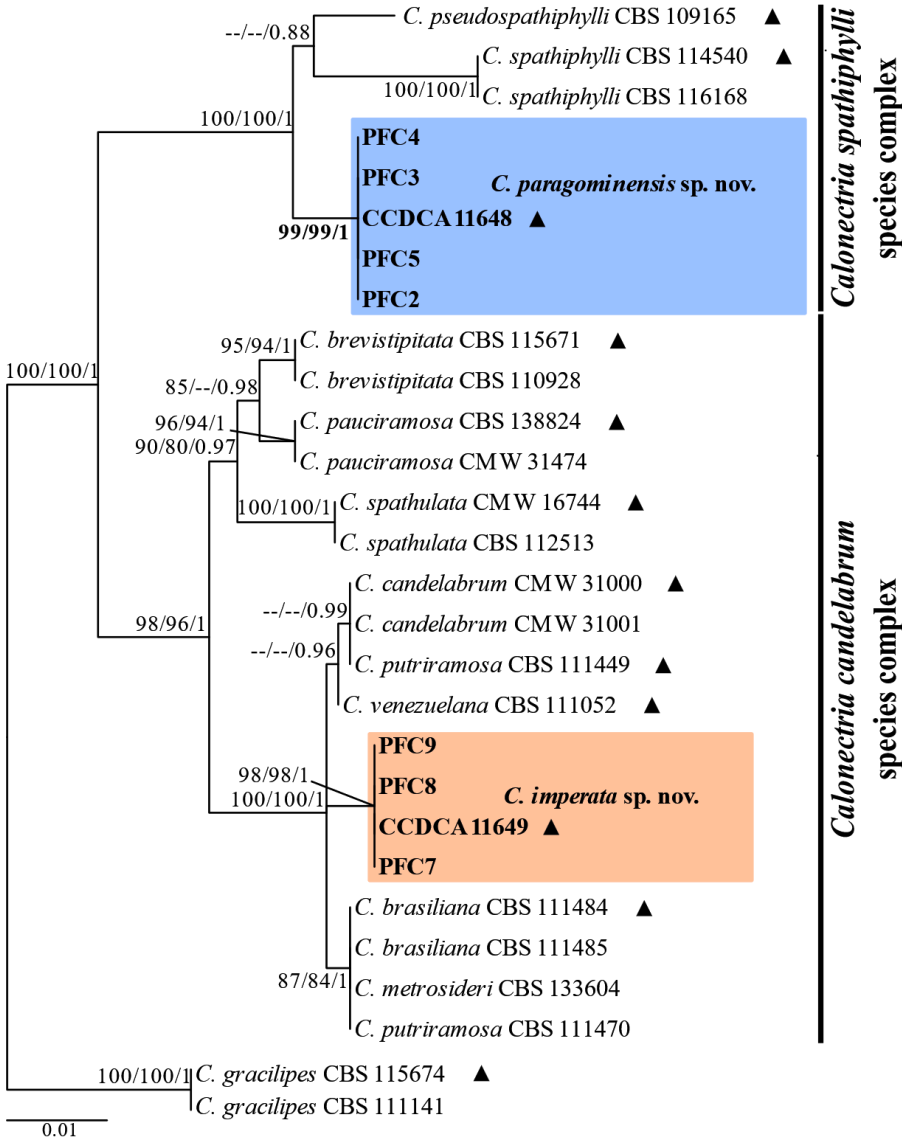

Figure 4S. Phylogenetic tree based on maximum likelihood analysis of *rpb2* gene region. Bootstrap support values ≥ 80% for maximum parsimony (MP), Ultrafast bootstrap support values ≥ 95% for maximum likelihood (ML), and posterior probability (PP) values ≥ 0.95 from BI analyses are presented at the nodes (MP/ML/PP). Bootstrap values below 80% (MP), 95% (ML) and posterior probabilities below 0.80 are marked with "-". Ex-type isolates are indicated by "▲", isolates highlighted in bold were sequenced in this study, and novel species are in blue and orange. *C. gracilipes* was used as outgroup. The scale bar indicates the number of nucleotide substitutions per site.

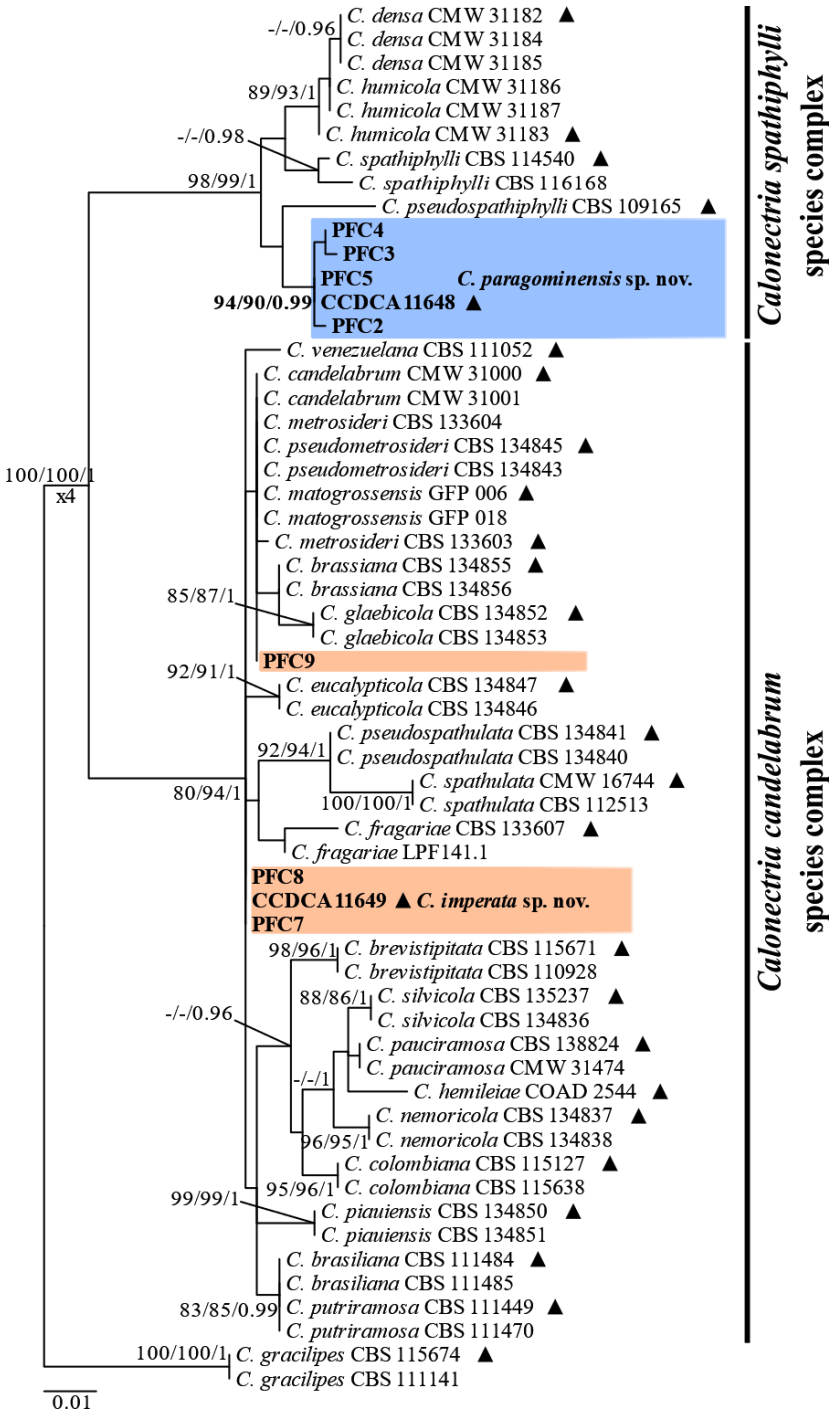

Figure 5S. Phylogenetic tree based on maximum likelihood analysis of *tef1* gene region. Bootstrap support values ≥ 80% for maximum parsimony (MP), Ultrafast bootstrap support values ≥ 95% for maximum likelihood (ML), and posterior probability (PP) values ≥ 0.95 from BI analyses are presented at the nodes (MP/ML/PP). Bootstrap values below 80% (MP), 95% (ML) and posterior probabilities below 0.80 are marked with "-". Ex-type isolates are indicated by "▲", isolates highlighted in bold were sequenced in this study, and novel species are in blue and orange. *C. gracilipes* was used as outgroup. The scale bar indicates the number of nucleotide substitutions per site.

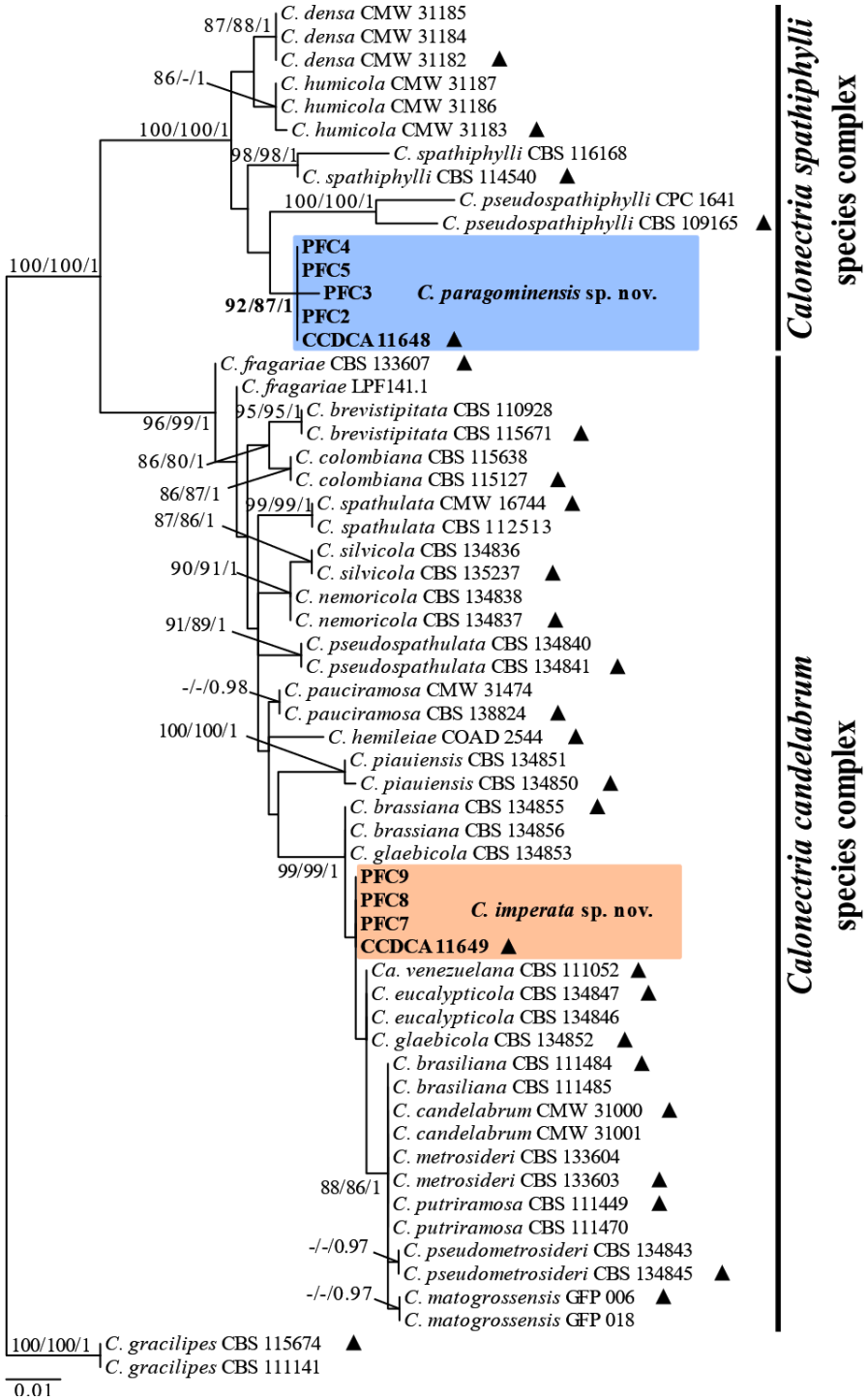

Figure 6S. Phylogenetic tree based on maximum likelihood analysis of *tub2* gene region. Bootstrap support values ≥ 80% for maximum parsimony (MP), Ultrafast bootstrap support values ≥ 95% for maximum likelihood (ML), and posterior probability (PP) values ≥ 0.95 from BI analyses are presented at the nodes (MP/ML/PP). Bootstrap values below 80% (MP), 95% (ML) and posterior probabilities below 0.80 are marked with "-". Ex-type isolates are indicated by "▲", isolates highlighted in bold were sequenced in this study, and novel species are in blue and orange. *C. gracilipes* was used as outgroup. The scale bar indicates the number of nucleotide substitutions per site.

Table 1. *Calonectria* species and GenBank accession numbers of DNA sequences used in this study.

Species complex	Species	Isolate representing the species[‡,§]	Other isolate numbers	Host/ Substrate	Country	Genbank accession numbers					
						act[|]	***cmdA***	***his3***	***rpb2***	***tef1***	***tub2***
Calonectria spathiphylli species complex	*C. densa*	**CMW 31182**		Soil	Ecuador	GQ280525	GQ267444	GQ267281	N/A	GQ267352	GQ267232
		CMW 31184		Soil	Ecuador	GQ280523	GQ267442	GQ267279	N/A	GQ267350	GQ267230
		CMW 31185		Soil	Ecuador	GQ280524	GQ267443	GQ267280	N/A	GQ267351	GQ267231
	C. humicola	**CMW 31183**		Soil	Ecuador	GQ280526	GQ267445	GQ267282	N/A	GQ267353	GQ267233
		CMW 31186		Soil	Ecuador	GQ280527	GQ267446	GQ267283	N/A	GQ267354	GQ267234
		CMW 31187		Soil	Ecuador	GQ280528	GQ267447	GQ267284	N/A	GQ267355	GQ267235
	***C. paragominensis* sp. nov.**[†]	**CCDCA 11648**		*E. grandis* × *E. brassiana*	Brazil	**ON009346**	**OM974325**	**OM974334**	**OM974343**	**OM974352**	**OM974361**
		PFC2		*E. grandis* × *E. brassiana*	Brazil	**ON009347**	**OM974326**	**OM974335**	**OM974344**	**OM974353**	**OM974362**
		PFC3		*E. grandis* × *E. brassiana*	Brazil	**ON009348**	**OM974327**	**OM974336**	**OM974345**	**OM974354**	**OM974363**
		PFC4		*E. grandis* × *E. brassiana*	Brazil	**ON009349**	**OM974328**	**OM974337**	**OM974346**	**OM974355**	**OM974364**
		PFC5		*E. grandis* × *E. brassiana*	Brazil	**ON009350**	**OM974329**	**OM974338**	**OM974347**	**OM974356**	**OM974365**
	C. pseudospathiphylli	**CBS 109165**	CPC 1623	Soil	Ecuador	GQ280493	GQ267412	AF348241	KY653435	FJ918562	AF348225
		CPC 1641		Soil	Ecuador	N/A	N/A	AF348233	N/A	N/A	AF348217
	C. spathiphylli	**CBS 114540**	ATCC44730, CSF11330	*Spathiphyllum* sp.	USA	GQ280505	GQ267424	AF348230	MT412666	GQ267330	AF348214
		CBS 116168	CSF 11401	*Spathiphyllum* sp.	Switzerland	GQ280506	GQ267425	FJ918530	MT412667	FJ918561	FJ918512
Calonectria candelabrum species complex	*C. brasiliana*	**CBS 111484**	CSF 11249	Soil	Brazil	MT334968	MT335198	MT335438	MT412502	MT412729	MT412951
		CBS 111485	CSF 11250	Soil	Brazil	MT334969	MT335199	MT335439	MT412503	MT412730	MT412952
	C. brassiana	**CBS 134855**		Soil	Brazil	N/A	KM396056	KM396139	N/A	KM395882	KM395969
		CBS 134856		Soil	Brazil	N/A	KM396057	KM396140	N/A	KM395883	KM395970
	C. brevistipitata	**CBS 115671**	CSF 11288	Soil	Mexico	MT334973	MT335203	MT335443	MT412507	MT412734	MT412956
		CBS 110928	CSF 11235	Soil	Mexico	MT334974	MT335204	MT335444	MT412508	MT412735	MT412957
	C. candelabrum	CMW 31000	CSF 11404	*Eucalyptus* sp.	Brazil	MT334977	MT335207	MT335447	MT412511	MT412738	MT412959
		CMW 31001	CSF 11405	*Eucalyptus* sp.	Brazil	MT334978	MT335208	MT335448	MT412512	MT412739	MT412960
	C. colombiana	**CBS 115127**		Soil	Colombia	GQ280538	GQ267455	FJ972442	N/A	FJ972492	FJ972423
		CBS 115638		Soil	Colombia	GQ280539	GQ267456	FJ972441	N/A	FJ972491	FJ972422
	C. eucalypticola	**CBS 134847**		*Eucalyptus* sp.	Brazil	N/A	KM396051	KM396134	N/A	KM395877	KM395964
		CBS 134846		*Eucalyptus* sp.	Brazil	N/A	KM396050	KM396133	N/A	KM395876	KM395963
	C. fragariae	**CBS 133607**		*Fragaria* × *ananassa*	Brazil	N/A	KM998966	KM998964	N/A	KM998963	KM998965
		LPF141.1		*Fragaria* × *ananassa*	Brazil	N/A	KX500191	KX500194	N/A	KX500197	KX500195
	C. glaebicola	**CBS 134852**		Soil	Brazil	N/A	KM396053	KM396136	N/A	KM395879	KM395966
		CBS 134853		*Eucalyptus* sp.	Brazil	N/A	KM396054	KM396137	N/A	KM395880	KM395967
	C. hemileiae	**COAD 2544**		*Hemileia vastatrix*	Brazil	N/A	MK037392	MK006026	N/A	MK006027	MK037391
	C. imperata sp. nov.[†]	**CCDCA 11649**		*E. urophylla*	Brazil	**ON009351**	**OM974330**	**OM974339**	**OM974348**	**OM974357**	**OM974366**
		PFC7		*E. urophylla*	Brazil	**ON009352**	**OM974331**	**OM974340**	**OM974349**	**OM974358**	**OM974367**
		PFC8		*E. urophylla*	Brazil	**ON009353**	**OM974332**	**OM974341**	**OM974350**	**OM974359**	**OM974368**
		PFC9		*E. urophylla*	Brazil	**ON009354**	**OM974333**	**OM974342**	**OM974351**	**OM974360**	**OM974369**
	C. matogrossensis	**GFP 006**		*E. urophylla*	Brazil	N/A	MH837653	MH837648	N/A	MH837659	MH837664
		GFP 018		*E. urophylla*	Brazil	N/A	MH837657	MH837652	N/A	MH837663	MH837668
	C. metrosideri	**CBS 133603**		*Metrosideros polymorpha*	Brazil	N/A	KC294304	KC294307	N/A	KC294310	KC294313
		CBS 133604	CSF 11309	*Metrosideros polymorpha*	Brazil	MT335056	MT335288	MT335528	MT412585	MT412819	MT413033
	C. nemoricola	**CBS 134837**		Soil	Brazil	N/A	KM396066	KM396149	N/A	KM395892	KM395979
		CBS 134838		Soil	Brazil	N/A	KM396067	KM396150	N/A	KM395893	KM395980
	C. pauciramosa	**CBS 138824**	CSF 16461	Soil	South Africa	MT335093	MT335325	MT335565	MT412618	MT412856	MT413068
		CMW 31474	CSF 11422	*E. urophylla* × *E. grandis*	China	MT335104	MT335336	MT335576	MT412629	MT412867	MT413079
	C. piauiensis	**CBS 134850**		Soil	Brazil	N/A	KM396060	KM396143	N/A	KM395886	KM395973
		CBS 134851		Soil	Brazil	N/A	KM396061	KM396144	N/A	KM395887	KM395974
	C. pseudometrosideri	**CBS 134845**		Soil	Brazil	N/A	KM395995	KM396083	N/A	KM395821	KM395909
		CBS 134843		*Metrosideros polymorpha*	Brazil	N/A	KM395993	KM396081	N/A	KM395819	KM395907
	C. pseudospathulata	**CBS 134841**		Soil	Brazil	N/A	KM396070	KM396153	N/A	KM395896	KM395983
		CBS 134840		Soil	Brazil	N/A	KM396069	KM396152	N/A	KM395895	KM395982
	C. putriramosa	**CBS 111449**	CSF 11246	*Eucalyptus* cutting	Brazil	MT335129	MT335364	MT335604	MT412657	MT412895	MT413105
		CBS 111470	CSF 11247	Soil	Brazil	MT335130	MT335365	MT335605	MT412658	MT412896	MT413106
	C. silvicola	**CBS 135237**	LPF081	Soil	Brazil	N/A	KM396065	KM396148	N/A	KM395891	KM395978
		CBS 134836		Soil	Brazil	N/A	KM396062	KM396145	N/A	KM395888	KM395975
	C. spathulata	**CMW 16744**	CSF 11331	*E. viminalis*	Brazil	MT335139	MT335376	MT335616	MT412668	MT412907	MT413117
		CBS 112513	CSF 11259	*Eucalyptus* sp.	Colombia	MT335140	MT335377	MT335617	MT412669	MT412908	MT413118
	C. venezuelana	**CBS 111052**	CSF 11238	Soil	Venezuela	MT335155	MT335394	MT335634	MT412685	MT412925	MT413132
Calonectria gracilipes species complex	*C. gracilipes*	**CBS 115674**	CSF 11289	Soil	Colombia	MT335022	MT335252	MT335492	MT412554	MT412783	MT413001
		CBS 111141	CSF11239	Soil	Colombia	MT335023	MT335253	MT335493	MT412555	MT412784	MT413002

† New *Calonectria* species reported in the present study.

‡ Ex-type isolates of the *Calonectria* species are marked in bold.

§ ATCC: American Type Culture Collection, Virginia, USA; CBS: Westerdijk Fungal Biodiversity Institute, Utrecht, The Netherlands; CCDCA: Coleção de Culturas de Microrganismos do Departamento de Ciência dos Alimentos/UFLA, Lavras, Brazil; CMW: Culture collection of the Forestry and Agricultural Biotechnology Institute (FABI), University of Pretoria, Pretoria, South Africa; COAD: Coleção Octávio de Almeida Drumond, Universidade Federal de Viçosa, Viçosa, Brazil; CPC: Pedro Crous working collection housed at Westerdijk Fungal Biodiversity Institute; CSF: Culture Collection located at China Eucalypt Research Centre (CERC), Chinese Academy of Forestry, ZhanJiang, GuangDong Province, China; GFP: Universidade Federal de Brasilia, Brasilia, Brazil; LPF: Laboratorio de Patologia Florestal, Universidade Federal de Viçosa, Viçosa, Brazil; PFC: Laboratorio de Patologia Florestal, Universidade Federal de Lavras, Lavras, Brazil.

| *act*: actin; *cmdA*: calmodulin; *his3*: histone H3; *rpb2*: the second largest subunit of RNA polymerase; *tef1*: translation elongation factor 1-alpha; *tub2*: β-tubulin. GenBank accession number obtained in this study are marked in bold.

Table 2. Single nucleotide polymorphisms unique to *C. paragominensis* in comparison with their phylogenetically closely related species in the six gene regions.

Species	act†										cmdA									
	188‡	189	190	191	192	193	194	195	196	197	142	144	170	185	217	270	437	444	455	483
C. paragominensis CCDCA 11648	a	g	a	a	a	a	a	g	a	a	t	a	c	c	t	c	a	a	g	a
C. densa CMW 31182	t	-	-	-	-	-	-	-	-	-	a	c	t	t	c	t	g	g	a	c
C. humicola CMW 31183	t	-	-	-	-	-	-	-	-	-	a	c	t	t	c	t	g	g	a	c
C. pseudospathiphylli CBS 109165	t	-	-	-	-	-	-	-	-	-	a	c	t	t	c	t	g	g	a	c
C. spathiphylli CBS 114540	t	-	-	-	-	-	-	-	-	-	a	c	t	t	c	t	g	g	a	c

Species	his3									rpb2						tef1					tub2
	6	43	47	52	53	54	247	259	274	81	141	315	474	630	735	32	123	208	434	459	15
C. paragominensis CCDCA 11648	c	t	t	-	-	-	a	g	a	t	c	t	t	a	g	c	t	g	g	c	a
C. densa CMW 31182	t	a	c	c	t	c	t	a	g							-	-	a	t	t	t
C. humicola CMW 31183	t	a	c	c	t	c	t	a	g							-	-	a	t	t	t
C. pseudospathiphylli CBS 109165	-	a	c	c	a	c	c	a	g	c	t	c	c	g	a	-	-	a	a	t	t
C. spathiphylli CBS 114540	-	a	c	c	c	c	c	a	g	c	t	c	c	g	a	-	-	a	t	t	t

† Only polymorphic nucleotides occurring in all the isolates are shown, not alleles that partially occur in individuals per phylogenetic group.

‡ Numerical positions of the nucleotides in the DNA sequence alignments.

Table 3. Single nucleotide polymorphisms found in *Calonectria imperata* and its phylogenetically closely related species in the six gene regions.

Species	***act***[†]	***cmdA***												***his3***						
	57[‡]	62	71	121	171	187	210	319	376	403	405	418	444	8	44	46	53	56	60	66
C. imperata CCDCA 11649	**c**	a	c	c	g	g	c	c	t	**t**	c	**t**	t	c	c	t	c	c	g	a
C. brassiana CBS 134855		c	g	t	g	g	c	c	c	c	c	a	t	t	c	t	c	c	g	a
C. glaebicola CBS 134852		a	c	c	g	g	c	g	t	c	c	a	t	c	t	c	c	c	g	a
C. piauiensis CBS 134850		a	g	c	c	a	c	c	c	c	c	a	c	c	c	-	a	c	a	c
C. venezuelana CBS 111052	t	a	c	c	g	g	a	g	t	c	t	a	t	c	c	t	c	t	g	a
Species	***his3***																			
	93	99	105	114	156	189	234	235	238	244	245	250	251	252	254	255	257	262	275	276
C. imperata CCDCA 11649	c	c	c	a	t	t	t	t	c	c	a	c	c	a	g	c	a	a	t	g
C. brassiana CBS 134855	c	c	c	t	t	t	t	t	c	c	a	c	c	a	g	c	a	a	t	g
C. glaebicola CBS 134852	c	c	c	a	t	t	t	t	c	a	a	c	c	a	g	c	a	a	t	g
C. piauiensis CBS 134850	t	t	c	a	c	t	c	g	t	g	g	t	a	g	a	t	g	g	c	a
C. venezuelana CBS 111052	c	c	a	a	t	c	t	t	c	c	a	c	c	a	g	c	a	a	t	g

Table 3. Continuation.

Species	*his3*							*rpb2*					*tef1*							
	277	278	333	336	351	405	420	105	603	624	693	840	47	81	110	112	135	220	239	357
C. imperata CCDCA 11649	c	t	t	c	g	c	t	**g**	**a**	**c**	**t**	**a**	c	g	a	t	t	c	c	c
C. brassiana CBS 134855	c	t	t	c	g	t	t	n	n	n	n	n	c	g	t	t	t	c	c	c
C. glaebicola CBS 134852	c	t	t	c	a	c	t	n	n	n	n	n	c	a	a	t	t	c	c	c
C. piauiensis CBS 134850	t	t	c	t	g	c	g	n	n	n	n	n	t	g	a	a	c	a	t	c
C. venezuelana CBS 111052	c	c	t	c	g	c	t	t	g	t	c	t	c	g	a	t	t	c	c	t
Species	***tef1a***					***tub2***														
	417	421	422	425	453	50	99	120	132	174	175	188	191	220	377	398	408	409		
C. imperata CCDCA 11649	c	c	c	a	a	c	a	g	t	c	c	g	c	t	t	t	-	-		
C. brassiana CBS 134855	c	t	t	a	a	c	a	g	t	c	c	g	c	t	t	t	a	c		
C. glaebicola CBS 134852	c	t	t	a	a	c	a	g	t	c	c	g	c	t	t	t	a	c		
C. piauiensis CBS 134850	t	c	c	a	a	g	g	a	c	t	t	a	a	c	c	g	a	c		
C. venezuelana CBS 111052	c	c	c	c	g	c	a	g	t	c	c	g	c	t	t	t	a	c		

† Only polymorphic nucleotides occurring in all the isolates are shown, not alleles that partially occur in individuals per phylogenetic group.

‡ Numerical positions of the nucleotides in the DNA sequence alignments.

Table 4. Morphological characteristics of two new *Calonectria* species and their phylogenetically closely related species.

Species complex	Species	Conidiogenus apparatus		Stipe		Macroconidia			Vesicle		Reference
		Size (L × W)†,‡,§	Branches	Size (L × W)†,‡,§	Extension (L × W)†,‡,§	Size (L × W)†,‡,§,|	Average (L × W)†,‡,§	Septa	Diameter†,§	Shape	
***Calonectria spathiphylli* species complex**	***C. paragominensis***	40–113 × 45–129	(–4)	112–281 × 2–4	123–295 × 1.5–3	(47–)56–66(–71) × (4–)4.8–5.9(–7)	61 × 5	1(–3)	8–12	globoid to sphaeropedunculate	This study
	C. densa	49–78 × 63–123	(–4)	54–90 × 6–10	149–192 × 5–6	(47–)50–58(–62) × (5–)6	54 × 6	1	10–12	ovoid to ellipsoid to sphaeropedunculate	Lombard et al., 2010b
	C. humicola	43–71 × 42–49	3	44–90 × 6–8	126–157 × 4–5	(45–)48–54(–56) × (4–)5	51 × 5	1	10–12	globoid to ovoid to sphaeropedunculate	Lombard et al., 2010b
	C. pseudospathiphylli	70–100 × 25–70	4	100–350 × 5–6	100–250 × 2.5–3.5	(40–)47–55(–60) × 4–5	52 × 4	1(–3)	8–12	sphaeropedunculate to ellipsoid	Kang et al., 2001; Crous 2002
	C. spathiphylli	60–150 × 40–90	4	120–150 × 6–8	170–260 × 3–4	(45–)65–80(–120) × (5–)6(–7)¶	70 × 6	1(–3)	8–15	globoid or ellipsoid to obpyriform	Crous 2002
***Calonectria candelabrum* species complex**	***C. imperata***	50–127 × 41–110	(–3)	135–227 × 2–4	151–254 × 1.5–3	(38–)43–49(–52) × (2–)2.7–3.2(–4)	46 × 3	(–1)	3–6	ellipsoid to narrowly obpyriform	This study
	C. piauiensis	20–60 × 35–80	2	50–110 × 4–6	95–130 × 2–3	(38–)47–52(–60) × 3–5	49 × 4.5	1	3–7	ellipsoid to narrowly obpyriform	Alfenas et al., 2015
	C. brassiana	50–80 × 50–135	3	55–155 × 5–8	90–172 × 2–3	(35–)50–56(–65) × 3–5	53 × 4	1	3–7	ellipsoid to narrowly obpyriform	Alfenas et al., 2015
	C. glaebicola	27–45 × 25–40	2	50–130 × 5–7	100–165 × 2–4	(45–)50–52(–55) × 3–5	50 × 4	1	3–5	ellipsoid to narrowly obpyriform	Alfenas et al., 2015
	C. venezuelana	25–65 × 25–60	3	35–100 × 4–8	85–190 × 3–6	(48–)54–62(–65) × (4–)4.5–5.5(–7)	58 × 5	1	5–9	fusiform to ovoid to ellipsoid	Lombard et al., 2016

† All measurements are in µm.

‡ L × W = length × width.

§ Minimum–maximum.

| Measurements are presented in the format [(minimum–) (average – standard deviation) – (average + standard deviation) (–maximum)].

¶ Measurements are presented in the format [(minimum–) (average) (–maximum)].

ARTICLE 2 – MOLECULAR AND MORPHOLOGICAL CHARACTERIZATION OF *Calonectria quinqueramosa* CAUSING LEAF BLIGHT ON *Eucalyptus urophylla* IN BRAZIL

Enrique I. Sanchez-Gonzalez[1], Thaissa de Paula Farias Soares[2], Talyta Galafassi Zarpelon[2], Edival Angelo Valverde Zauza[2], Reginaldo Gonçalves Mafia[2], Maria Alves Ferreira[1]

[1] Universidade Federal de Lavras, Departamento de Fitopatologia, Lavras, MG, 37200-900, Brasil

[2] Suzano Papel e Celulose S. A. Centro de Tecnologia, Aracruz, ES, 29197-900, Brasil

*Corresponding author: M. A. Ferreira; mariaferreira@ufla.br

Article accepted in the *Journal of Phytopathology* 2023, presented according to journal guidelines.

Original Article

Molecular and morphological characterization of *Calonectria quinqueramosa* causing leaf blight on *Eucalyptus urophylla* in Brazil

Enrique Ignacio Sánchez-González[1], Thaissa de Paula Farias Soares[2], Talyta Galafassi Zarpelon[2], Edival Angelo Valverde Zauza[2], Reginaldo Gonçalves Mafia[2], Maria Alves Ferreira[1]

[1] Universidade Federal de Lavras, Departamento de Fitopatologia, Lavras, MG, 37200-900, Brasil
E.I.S.G.: ei_sanchez@hotmail.com; ORCID: 0000-0002-0180-8154
M.A.F.: mariaferreira@ufla.br; ORCID: 0000-0001-9401-7142
[2] Suzano Papel e Celulose S. A. Centro de Tecnologia, Aracruz, ES, 29197-900, Brasil
T.P.F.S: ThaissaSoares.inova@suzano.com.br
T.G.Z.: talyta.zarpelon@suzano.com.br
E.A.V.Z.: edivalzauza@suzano.com.br; ORCID: 0000-0001-8322-7689
R.G.M.: rgoncalves@suzano.com.br

Correspondence
Maria Alves Ferreira, Universidade Federal de Lavras, Departamento de Fitopatologia, Laboratorio de Patologia Florestal, Lavras, MG, 37200-900, Brasil.
Email: mariaferreira@ufla.br; Tel: +55 (35) 3829-1799

Funding Information
This research was financed by Suzano Papel e Celulose S. A.

CONFLICTS OF INTEREST
The authors declare no conflict of interest.

Abstract
One of the most damaging diseases of *Eucalyptus* is Calonectria leaf blight, and it causes significant economic losses. In March 2021, symptoms of leaf blight disease were observed in a *Eucalyptus* commercial plantation in northeastern Brazil. The present study aimed to identify the causal agent based on morphological features, phylogenetic analyses, and pathogenicity tests. Based on phylogenetic analyses of the *cmdA*, *his3*, *tef1*, and *tub2* gene regions and morphological characteristics, the fungal isolates were identified as *Calonectria quinqueramosa*, and their pathogenicity to *Eucalyptus urophylla* was confirmed. The results of this study confirmed the importance of multi-locus phylogeny supported by morphological characteristics for the proper identification of *Calonectria* species. To the best of our knowledge, this study highlights the first report of *C. quinqueramosa* causing leaf blight on *E. urophylla* trees in northeastern Brazil. This information will be valuable to promote the development of disease management strategies and to lead the development of *Eucalyptus* genotypes with resistance to *Calonectria*.

KEYWORDS
leaf blight disease; multi-locus phylogeny; pathogenicity test; tree pathogen

1. INTRODUCTION

Plant pathogenic fungi belonging to the *Calonectria* genus have a global distribution and can infect more than 335 different plant species belonging to almost 100 different plant families, including agricultural, horticultural, and forestry crops in tropical and subtropical climates. (Crous, 2002; Liu & Chen, 2022). To date, in Brazil have been described 37 species of *Calonectria*: one mycoparasite species, six were isolated from tropical rainforests (soil samples), seven were isolated from different plant species, and twenty three were isolated from diseased tissues or soil samples of *Eucalyptus* plantations (Crous et al., 2018, 2019; Liu et al., 2020; Sanchez-Gonzalez et al., 2022); all them are distributed in the species complexes of *C. brassicae*, *C. candelabrum*, *C. cylindrospora*, *C. gracilipes*, *C. naviculata*, *C. pteridis*, and *C. spathiphylli* (Crous et al., 2018, 2019; Liu et al., 2020; Sanchez-Gonzalez et al., 2022).

In Brazil, diseases associated with *Calonectria,* such as root rot, cutting rot, damping-off, and Calonectria leaf blight (CLB), have been reported in nurseries and commercial plantations of *Eucalyptus* (Soares et al., 2018), and according to Liu and Chen (2022), CLB causes significant economic losses in *Eucalyptus* plantations, and it is one of the most damaging diseases worldwide. Since *Eucalyptus* trees are propagated clonally, the *Eucalyptus* plantations are genetically homogeneous, which gives an advantage for fungal pathogens to become a threat to commercial plantations (Bose et al., 2022a).

Calonectria leaf blight is the primary fungal leaf disease in commercial *Eucalyptus* plantations in the warm and humid regions of northern and northeastern Brazil (Alfenas et al., 2015), and strategies to control this disease include the selection and cultivation of resistant genotypes as well as chemical methods and integrated cultivation (Soares et al., 2018). Therefore, a proper identification of the pathogen species may be valuable to promote the development of disease management strategies and to lead the development of *Eucalyptus* genotypes with resistance to *Calonectria*. In March 2021, occurrence of leaf blight was observed in a *Eucalyptus* commercial plantation localized in the municipality of Cidelândia, in the state of Maranhão, Brazil. However, the identity of the causal agent was unclear. Thus, in this study the aims were to identify the causal agent of leaf blight on *Eucalyptus* trees in northeastern Brazil through molecular phylogenetic analyses and morphology, and to confirm their pathogenicity to *Eucalyptus urophylla*.

2. MATERIALS AND METHODS

2.1 Fungal isolation

In March 2021, during a disease survey conducted in a one-year-old *E. urophylla* commercial plantation localized in the municipality of Cidelândia (5°09'13.5"S, 47°37'19.9"W), in the state of Maranhão, Brazil. The *Eucalyptus* trees presented leaf blight and leaf spot symptoms (Figure 1). Twenty-five diseased leaves were randomly collected through the plantation, one leaf per tree. The distance between sampled trees ranged from 50 to 100 m. The samples were kept in paper bags and brought to the Laboratory of Forest Pathology at the Universidade Federal de Lavras (UFLA) for fungal isolation, and morphological and molecular characterization.

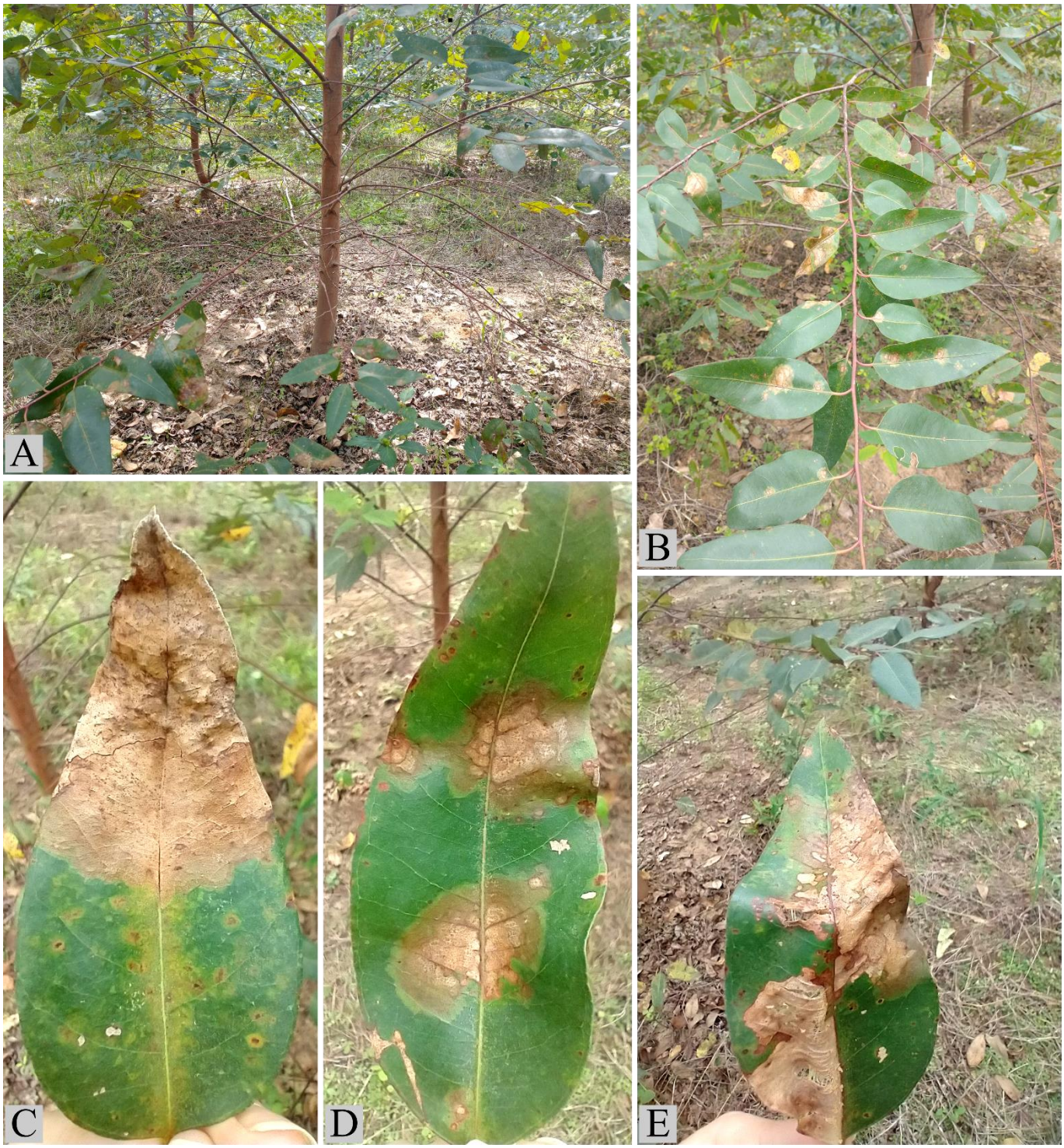

FIGURE 1 Calonectria leaf blight symptoms on one-year-old *Eucalyptus urophylla* trees under field conditions. (**A**) Defoliation due to leaf blight; (**B**) Leaf spot on leaves; (**C –E**) Leaves becoming blighted.

Based on preliminary isolation yielding *Calonectria*-like morphology fungal isolates, the same procedures used by Sanchez-Gonzalez et al. (2022) were followed for *Calonectria* isolation and single spore cultures obtainment. The pure cultures were stored and maintained in dry culture and in sterile water (Castellani, 1939), and deposited in the mycological collection of the Laboratory of Forest Pathology at UFLA.

2.2 DNA extraction, PCR amplification, and sequencing

All the *Calonectria* isolates obtained were used for DNA extraction and sequence analysis. Based on previous studies (Liu & Chen, 2017; Liu et al., 2021; Wu & Chen, 2021), calmodulin (*cmdA*), histone H3 (*his3*), translation elongation factor 1-alpha (*tef1*), and β-tubulin (*tub2*) partial gene regions were used as DNA

barcodes to identify *Calonectria* species. The DNA extraction, and PCR mixture and amplification were performed following the same procedures and conditions used by Sanchez-Gonzalez et al. (2022). The PCR products were separated in a 1.2% agarose gel by electrophoresis at 120 V for 1 h, stained with Diamond Nucleic Acid Dye (Promega, Madison, WI, USA), and visualized in an ultraviolet light transilluminator. PCR products were sent to Macrogen Inc. (Macrogen, Seoul, Korea) for purification and bidirectional sequencing service. The raw sequences were edited using Chromas v. 2.6.6 (Technelysium Pty Ltd, South Brisbane, QLD, Australia) software, and assembled using SeqAssem software v. 07/2008 (Hepperle, 2004). The sequences were deposited in the GenBank/NCBI database (http://www.ncbi.nlm.nih.gov).

2.3 Phylogenetic analyses

The sequences of *cmdA*, *his3*, *tef1*, and *tub2* were used for standard nucleotide BLAST search, and sequences of closely related *Calonectria* species, including the ex-type isolates, were downloaded from GenBank (Table 1) and used for the phylogenetic analyses. Sequence alignments were performed in the online interface of MAFFT v. 7.0 (Katoh et al., 2019; http://mafft.cbrc.jp/alignment/server) following the alignment strategy FFT-NS-i (Slow; interactive refinement method) and manually corrected using MEGA7 (Kumar et al., 2016) when necessary.

Maximum Likelihood (ML) and Bayesian Inference (BI) approaches were used to determine the phylogenetic relationships among species, on the individual gene regions and their concatenated dataset. The individual and partitioned ML analyses were conducted using IQ-TREE (Nguyen et al., 2015) in the IQ-TREE web server (Trifinopoulos et al., 2016; Chernomor et al., 2016; http://iqtree.cibiv.univie.ac.at). For each gene region, the best nucleotide substitution model was selected according to the Bayesian Information Criterion (BIC) using ModelFinder (Kalyaanamoorthy et al., 2017). The ML models used were TNe+I (*cmdA*), TIM2+F+G4 (*his3*), HKY+F+I+G4 (*tef1*) and K2P+I (*tub2*). An ultrafast bootstrapping (UFBoot2) with 10,000 replicates was performed to determine the branch support values (Hoang et al., 2018).

The individual and partitioned BI analyses were conducted using MrBayes v.3.2.7a (Ronquist et al., 2012) on XSEDE at the CIPRES Science Gateway v.3.3 (http://www.phylo.org/, accessed on 20 November 2022). For each gene region, the best nucleotide substitution model was selected according to the Akaike Information Criterion (AIC) using MrModeltest v. 2 (Nylander, 2004). The BI models used were SYM+I (*cmdA*) GTR+G (*his3*), GTR + I + G (*tef1*) and HKY + I + G (*tub2*). Two independent runs of four Markov Chain Monte Carlo (MCMC) chains (three hot and one cold) were simultaneously run in parallel, starting from a random tree for 10^7 generations, and sampling trees every 1,000 generations. To verify if the chains had converged, and the stationary phase of each search was reached, the log-likelihood scores distribution was examined with Tracer v.1.5 (Rambaut & Drummond, 2007). Also, the convergent diagnostics of the effective sampling site (ESS), the potential scale reduction factor (PSRF), and the average standard deviation of split frequencies (ASDSF) (Ronquist et al., 2019) were assessed. As the "burn-in" phase, the first 25% of saved trees were discarded, and posterior probabilities (PP) were calculated with the remaining trees. The obtained trees were visualized in FigTree v. 1.4.4 (Rambaut, 2009) and edited in Inkscape v. 1.0 (https://inkscape.org).

TABLE 1 *Calonectria* species and GenBank accession numbers of DNA sequences used in this study.

Calonectria species	Isolate representing the species[a,b,c]	Host/ Substrate	Country	Genbank accession numbers[d,e]			
				cmdA	***his3***	***tef1***	***tub2***
C. brachiatica	**CMW25298,** CSF11364	*Pinus maximinoi*	Colombia	MT335195	MT335435	MT412726	MT412948
	CMW25302, CSF11365	*Pi. tecunumanii*	Colombia	MT335196	MT335436	MT412727	MT412949
C. brassicae	**CBS111869,** CSF11255	*Argyreia splendens*	Indonesia	MT335202	MT335442	MT412733	MT412955
C. clavata	**CMW23690,** CSF11353	*Callistemon viminalis*	USA	MT335223	MT335463	MT412754	MT412975
	CMW30994, CSF11400	Root debris in peat	USA	MT335224	MT335464	MT412755	MT412976
C. duoramosa	**CBS134656**	Soil (tropical rainforest)	Brazil	KM396027	KM396110	KM395853	KM395940
	LPF453	Soil (*Eucalyptus* plantation)	Brazil	KM396028	KM396111	KM395854	KM395941
C. ecuadorae	**CMW23677,** CSF11344	Soil	Ecuador	MT335242	MT335482	MT412773	MT412991
	CBS111706, CSF16433	Soil	Ecuador	MT335240	MT335480	MT412771	MT412989
C. gracilis	**CBS111807,** AR2677	*Manilkara zapota*	Brazil	GQ267407	DQ190646	GQ267323	AF232858
	CBS111284	Soil	Brazil	GQ267408	DQ190647	GQ267324	DQ190567
C. octoramosa	**CBS111423,** CSF16431	Soil	Ecuador	MT335303	MT335543	MT412834	MT413048
C. orientalis	**CMW20291,** CSF11336	Soil	Indonesia	MT335304	MT335544	MT412835	MT413049
	CMW20273, CSF11335	Soil	Indonesia	MT335305	MT335545	MT412836	MT413050
C. paraensis	**CBS134669**	Soil (*Eucalyptus* plantation)	Brazil	KM396011	KM396094	KM395837	KM395924
	LPF429	Soil (tropical rainforest)	Brazil	KM396015	KM396098	KM395841	KM395928
C. parvispora	**CBS111465,** CSF16432	Soil	Brazil	MT335314	MT335554	MT412845	MT413057
	CMW30981, CSF11388	Soil	Brazil	MT335313	MT335553	MT412844	MT413056
C. pauciphialidica	**CMW30980,** CSF11387	Soil	Ecuador	MT335315	MT335555	MT412846	MT413058
C. pini	**CMW31209,** CSF11410	*Pi. patula*	Colombia	MT335339	MT335579	MT412870	MT413082
	CMW31210	*Pi. patula*	Colombia	GQ267437	GQ267274	GQ267345	GQ267225
C. pseudobrassicae	**CBS134662**	Soil (*Eucalyptus* plantation)	Brazil	KM396023	KM396106	KM395849	KM395936
	CBS134661	Soil (*Eucalyptus* plantation)	Brazil	KM396022	KM396105	KM395848	KM395935
C. pseudoecuadoriae	**CBS111402**	Soil	Ecuador	KX784589	N/A	KX784723	KX784652
C. quinqueramosa	**CBS134654**	Soil (*Eucalyptus* plantation)	Brazil	KM396029	KM396112	KM395855	KM395942
	CBS134655	Soil (*Eucalyptus* plantation)	Brazil	KM396030	KM396113	KM395856	KM395943
	CBS134863	Soil (*Eucalyptus* plantation)	Brazil	KM396031	KM396114	KM395857	KM395944
	MA12*	*E. urophylla* (leaf)	Brazil	**OP910222**	**OP910226**	**OP910230**	**OP910234**
	MA15*	*E. urophylla* (leaf)	Brazil	**OP910223**	**OP910227**	**OP910231**	**OP910235**
	MA18*	*E. urophylla* (leaf)	Brazil	**OP910224**	**OP910228**	**OP910232**	**OP910236**
	MA22*	*E. urophylla* (leaf)	Brazil	**OP910225**	**OP910229**	**OP910233**	**OP910237**
C. robigophila	**CBS134652**	*Eucalyptus* sp. (leaf)	Brazil	KM396024	KM396107	KM395850	KM395937
	CBS134653	*Eucalyptus* sp. (leaf)	Brazil	KM396025	KM396108	KM395851	KM395938
C. paragominensis	**CCDCA11648**	*E. grandis* × *E. brassiana*	Brazil	OM974325	OM974334	OM974352	OM974361
	PFC2	*E. grandis* × *E. brassiana*	Brazil	OM974326	OM974335	OM974353	OM974362

[a] Ex-type isolates are marked in bold.

[b] Isolates obtained in this study are marked in with "*"

[c] CBS: Westerdijk Fungal Biodiversity Institute, Utrecht, The Netherlands; CCDCA: Coleção de Culturas de Microrganismos do Departamento de Ciência dos Alimentos/UFLA, Lavras, Brazil; CMW: Culture collection of the Forestry and Agricultural Biotechnology Institute (FABI), University of Pretoria, Pretoria, South Africa; CSF: Culture Collection located at Research Institute of Fast-growing Trees (RIFT)/China Eucalypt Research Centre (CERC), Chinese Academy of Forestry, ZhanJiang, GuangDong Province, China; LPF: Laboratorio de Patologia Florestal, Universidade Federal de Viçosa, Viçosa, Brazil; MA, PFC: Laboratorio de Patologia Florestal, UFLA, Lavras, Brazil.

[d] *cmdA*: calmodulin; *his3*: histone H3; *tef1*: translation elongation factor 1-alpha; *tub2*: β-tubulin.

[e]GenBank accession number marked in bold were obtained in this study.

2.4 Morphological characterization

Based on phylogenetic analyses, four *Calonectria* isolates were selected for morphological characterization. The size of macroconidia, macroconidia septation and width of vesicles are typical characteristics used for morphological comparisons for *Calonectria* species (Liu et al., 2021; Wu & Chen, 2021). Sexual and asexual structures were induced by transferring agar plugs (5 mm in diameter) from the periphery of actively growing pure cultures on 2% malt extract agar (MEA; malt extract 20 g·L^{-1}, agar 20 g·L^{-1}, yeast extract 2 g·L^{-1}, sucrose 5 g·L^{-1}) plates in synthetic nutrient-poor agar (SNA) (Nirenberg, 1981) plates and incubating for 7 to 10 days at 25°C (three replicates per isolate were used). In case of sexual structures, one representative isolate was selected for perithecia, asci and ascospores characterization.

The fungal structures were put in 85% lactic acid on glass slides and examined under a Labomed LX400 microscope (Lab America, Inc., CA, USA) and an Opton 5.1MP digital camera model TA-0120-B with OptView software (Anatomic, Ltd., SP, BR). For each isolate, thirty replicate measurements were made for each morphological structure. Minimum, maximum, and mean values were determined and presented as follows: (minimum–) (mean – standard deviation) – (mean + standard deviation) (–maximum). Optimal growth temperature was determined by incubating at temperatures of 20°C, 25°C and 30°C on MEA plates in the dark (four replicates per isolate were used) and measuring the colony diameters after seven days. Texture and color of colonies were determined using seven-day-old cultures on MEA incubated at 25°C.

2.5 Pathogenicity test

To verify if the fungal isolates can cause disease in *Eucalyptus* tree leaves, the same four *Calonectria* isolates used for morphological characterization were inoculated on healthy leaves of short, detached branches from an approximately one-year-old healthy tree of *E. urophylla* genotype kept in greenhouse. The same *E. urophylla* genotype from which the isolates were obtained was chosen for inoculation. The mycelial plug method was used for inoculation (Wu & Chen, 2021; Liu & Chen, 2022). Mycelial plugs (5 mm in diameter) from the periphery of 14-day-old fungal colonies grown on MEA at 25°C were cut and placed upside down on the abaxial surface of six to eight leaves without wounds using sterile needles. Sterile MEA plugs were used to inoculate leaves as negative controls. The branches with inoculated leaves were kept in moist plastic chambers and maintained at 25 ± 2°C for 7 days at laboratory. For each lesion, two measurements of diameter perpendicular to each other were registered at three and five days-post-inoculation (dpi). The experiment was performed during November 2022 and was repeated once using the same approach. To fulfill Koch´s postulates, re-isolations were conducted from the disease leaves, and the identity of the re-isolated fungi was verified by morphological characteristics in comparison with the same isolate used for inoculation.

3. RESULTS

3.1 Fungal isolates

From the collected diseased leaves of the *E. urophylla* trees, twenty isolates with *Calonectria*-like morphology were obtained. Then, four isolates were selected for further studies based on preliminary phylogenetic analyses of the *tub2* and *tef1* gene regions, since the other isolates corresponded to species of *Calonectria* already known to cause leaf blight in *E. urophylla* (data not shown) (Table 1).

3.2 Phylogenetic analyses

The BLAST search results performed with *cmdA*, *his3*, *tef1*, and *tub2* showed that the four isolates belong to the *Calonectria brassicae* species complex (CBSC). Then, sequences from 31 isolates, including ex-type specimens of 17 *Calonectria* species closely related to the isolates selected in this study were downloaded from GenBank (Table 1). For phylogenetic analyses, the sequences were combined in a single sequence dataset, and two strains of *Calonectria paragominensis* were included as the outgroup taxa.

For each gene region and the concatenated dataset, the alignments were as follows: *cmdA* (35 taxa, 690 bp), *his3* (34 taxa, 436 bp), *tef1* (35 taxa, 500 bp), *tub2* (35 taxa, 520 bp) and concatenated (35 taxa, 2146 bp). For the phylogenetic trees derived from the ML and BI analyses of *cmdA*, *his3*, *tef1*, and *tub2* the topologies were similar, but the positions of some *Calonectria* species was slightly different. In the ML and BI analyses of the concatenated dataset well-supported lineages were formed. The ML trees are showed in this study (Figure 2, Supplementary Figures S1–S4). The full alignment had 320 parsimony-informative characters, 46 parsimony-uninformative characters, and 1,780 constant characters., The convergence of the chains for the individual and partitioned BI analyses was confirmed by an ESS > 200, a PSRF equal to 1, and an ASDSF ≤ 0.003.

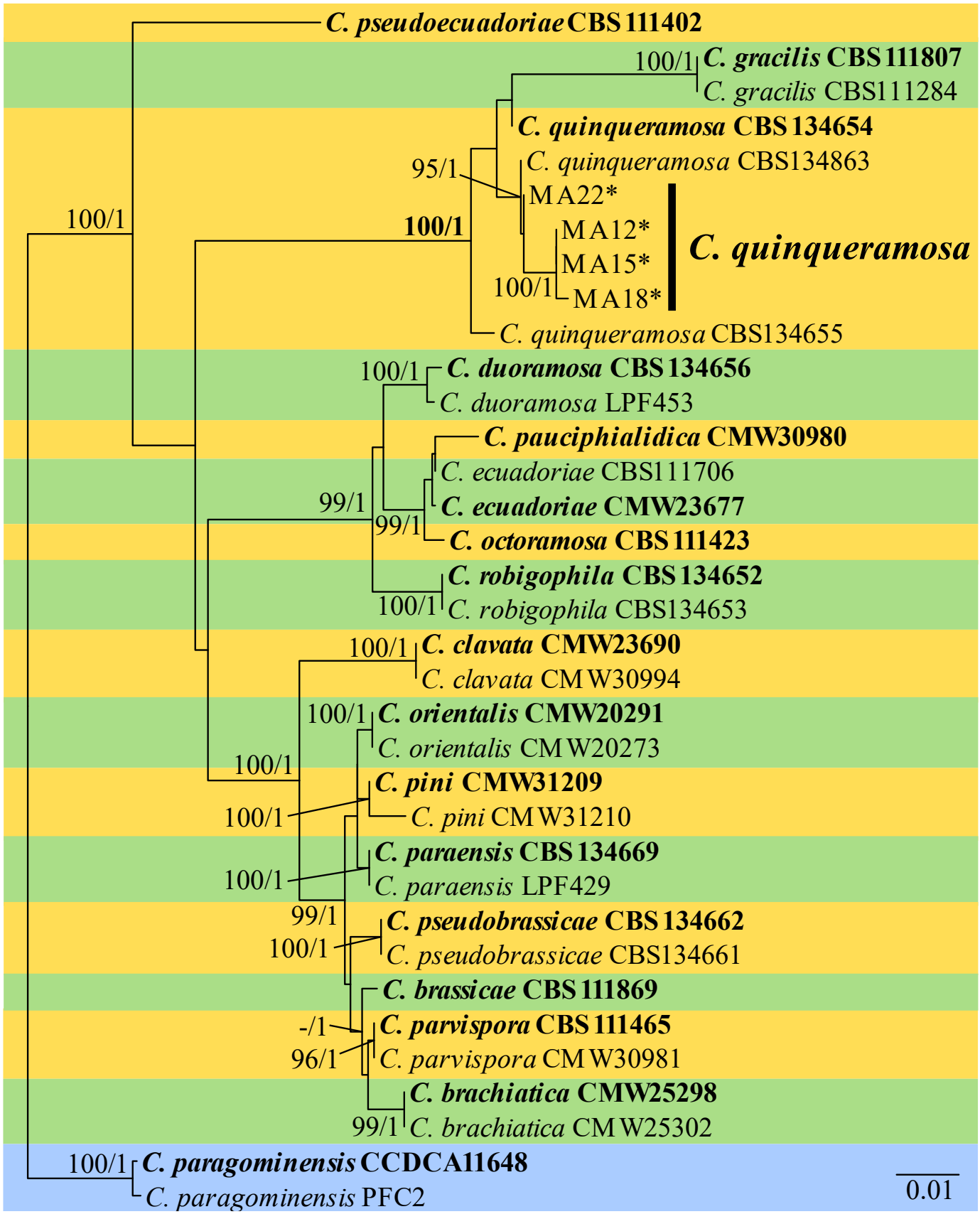

FIGURE 2 Phylogenetic tree of *Calonectria brassicae* species complex based on maximum likelihood analysis of concatenated gene regions *cmdA*, *his3*, *tef1* and *tub2*. Support values of UFBoot2 (≥ 95%) and PP (≥ 0.95) are presented at the nodes (ML/BI). Values below 95% (UFBoot2) and 0.95 (PP) are marked with "-". Ex-type isolates are highlighted in bold, and "*" indicates isolates sequenced in this study. *C. paragominensis* was used as outgroup taxa. The number of nucleotide substitutions per site is indicated by the scale bar.

For *cmdA* data set, the phylogenetic analyses showed that the isolates MA12, MA15 and MA18 formed a clade strongly supported (ML/PP = 100%/1) together with an isolate of *C. quinqueramosa* species (CBS134655) (Supplementary Figure S1). In the phylogenetic analyses based on each of *his3*, *tef1*, and *tub2* data sets, the isolates MA12, MA15 and MA18 were clustered in an independent clade supported by high bootstrap (ML) and high posterior probability (PP) values (*his3*: ML/PP = 100%/1; *tef1*: ML/PP = 98%/0.99; *tub2*: ML/PP = 89%/0.96) (Supplementary Figures S2–S4). In case of the isolate MA22, the phylogenetic analyses based on *cmdA*, *tef1*, and *tub2* data sets, showed that it formed a clade together with isolates of *C. quinqueramosa* species (ex-type CBS134654 and/or CBS134863) with high bootstrap and posterior probability values (*cmdA*: ML/PP = 95%/1; *tef1*: ML/PP = 100%/1; *tub2*: ML/PP = 88%/0.9) (Supplementary Figures S1, S3 and S4). For *his3* data set, the isolate MA22 formed a clade with two isolates of *C. gracilis* species (ex-type AR2677 and CBS111284), with high bootstrap and posterior probability values (ML/PP = 92%/0.99) (Supplementary Figure S2).

The four isolates formed two strongly defined phylogenetic subclades, based on the four genes concatenated dataset. Subclade 1 was formed by the isolate MA22 and CBS134655 (ML/PP = 95%/1) and the subclade 2 was formed by the isolates MA12, MA15 and MA18 (ML/PP = 100%/1) (Figure 2). Both subclades were clustered within a major clade including the ex-type culture of *C. quinqueramosa* CBS134654 with high support values of bootstrap and posterior probability (ML/PP = 100%/1) (Figure 2). Fixed unique single nucleotide polymorphisms (SNPs) were identified in the four isolates in comparison with *C. quinqueramosa* species (Table 2). The isolate MA22 presented one SNP difference (*his3*: 1), the isolates MA12 and MA15 presented eight SNP differences (*his3*: 5; *tef1*: 2; and *tub2*: 1) and the isolate MA18 presented 12 SNP differences (*cmdA*: 4; *his3*: 5; *tef1*: 2; and *tub2*: 1).

TABLE 2 Fixed unique single nucleotide polymorphisms identified in the isolates obtained in this study in comparison with *Calonectria quinqueramosa* species in the four gene regions.

Species	Isolate Code[a]	*cmdA*				*his3*					*tef1*		*tub2*
		7[b]	10	11	12	697	800	934	940	980	1205	1324	1836
C. quinqueramosa	**CBS134654**	C	T	C	T	T	C	T	C	C	C	C	G
	CBS134655	C	T	C	T	T	C	T	C	C	C	C	G
	CBS134863	C	T	C	T	T	C	T	C	C	C	C	G
	MA22*	C	T	C	T	C[c]	C	T	C	C	C	C	G
	MA12*	C	T	C	T	C	T	C	A	T	T	T	A
	MA15*	C	T	C	T	C	T	C	A	T	T	T	A
	MA18*	T	C	T	C	C	T	C	A	T	T	T	A

[a] Ex-type isolate is marked in bold; "*" indicates isolates obtained in this study. [b] Numerical positions of the nucleotides in the DNA sequence alignment. [c] Polymorphic nucleotides are highlighted in gray shade.

3.3 Morphological characterization

The four isolates were homothallic, and showed similar morphology for size of macroconidia, macroconidia septation and width of vesicles (Table 3), therefore, the isolate MA18 was selected for describing morphology in this study (Figure 3). **Description:** The perithecia produced on SNA plates were solitary or aggregated in groups, orange to red brown, becoming dark with age, subglobose to pyriform, and measured (235–)275–362(–402) × (165–)206–258(–264) µm (average 318 × 232 µm). Asci were clavate, contained eight spores, tapered to a long thin stalk, and measured (52–)59–80(–98) × (16–)18–23(–25) µm (average 69 × 20 µm). Ascospores were guttulate, hyaline, straight to curved, fusoid with rounded ends, 1-septate, slightly constricted at the septum, aggregated in the upper third of the ascus, and measured (32–)36–43(–47) × (4–)5(–6) µm (average = 40 × 5 µm). Macroconidiophores consisted of a stipe, with fertile branches in a penicillate

arrangement, a stipe extension, and a terminal vesicle. Stipes were hyaline, septate and smooth. Stipe extensions were septate, straight to flexuous, (192–)227–302(–346) µm long, 2–3 µm wide at the apical septum, terminating in a narrowly clavate to clavate vesicle 3–4 µm diam. Macroconidia were cylindrical, rounded at both ends, straight, (51–)53–62(–65) × 4–6 µm (av. = 58 × 5 µm), 1-septate, lacking a visible abscission scar, held in parallel cylindrical clusters by colorless slime. **Culture characteristics:** Colonies formed a sparse aerial mycelium after seven days on MEA plates incubated at 25°C in the dark, with irregular margins and moderate sporulation. The surface was umber to fawn, and sienna-dark brick to amber in reverse with sparse chlamydospores forming microsclerotia. After seven days, colonies on MEA plates reached 29.7 mm, 37.3 mm, and 38.8 mm in diameter at 20°C, 25°C, and 30°C, respectively.

TABLE 3 Morphological comparison among *Calonectria quinqueramosa* species and isolates obtained in this study.

Species	Isolate Code[a]	Macroconidia Size (L × W)[b,c,d]	Macroconidia Average (L × W)[b,c,d]	Macroconidia Septation	Vesicle Width[b,d]	Vesicle Average Width[b]
C. quinqueramosa	**CBS134654**	(45–)57–61(–70) × 4–6	59 × 5	1	3–5	N/A
	MA12*	(56–)59–67(–70) × 4–6	63 × 5	1	3–5	3.9
	MA15*	(47–)52–60(–62) × 4–6	56 × 5	1	3–5	3.7
	MA18*	(51–)53–62(–65) × 4–6	58 × 5	1	3–4	3.7
	MA22*	(40–)41–54(–63) × 4–5	48 × 4	1	3–5	3.2

[a] Ex-type isolate is marked in bold; "*" indicates isolates obtained in this study. [b] All measurements are in µm (n = 30). [c] L × W = length × width. [d] Measurements are presented in the format [(minimum–) (mean – standard deviation) – (mean + standard deviation) (–maximum)].

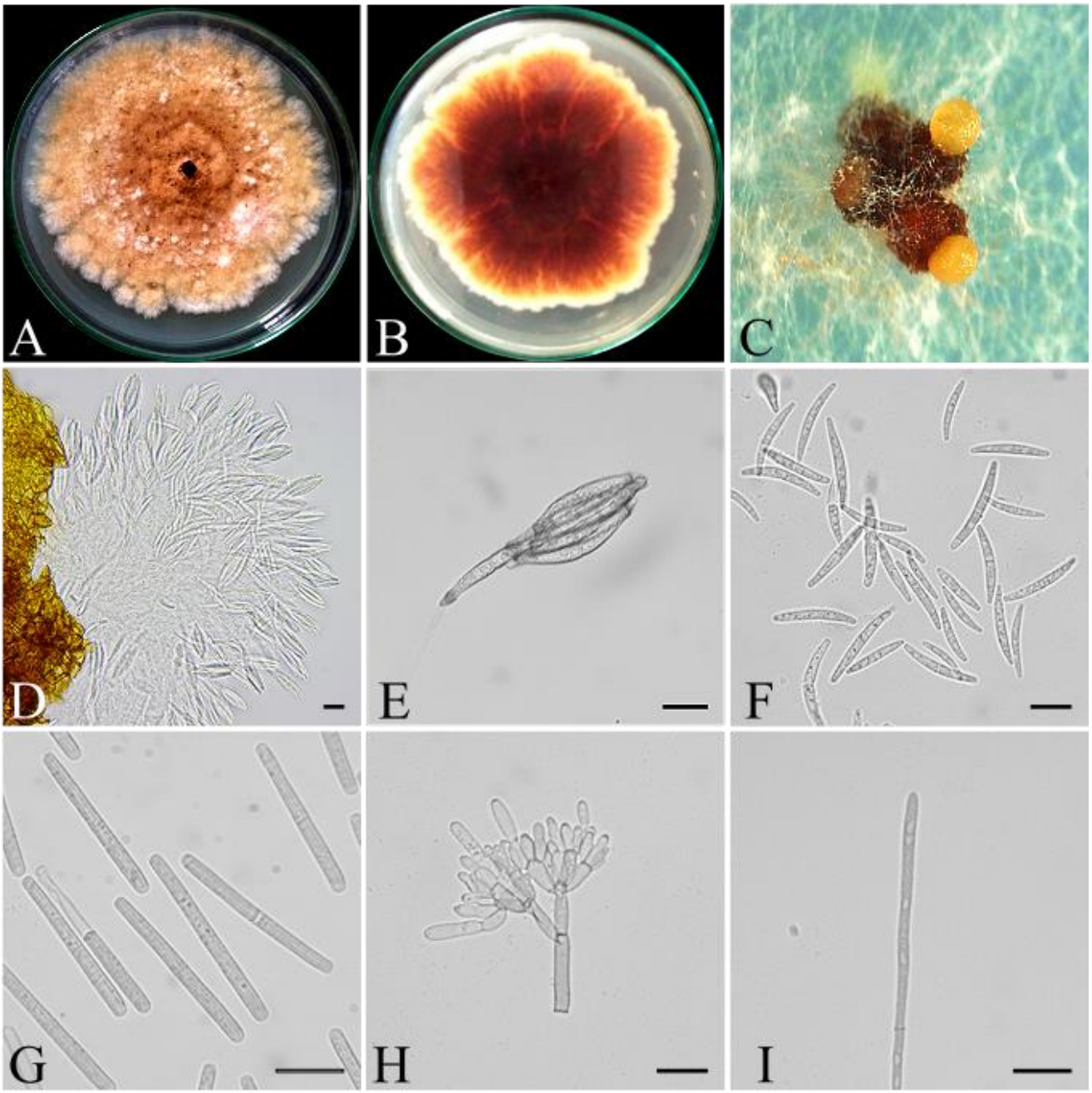

FIGURE 3 Morphological characteristics of *Calonectria quinqueramosa* (MA18). (**A)** Surface and (**B**) reverse sides of *C. quinqueramosa* after 14 days grown at 25°C on MEA plates; (**C**) Perithecium formed on SNA plates after 10 days at 25°C; (**D,E**) Asci; (**F**) Ascospores; (**G**) Macroconidia; (**H**) Conidiogenus apparatus with doliiform to reniform phialides on conidiophore branches; (**I**) Narrowly clavate vesicle.

3.4 Pathogenicity test

The mycelial plugs of the four *Calonectria* isolates produced necrotic symptoms on leaves (Figure 4A–D) but not on the negative control inoculations (Figure 4F). At 3 dpi the lesion diameter of the isolates MA12, MA15, MA18 and MA22 reached 15.6 ± 6.60 mm, 5.15 ± 0.38 mm, 25.85 ± 11.33 mm, and 15 ± 1.08 mm, respectively. At 5 dpi the lesion diameter of the isolates MA12, MA15, MA18 and MA22 reached 21.15 ± 10.64 mm, 8.31 ± 0.63 mm, 36.54 ± 12.63 mm, and 22.15 ± 4.38 mm, respectively. Sporulation occurred on the inoculated leaves 7 dpi. From inoculated leaves, fungi were reisolated and identified by the same morphological characteristics as the originally inoculated isolates. No fungi were isolated from the negative controls. Thus, the requirements of Koch's postulates were fulfilled.

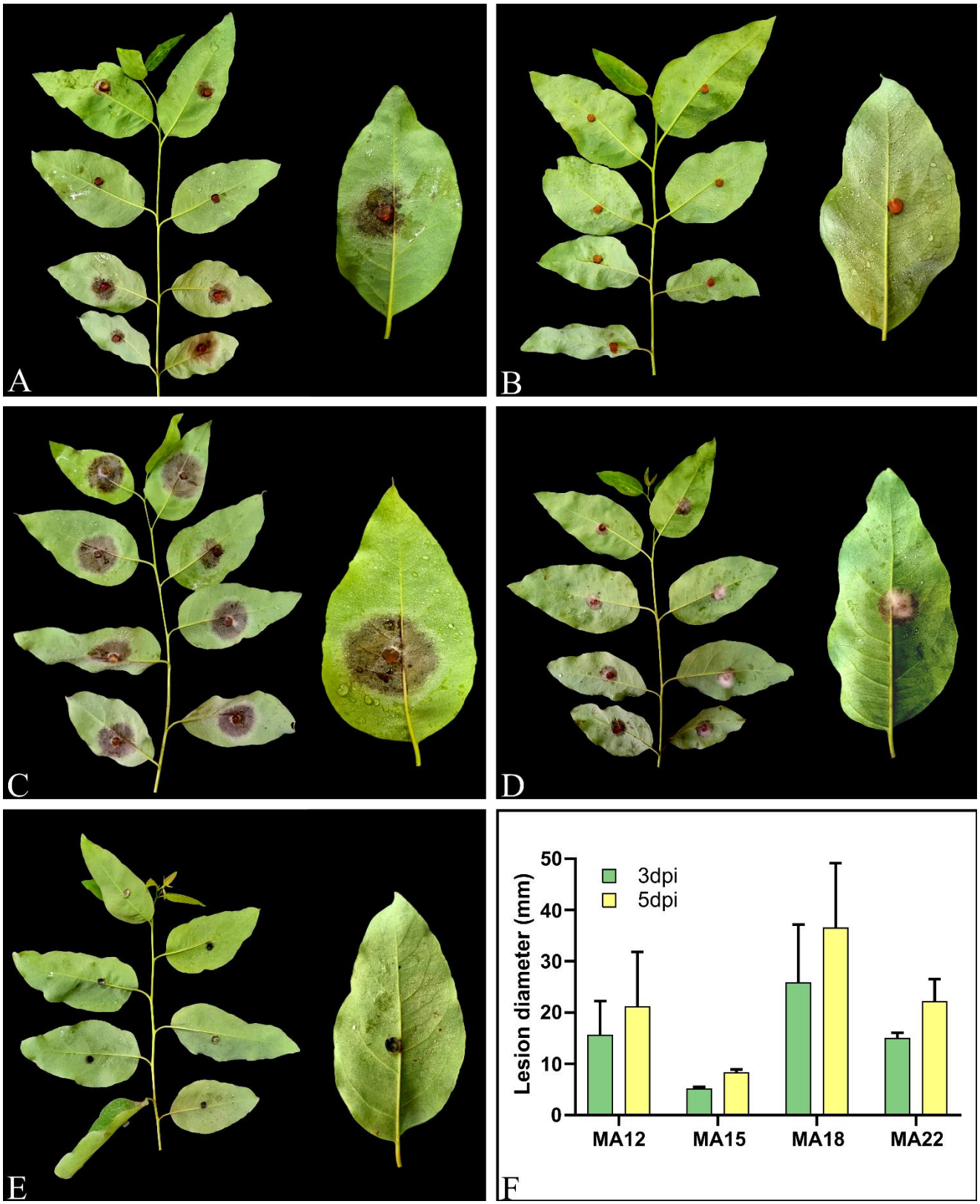

FIGURE 4 Necrotic symptoms on leaves of *Eucalyptus urophylla* genotype inoculated by *Calonectria quinqueramosa* mycelial plugs at 3 dpi. (A) Leaves inoculated with MA12; (B) Leaves inoculated with MA15; (C) Leaves inoculated with MA18; (D) Leaves inoculated with MA22; (E) No necrotic symptoms on leaves inoculated with sterile MEA plugs; (F) Lesion diameters at 3 and 5 dpi.

4. DISCUSSION

Based on phylogenetic analyses of four gene regions and on morphological comparisons, the *Calonectria* isolates obtained in this study were identified. The *cmdA, his3, tef1,* and *tub2* gene regions have been indicated to be adequate DNA barcodes to correctly identify *Calonectria* species (Liu et al., 2020; Wu & Chen, 2021). Previous studies in *Calonectria* have shown that isolates from the same species may show differences in nucleotides during comparisons of DNA sequences (Liu et al., 2022), even to form subclades with high support values (Wang et al., 2019). However, an integrative taxonomy is encouraged, combining phylogeny, phenotype, and reproductive biology (when feasible) for species delimitation, rather than a single approach *per se* (Lücking et al., 2020). In this study, although the isolates MA12, MA15, MA18 and MA22 formed subclades with high support values in the phylogenetic analyses, the morphological characteristics and dimensions from sexual and asexual structures examined were like the originally described for the species *C. quinqueramosa* (Alfenas et al., 2015), except for the isolate MA22, which was slightly shorter in terms of macroconidia size. These morphological variations among isolates within the same species have been reported for other *Calonectria* species in previous studies (Liu et al., 2020; Wu & Chen, 2021). Therefore, we considered these isolates members of the *C. quinqueramosa* species, and that the molecular differences found reflect intraspecific rather than interspecific variability (Liu et al., 2020).

Calonectria quinqueramosa resides in the *C. brassicae* complex, in the Prolate Group, species from this complex are characterized by their clavate vesicles, 1-septate macroconidia, orange to red brown perithecia, 8-spored asci and 1-septate ascospores, in either heterothallic and homothallic species, and are primarily distributed in South America, North America, and Asia (Liu et al., 2020). Of the 16 species in the *C. brassicae* complex, seven have been described in Brazil (Alfenas et al., 2015; Crous, 2002; Li et al., 2020; Marin-Felix, et al., 2017) and from these seven, only *C. robigophila* had been reported to be associated with CLB in *Eucalyptus* (Alfenas et al., 2015).

The mycelial plug method employed for the inoculation of *E. urophylla* leaves has showed the pathogenicity of the four *Calonectria* isolates, coinciding with the results of other studies where this method has been used to test *Calonectria* isolates that present a moderate or failed sporulation on the culture media (Bose et al., 2022b; Liu & Chen, 2022; Wu & Chen, 2021) Also, visual variations were observed in terms of the pathogenicity among the *Calonectria* isolates, which coincides with the reported by Liu and Chen (2022), where they found that within the same *Calonectria* species, the pathogenicity of the isolates can be different.

According to Liu and Chen (2017), a precise diagnosis of plant diseases and identification of its casual agents promote the development of effective disease management strategies. Thus, the results of the present study confirmed the importance of multi-locus phylogeny supported by morphological characteristics for the proper identification of *Calonectria* species. *Calonectria quinqueramosa* was originally described from soil in *Eucalyptus* plantation in Brazil, and its pathogenicity on *Eucalyptus* was not assessed (Alfenas et al., 2015). Thus, to the best of our knowledge, and based on the results of phylogenetic analyses, morphology characterization and pathogenicity tests, this study highlights the first report of *C. quinqueramosa* causing leaf blight on *E. urophylla* trees in northeastern Brazil.

ACKNOWLEDGEMENTS

We thank the Laboratory of Electron Microscopy and Ultrastructural Analysis at Universidade Federal de Lavras (UFLA) for the facilities granted during the completion of this study. The first author thanks for the doctorate scholarship assigned by the “Coordenação de Aperfeiçoamento de Pessoal de Nível Superior (CAPES)” through Brazil’s PAEC OAS-GCUB Scholarships Program.

AUTHOR CONTRIBUTIONS

Project conceptualization: E.I.S.G., T.G.Z., R.G.M., and M.A.F.; Experimentation: T.P.F.S., and E.I.S.G.; Data analysis: T.G.Z., T.P.F.S., and E.I.S.G.; Resources: E.A.V.Z., T.G.Z., and R.G.M.; Preparation of the draft manuscript, its review and editing: E.I.S.G., T.P.F.S., T.G.Z., E.A.V.Z., R.G.M., and M.A.F. All authors agree to be accountable for all aspects of the work. All authors read and approved the final version of the manuscript.

REFERENCES

Alfenas, R. F., Lombard, L., Pereira, O. L., Alfenas, A. C., & Crous, P. W. (2015). Diversity and potential impact of *Calonectria* species in *Eucalyptus* plantations in Brazil. *Studies in Mycology, 80*, 89–130. https://doi.org/10.1016/j.simyco.2014.11.002

Bose, R., Banerjee, S., Pandey, A., Bhandari, M. S., Barthwal, S., & Pandey, S. (2022a). Calonectria leaf blight of *Eucalyptus*: A global review. *Annals of Applied Biology*, 1–23. https://doi.org/10.1111/aab.12800

Bose, R., Banerjee, S., Negi, N., Pandey, A., Bhandari, M. S., & Pandey, S. (2022b). Identification and pathogenicity of *Calonectria pseudoreteaudii* causing leaf blight of Eucalyptus—a new record for India. *Physiological and Molecular Plant Pathology, 122*, 101917.

Castellani, A. (1939). Viability of some pathogenic fungi in distilled water. *Journal of Tropical Medicine and Hygiene, 42*, 225–226.

Chernomor, O., von Haeseler, A., & Minh, B. Q. (2016). Terrace aware data structure for phylogenomic inference from supermatrices. *Systematic Biology, 65*, 997–1008. https://doi.org/10.1093/sysbio/syw037

Crous, P.W. (2002). *Taxonomy and pathology of Cylindrocladium* (*Calonectria*) *and allied genera*, The American Phytopathological Society: St. Paul, MN, USA.

Crous, P. W., Luangsa-ard, J. J., Wingfield, M. J., Carnegie, A. J., Hernández-Restrepo, M., Lombard, L., Roux, J., Barreto, R. W., Baseia, I. G., Cano-Lira, J. F., et al. (2018). Fungal Planet description sheets: 785–867. *Persoonia, 41*, 238–417. https://doi.org/10.3767/persoonia.2018.41.12

Crous, P. W., Carnegie, A. J., Wingfield, M. J., Sharma, R., Mughini, G., Noordeloos, M. E., Santini, A., Shouche, Y. S., Bezerra, J. D. P., Dima, B., et al. (2019) Fungal Planet description sheets: 868–950. *Persoonia, 42*, 291–473. https://doi.org/10.3767/persoonia.2019.42.11

Hepperle, D. (2004). SeqAssem. Win32–Version. A sequence analysis tool contig assembler and trace data visualization tool for molecular sequences. Win32-Version. Distributed by the author via: http://www.sequentix.de (accessed 24 July 2022)

Hoang, D. T., Chernomor, O., von Haeseler, A., Minh, B. Q., & Vinh, L. S. (2018). UFBoot2: Improving the ultrafast bootstrap approximation. *Molecular Biology and Evolution, 35*, 518–522. https://doi.org/10.1093/molbev/msx281

Kalyaanamoorthy, S., Minh, B. Q., Wong, T. K., von Haeseler, A., & Jermiin, L. S. (2017). ModelFinder: fast model selection for accurate phylogenetic estimates. *Nature Methods, 14*, 587–589. https://doi.org/10.1038/nmeth.4285

Katoh, K., Rozewicki, J., & Yamada, K. D. (2019). MAFFT online service: Multiple sequence alignment, interactive sequence choice and visualization. *Briefings in Bioinformatics, 20*, 1160–1166. https://doi.org/10.1093/bib/bbx108

Kumar, S., Stecher, G., & Tamura, K. (2016). MEGA7: Molecular evolutionary genetics analysis version 7.0 for bigger datasets. *Molecular Biology and Evolution*, *33*, 1870–1874. https://doi.org/10.1093/molbev/msw054

Li, J. Q., Wingfield, B. D., Wingfield, M. J., Barnes, I., Fourie, A., Crous, P. W., & Chen, S. F. (2020). Mating genes in *Calonectria* and evidence for a heterothallic ancestral state. *Persoonia*, *45*, 163–176. https://doi.org/10.3767/persoonia.2020.45.06

Liu, Q., & Chen, S. (2017). Two novel species of *Calonectria* isolated from soil in a natural forest in China. *MycoKeys*, *26*, 25–60. https://doi.org/10.3897/mycokeys.26.14688

Liu, Q. L., Li, J. Q., Wingfield, M. J., Duong, T. A., Wingfield, B. D., Crous, P. W., & Chen, S. F. (2020). Reconsideration of species boundaries and proposed DNA barcodes for *Calonectria*. *Studies in Mycology*,. *97*, e100106. https://doi.org/10.1016/j.simyco.2020.08.001

Liu, L., Wu, W., & Chen, S. (2021). Species Diversity and Distribution Characteristics of *Calonectria* in Five Soil Layers in a *Eucalyptus* Plantation. *Journal of Fungi*, *7*, 857. https://doi.org/10.3390/jof7100857

Liu, L., & Chen, S. (2022). Pathogenicity of six *Calonectria* species isolated from five soil layers in a *Eucalyptus* plantation. *Journal of Phytopatholgy*, *170*, 445–452. https://doi.org/10.1111/jph.13096

Liu, Q., Wingfield, M. J., Duong, T. A., Wingfield, B. D., & Chen, S. (2022). Diversity and Distribution of *Calonectria* Species from Plantation and Forest Soils in Fujian Province, China. *Journal of Fungi*, *8*, 811. https://doi.org/10.3390/jof8080811

Lücking, R., Aime, M. C., Robbertse, B., Miller, A. N., Ariyawansa, H. A., Aoki, T., Cardinali, G., Crous, P. W., Druzhinina, I. S., Geiser, D. M., et al. (2020). Unambiguous identification of fungi: where do we stand and how accurate and precise is fungal DNA barcoding? *IMA fungus*, *11*, 1–32. https://doi.org/10.1186/s43008-020-00033-z

Marin-Felix, Y., Groenewald, J. Z., Cai, L., Chen, Q., Marincowitz, S., Barnes, I., Bensch, K., Braun, U., Camporesi, E., Damm, U., et al. (2017). Genera of phytopathogenic fungi. *Studies in Mycology*, *86*, 99–216. https://doi.org/10.1016/j.simyco.2017.04.002

Nguyen, L. T., Schmidt, H. A., von Haeseler, A., & Minh, B. Q. (2015). IQ-TREE: A fast and effective stochastic algorithm for estimating maximum-likelihood phylogenies. *Molecular Biology and Evolution*, *32*, 268–274. https://doi.org/10.1093/molbev/msu300

Nirenberg, H. I. (1981). A simplified method for identifying *Fusarium* spp. occurring on wheat. *Canadian Journal of Botany*, *59*, 1599–1609. https://doi.org/10.1139/b81-217

Nylander, J. A. A. (2004). MrModeltest v2. Program distributed by the author. Evolutionary Biology Centre, Uppsala University. Available online: https://github.com/nylander/MrModeltest2/releases (accessed 20 November 2020)

Rambaut, A., & Drummond, A. J. (2007). Tracer v1.5. available online: http://tree.bio.ed.ac.uk/software/tracer/ (accessed 29 July 2020)

Rambaut, A**.** (2009). FigTree, a graphical viewer of phylogenetic trees. Available online http://tree.bio.ed.ac.uk/software/figtree/ (accessed 29 July 2020)

Ronquist, F., Teslenko, M., van Der Mark, P., Ayres, D. L., Darling, A., Höhna, S., Larget, B., Liu, L., Suchard, M. A., & Huelsenbeck, J. P. (2012). MrBayes 3.2: Efficient Bayesian phylogenetic inference and model choice across a large model space. *Systematic Biology*, *61*, 539–542. https://doi.org/10.1093/sysbio/sys029

Ronquist, F., Huelsenbeck, J., Teslenko, M., & Nylander, J. A. A. (2019). MrBayes version 3.2 manual: tutorials and model summaries. https://nbisweden.github.io/MrBayes/manual.html

Sanchez-Gonzalez, E. I., Soares, T. D. P. F., Zarpelon, T. G., Zauza, E. A. V., Mafia, R. G., & Ferreira, M. A. (2022). Two new species of *Calonectria* (Hypocreales, Nectriaceae) causing *Eucalyptus* leaf blight in Brazil. *MycoKeys*, *91*, 169–197. https://doi.org/10.3897/mycokeys.91.84896

Soares, T. P., Pozza, E. A., Pozza, A. A., Mafia, R. G., & Ferreira, M. A. (2018) Calcium and Potassium Imbalance Favours Leaf Blight and Defoliation Caused by *Calonectria pteridis* in *Eucalyptus* Plants. *Forests*, *9*, e782. https://doi.org/10.3390/f9120782

Trifinopoulos, J., Nguyen, L. T., von Haeseler, A., & Minh, B. Q. (2016). W-IQ-TREE: A fast online phylogenetic tool for maximum likelihood analysis. *Nucleic Acids Research, 44*, W232–W235. https://doi.org/10.1093/nar/gkw256

Wang, Q. C., Liu, Q. L., & Chen, S. F. (2019). Novel species of *Calonectria* isolated from soil near *Eucalyptus* plantations in southern China. *Mycologia*, *111*, 1028–1040. https://doi.org/10.1080/00275514.2019.1666597

Wu, W., & Chen, S. (2021). Species Diversity, Mating Strategy and Pathogenicity of Calonectria Species from Diseased Leaves and Soils in the *Eucalyptus* Plantation in Southern China. *Journal of Fungi*, *7*, 73. https://doi.org/10.3390/jof7020073

SUPPORTING INFORMATION

FIGURE 1S. Phylogenetic tree of *Calonectria brassicae* species complex based on maximum likelihood analysis of cmdA gene region, FIGURE 2S. Phylogenetic tree of *Calonectria brassicae* species complex based on maximum likelihood analysis of his3 gene region, FIGURE 3S. Phylogenetic tree of *Calonectria brassicae* species complex based on maximum likelihood analysis of tef1 gene region, FIGURE 4S. Phylogenetic tree of *Calonectria brassicae* species complex based on maximum likelihood analysis of tub2 gene region.

SUPPORTING INFORMATION

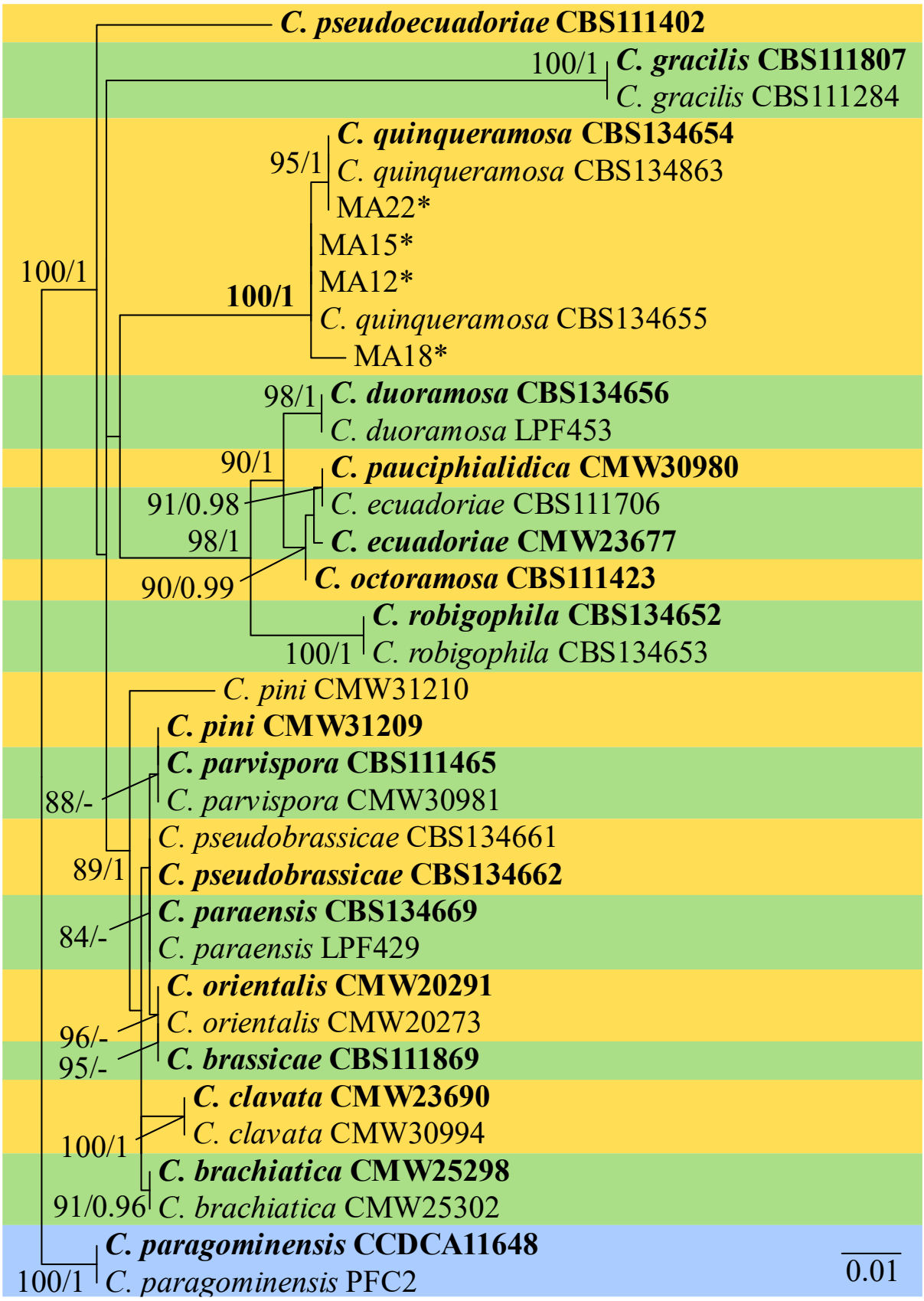

FIGURE 1S Phylogenetic tree of *Calonectria brassicae* species complex based on maximum likelihood analysis of *cmdA* gene region. Support values of UFBoot2 (≥ 80%) and PP (≥ 0.90) are presented at the nodes (ML/BI). Values below 80% (UFBoot2) and 0.90 (PP) are marked with "-". Ex-type isolates are highlighted in bold, and "*" indicates isolates sequenced in this study. *C. paragominensis* was used as outgroup taxa. The number of nucleotide substitutions per site is indicated by the scale bar.

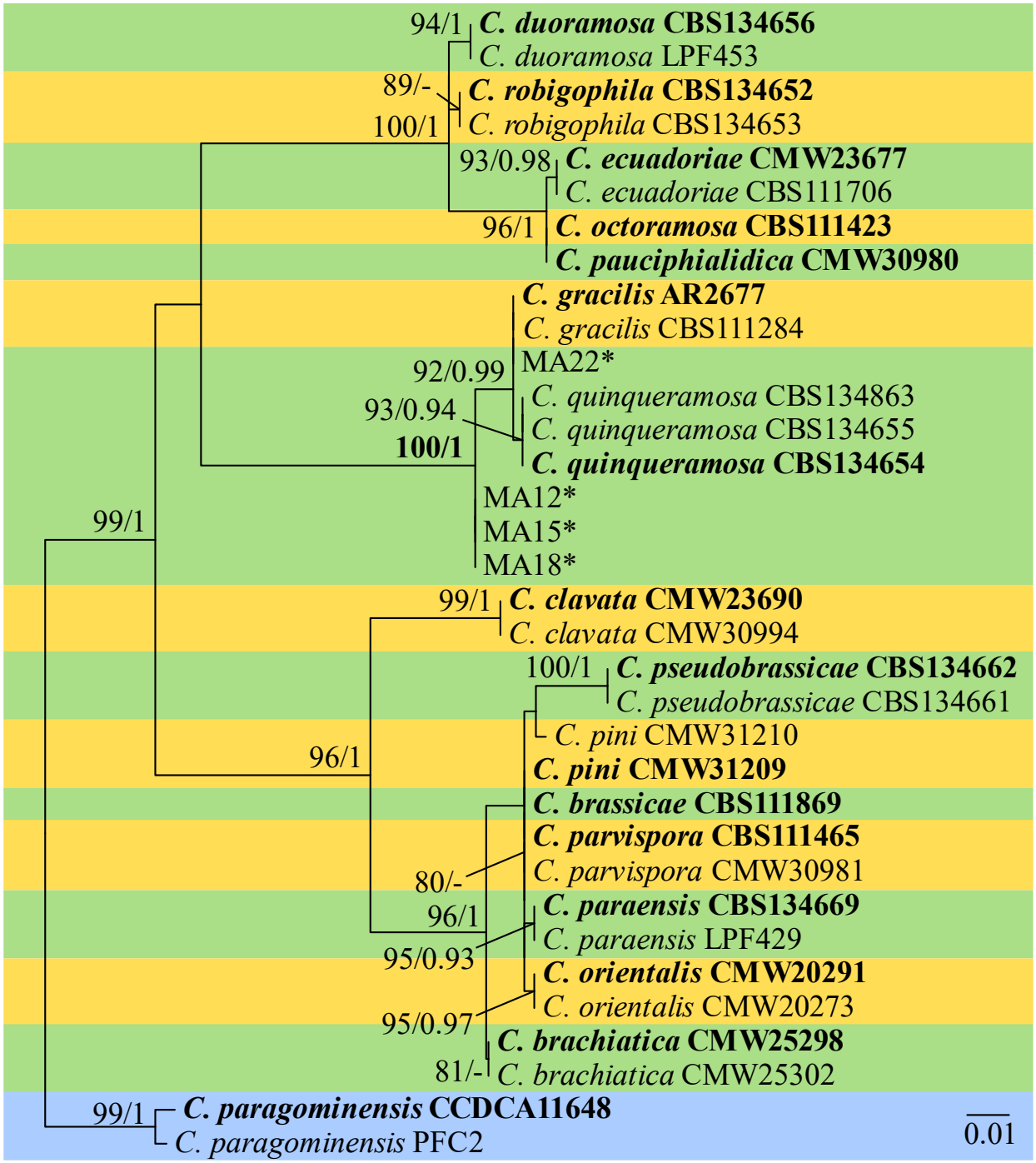

FIGURE 2S Phylogenetic tree of *Calonectria brassicae* species complex based on maximum likelihood analysis of *his3* gene region. Support values of UFBoot2 (≥ 80%) and PP (≥ 0.90) are presented at the nodes (ML/BI). Values below 80% (UFBoot2) and 0.90 (PP) are marked with "-". Ex-type isolates are highlighted in bold, and "*" indicates isolates sequenced in this study. *C. paragominensis* was used as outgroup taxa. The number of nucleotide substitutions per site is indicated by the scale bar.

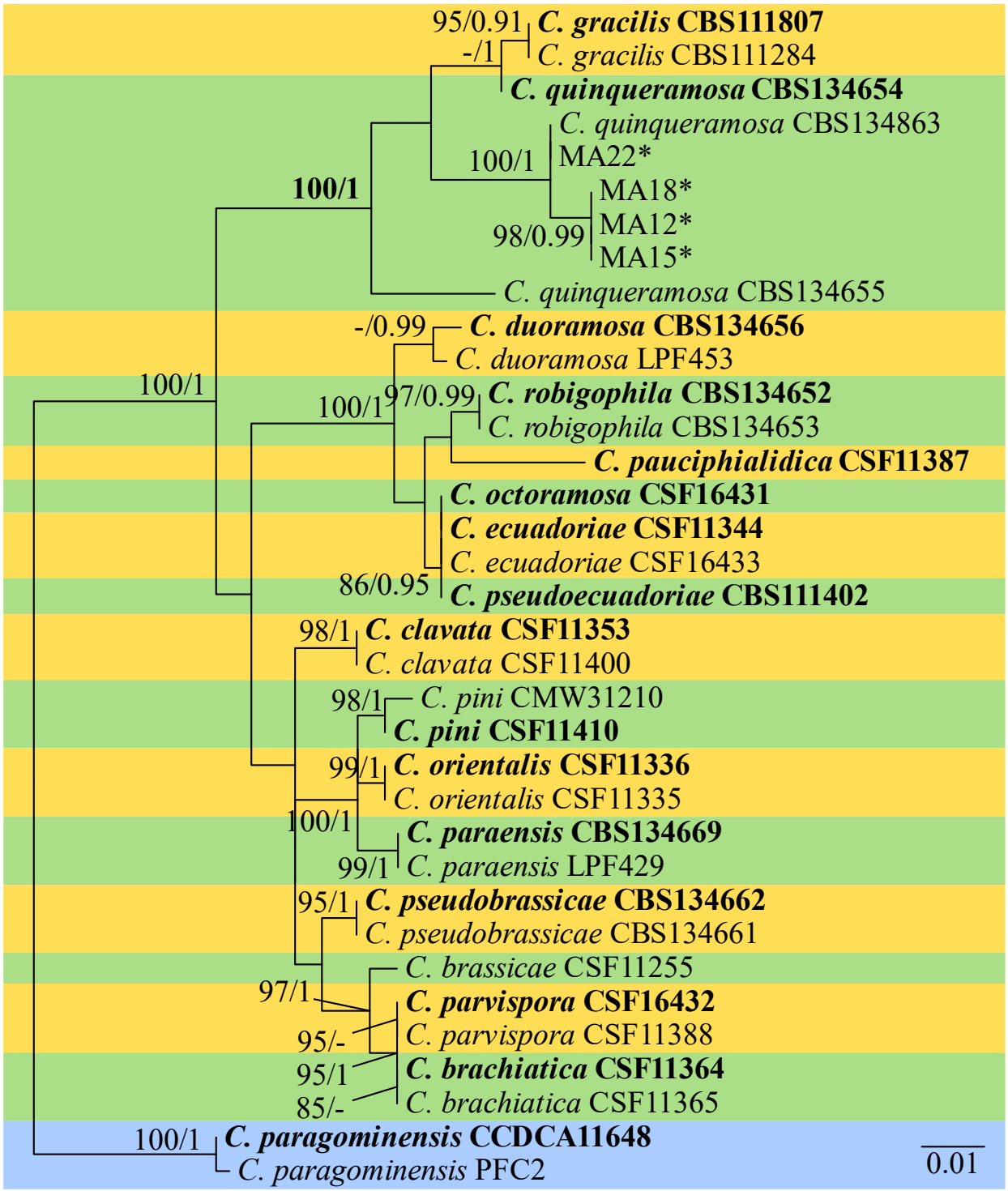

FIGURE 3S Phylogenetic tree of *Calonectria brassicae* species complex based on maximum likelihood analysis of *tef1* gene region. Support values of UFBoot2 (≥ 80%) and PP (≥ 0.90) are presented at the nodes (ML/BI). Values below 80% (UFBoot2) and 0.90 (PP) are marked with "-". Ex-type isolates are highlighted in bold, and "*" indicates isolates sequenced in this study. *C. paragominensis* was used as outgroup taxa. The number of nucleotide substitutions per site is indicated by the scale bar.

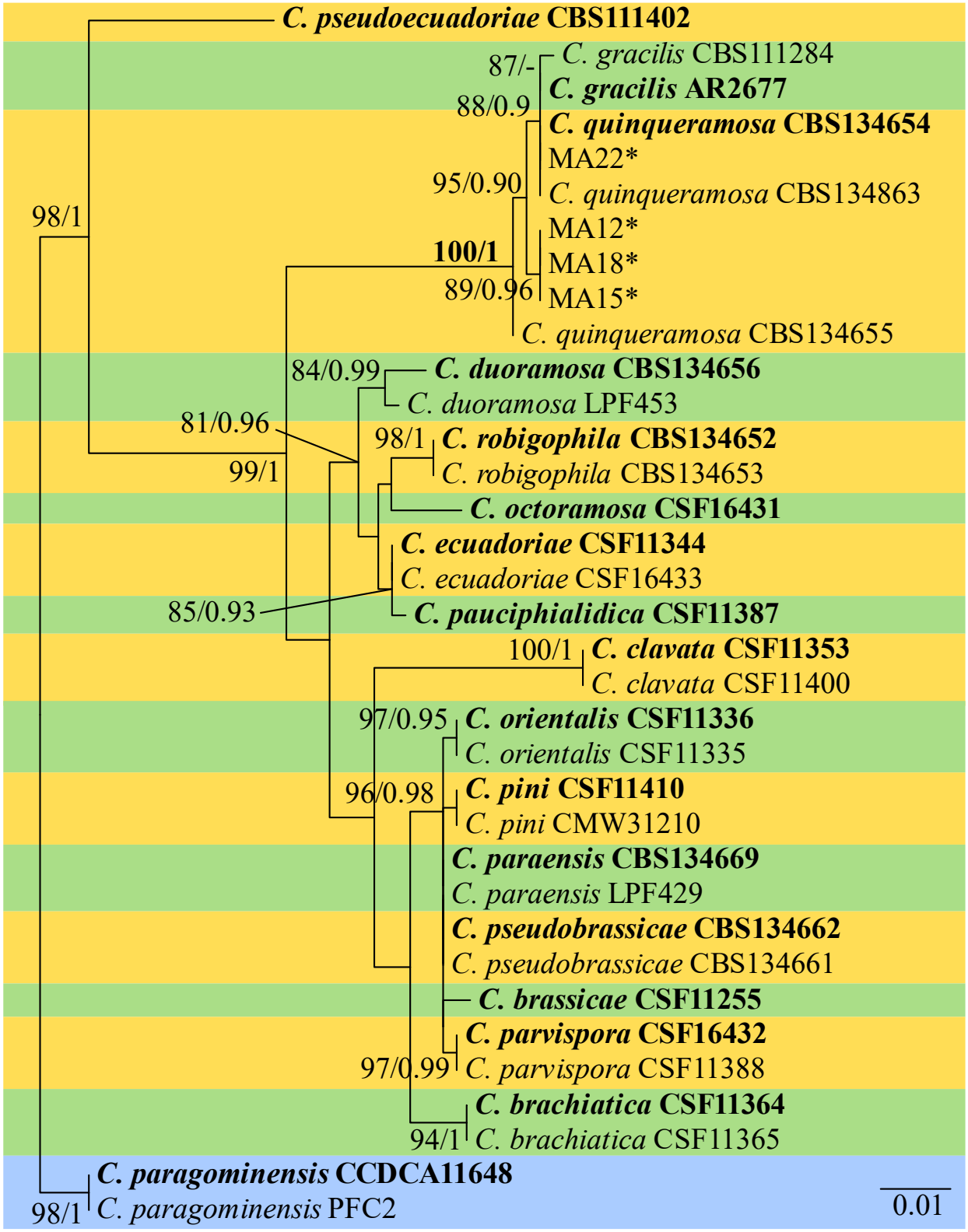

FIGURE 4S Phylogenetic tree of *Calonectria brassicae* species complex based on maximum likelihood analysis of *tub2* gene region. Support values of UFBoot2 (≥ 80%) and PP (≥ 0.90) are presented at the nodes (ML/BI). Values below 80% (UFBoot2) and 0.90 (PP) are marked with "-". Ex-type isolates are highlighted in bold, and "*" indicates isolates sequenced in this study. *C. paragominensis* was used as outgroup taxa. The number of nucleotide substitutions per site is indicated by the scale bar.

ARTICLE 3 – *Calonectria* SPECIES ASSOCIATED WITH *Eucalyptus* PLANTATIONS IN NORTHEASTERN BRAZIL: PHYLOGENY, MORPHOLOGY, AND MATING STRATEGY

Enrique I. Sanchez-Gonzalez[1], Thaissa de Paula Farias Soares[2], Talyta Galafassi Zarpelon[2], Edival Angelo Valverde Zauza[2], Reginaldo Gonçalves Mafia[2], Maria Alves Ferreira[1*]

[1] Universidade Federal de Lavras, Departamento de Fitopatologia, Lavras, MG, 37200-900, Brasil

[2] Suzano Papel e Celulose S. A. Centro de Tecnologia, Aracruz, ES, 29197-900, Brasil

*Corresponding author: M. A. Ferreira; mariaferreira@ufla.br

Article presented according with the guidelines of the *European Journal of Forest Research.*

Calonectria species associated with _Eucalyptus_ plantations in northeastern Brazil: phylogeny, morphology, and mating strategy

Enrique Ignacio Sánchez-González[1], Thaissa de Paula Farias Soares[2], Talyta Galafassi Zarpelon[2], Edival Angelo Valverde Zauza[2], Reginaldo Gonçalves Mafia[2], Maria Alves Ferreira[1]

[1] Universidade Federal de Lavras, Departamento de Fitopatologia, Lavras, MG, 37200-900, Brasil
E.I.S.G.: ei_sanchez@hotmail.com; ORCID: 0000-0002-0180-8154
M.A.F.: mariaferreira@ufla.br; ORCID: 0000-0001-9401-7142
[2] Suzano Papel e Celulose S. A. Centro de Tecnologia, Aracruz, ES, 29197-900, Brasil
T.P.F.S: ThaissaSoares.inova@suzano.com.br
T.G.Z.: talyta.zarpelon@suzano.com.br
E.A.V.Z.: edivalzauza@suzano.com.br; ORCID: 0000-0001-8322-7689
R.G.M.: rgoncalves@suzano.com.br

Correspondence
Maria Alves Ferreira, Email: mariaferreira@ufla.br; Tel: +55 (35) 3829-1799

Abstract
Calonectria leaf blight (CLB) has emerged as the main fungus-caused leaf disease in *Eucalyptus* plantations in the northern and northeastern Brazil's warm and humid regions. In order increase our knowledge about the species and genetic diversity, distribution, mating strategy and morphological characteristics of *Calonectria* in *Eucalyptus* plantations in northeastern Brazil, diseased leaves from *Eucalyptus* and soil samples were collected. Two hundred and two *Calonectria* isolates were obtained and identified based on multi-locus phylogenetic analyses of *act*, *cmdA, his3, rpb2, tef1* and t*ub*2 gene regions. The isolates were identified as *C. imperata* (48.7%), *C. amazonica* (24.9%), *C. ovata* (9.1%), *C. brasiliensis* (6.1%), *C. variabilis* (4.1%), *C. quinqueramosa* (3.6%), *C. paragominensis* (2%), and *C. maranhensis* (1.5%). The most prevalent species were *C. amazonica* and *C. imperata*, found in seven and six plantations, respectively. This is the first record of *C. amazonica* causing CLB in *E. urophylla.* MAT1-1-1 and MAT1-2-1 genes amplification showed that *C. maranhensis* is putative heterothallic, and that the asexual cycle is main reproductive mode of *C. amazonica*. *Calonectria imperata* presented the highest genetic diversity, with 17 genotypes in 96 isolates, followed by *C. brasiliensis* with 10 genotypes in 12 isolates. This study increased our knowledge about the species and genetic diversity, distribution, mating strategy and morphological characteristics of *Calonectria* in ten commercial *Eucalyptus* plantations located in the in northeastern Brazil, and this information could help build an efficient management plan for CLB in *Eucalyptus* plantations and the development of resistant *Eucalyptus* clones.

Keywords
Cylindrocladium, leaf blight, molecular phylogenetics, tree pathogen

1.Introducction

Calonectria species are among the most aggressive forestry pathogens, causing a variety of disease symptoms such as leaf and shoot blight, leaf spot, seedling blight, collar and root rot, cutting rot, damping-off and stem lesions (Crous 2002; Pham et al., 2022a). Brazil became one of the world's main producers of pulp, paper, and wood panels in 2021, with a productivity of 38.9 m^{3}·ha per year and a total area of 7.53 million hectares planted with *Eucalyptus* trees (IBÁ, 2022), and commercial *Eucalyptus* plantations have grown in recent years toward northern and northeastern Brazil's warm and humid regions, where Calonectria leaf blight (CLB) has emerged as the main fungus-caused leaf disease (Alfenas et al. 2015). The CLB has been reported in commercial plantations of *Eucalyptus*, primarily on *E. camaldulensis*, *E. benthanii*, *E. cloeziana*, *E. dunnii*, *E. grandis*, *E. saligna*, *E. tereticornis*, *E. urophylla* and the hybrid "urograndys" (*E. grandis* × *E. urophylla*) (Alfenas et al., 2009).

Various *Calonectria* species can cause CLB, affecting *Eucalyptus* plants from six months to 2–3 years after planting (Graça et al. 2009). The CLB is characterized in most *Eucalyptus* species by small, circular, or elongated pale grey to pale brown to dark brown spots that progress and extend throughout the leaf blade, resulting in leaf drop and, in some cases, severe defoliation (Alfenas et al. 2015). With the reduced photosynthetic area and the increased light entering through the subcanopy, the defoliation may decrease wood volume and encourage weed growth, which will cause *Eucalyptus* and understory plants to compete for resources, causing economic losses (Graça et al. 2009; Alfenas et al. 2015).

To date, 140 *Calonectria* species have been recognized based on multi-locus phylogenetic analysis and morphological comparisons (Crous et al. 2018, 2019, 2021a, 2021b; Wang et al. 2019; Liu et al. 2020, 2022; Mohali and Stewart 2021; Pham et al. 2022a, 2022b; Sanchez-Gonzalez et al. 2022; Zhang et al. 2022). These species are divided in eleven species complexes, which are *C. brassicae*, *C. candelabrum*, *C. colhounii*, *C. cylindrospora*, *C. gracilipes*, *C. mexicana*, *C. pteridis*, *C. reteaudii* and *C. spathiphylli* species complexes (in the Prolate Group), and *C. kyotensis* and *C. naviculata* species complexes (in the Sphaero-Naviculate Group) (Lombard et al. 2016; Liu et al. 2020). In Brazil, 37 *Calonectria* species have been described based in phylogenetic analyses and morphology, with 23 of them isolated from diseased tissues or soil samples of *Eucalyptus* plantations (Alfenas et al. 2015; Crous et al. 2018, 2019; Liu et al. 2020; Sanchez-Gonzalez et al. 2022).

Most species present in Brazil belong to the *C. candelabrum* species complex (17 species), followed by *C. brassicae* species complex (7 species), *C. cylindrospora* species complex (4 species), *C. pteridis* species complex (4 species), *C. gracilipes* species complex (2 species), *C. naviculata* species complex (2 species) and *C. spathiphylli* species complex (1 species), (Alfenas et al. 2015; Crous 2018, 2019; Liu et al. 2020; Sanchez-Gonzalez et al. 2022).

Species of the *C. pteridis* species complex are commonly reported to cause CLB on *Eucalyptus* plants in the field, while some species of the *C. candelabrum* species complex are reported to cause defoliation in the nurseries and *damping-off*. The highest species diversity found in *Eucalyptus* plantations appear to be

in the Brazilian states of Pará, Minas Gerais and Bahía, with fewer species recorded from the states of Maranhão and Piauí, and only single species from the states of Alagoas and Tocantins (Alfenas et al. 2015). *Calonectria* has both homothallic and heterothallic mating systems, but their sexual morphs are rarely seen in nature or laboratory culture (Li et al. 2020). Heterothallic species have a biallelic heterothallic mating system, with female structures (protoperithecia) spermatized by conidia or hyphae of an opposing mating type strain. Some species have retained the ability to recombine with other closely related species, though the progeny of these crosses has low fertility (Lombard et al. 2010a).

Previous studies have suggested that the species diversity of *Calonectria* associated with *Eucalyptus* plantations in Brazil can be high (Alfenas et al. 2015; Sanchez-Gonzalez et al. 2022). However, little is known about the diversity of *Calonectria* species found in *Eucalyptus* plantations in northeastern Brazil. During 2020 and 2021, disease surveys were carried out in ten *Eucalyptus* plantations located in the Brazilian´s states of Pará and Maranhão. Diseased leaves from *Eucalyptus* and soil samples were collected, and *Calonectria* isolates were obtained. Therefore, the aims of this study were (1) to identify the *Calonectria* isolates based on multi-locus phylogenetic analyses, (2) to determine the genotypic diversity within each *Calonectria* species, (3) to understand the mating strategy of each *Calonectria* species, (4) to determine the species diversity of *Calonectria* and its distribution in different *Eucalyptus* plantations.

2. Materials and Methods

2.1. Sample Collection and *Calonectria* isolation

During 2020 and 2021, disease surveys were performed in ten *Eucalyptus* plantations located in the states of Pará and Maranhão, Brazil. All the *Eucalyptus* genotypes presented typical symptoms of CLB (Fig. 1). Fifty diseased leaves and twenty-five soil samples (300 g in the 0–20 cm layer) were collected randomly from each *Eucalyptus* plantation (Table 1). The leaf samples were kept in paper bags, and the soil samples were stored in plastic bags to maintain moisture, both kind of samples were transferred to the Laboratory of Forest Pathology at the Universidade Federal de Lavras (UFLA) for further studies.

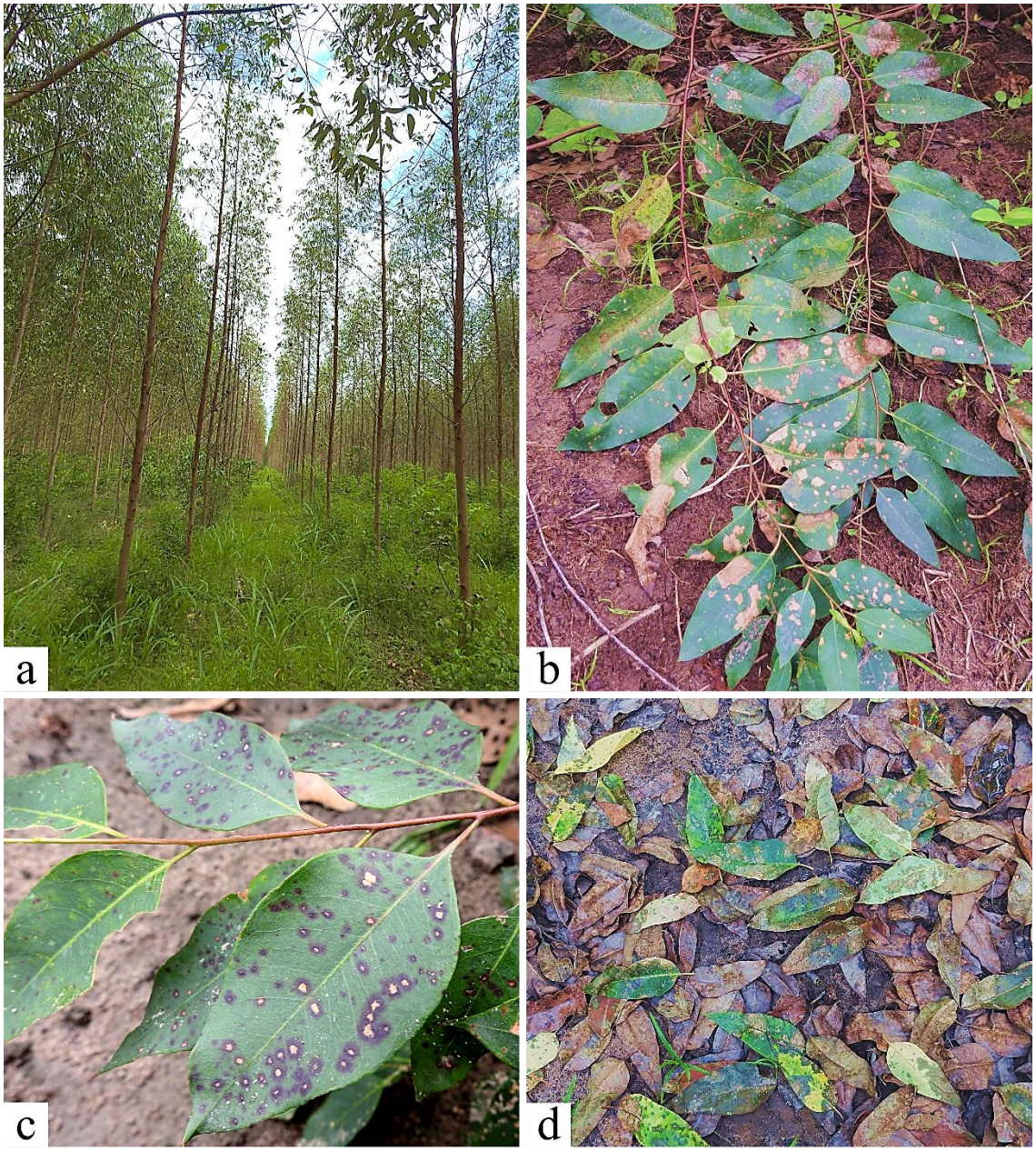

Fig. 1 *Eucalyptus* trees with Calonectria leaf blight symptoms under field conditions. (**a**) Defoliation associated to leaf blight; (**b**) Leaf blight symptoms ; (**c)** Leaf spot symptoms; (**d)** Infected leaves after defoliation on soil

Table 1 Number of *Calonectria* isolates obtained from leaves and soil samples per plantation sampled.

Plantation code	Location			Host	Age (years)	Isolates from leaves	Isolates from soil	Total Isolates
	City, State	Coordinates						
AN	Paragominas, Pará	3°06'47.1"S	47°28'17.4"W	*E. grandis x E. urophylla*	2.5	0	8	8
J	Paragominas, Pará	3°08'01.5"S	47°17'41.3"W	*E. urophylla*	0.5	5	5	10
VA	Paragominas, Pará	3°10'50.6"S	47°18'49.0"W	*E. grandis x E. brassiana*	1	23	0	23
AR	Dom Eliseu, Pará	4°05'23.4"S	47°33'57.2"W	*E. urophylla*	1	38	4	42
PR	Dom Eliseu, Pará	4°18'12.3"S	47°36'13.7"W	*E. urophylla*	0.5	1	0	1
P	Itinga do Maranhão, Maranhão	4°34'43.4"S	47°29'48.1"W	*E. urophylla*	2	14	11	25
SM	Açailândia, Maranhão	4°44'15.4"S	47°33'06.1"W	*E. urophylla*	0.5	46	5	51
MA	Cidelândia, Maranhão	5°09'13.5"S	47°37'19.9"W	*E. urophylla*	1	12	4	16
I	Imperatriz, Maranhão	5°12'43.9"S	47°37'21.0"W	*E. urophylla*	2.5	19	0	19
BF	Cidelândia, Maranhão	5°09'23.6"S	47°46'26.0"W	*E. urophylla*	0.5	2	0	2
Total						160	37	197

For *Calonectria* isolation from leaves and single spore cultures obtainment, the procedures indicated in our previous work (Sanchez-Gonzalez et al. 2022) were followed. For *Calonectria* isolation from the soil, each 200 g soil sample was deposited in plastic boxes (11 cm × 11 cm × 3.5 cm) and moistened with sterile distilled water. Leaves of *E. urophylla* were surface disinfested with 70% ethanol for 30 s, with 1% sodium hypochlorite for 1 min, and washed with sterilized water three times, then placed on the soil surface as biological bait. After 7 to 10 days at room temperature (26 ± 2 °C), conidiophores typical of *Calonectria* were observed on the leaves surface, and with a sterile needle conidia masses were scattered onto 2% malt extract agar (MEA; malt extract 20 $g \cdot L^{-1}$, agar 20 $g \cdot L^{-1}$, yeast extract 2 $g \cdot L^{-1}$, sucrose 5 $g \cdot L^{-1}$) plates and incubated at 25 °C for two hours. Single spore cultures were obtained by transferring the germinated conidia individually to fresh MEA plates and incubated at 25 °C for seven days. All the pure cultures were deposited as dry culture and in sterile water (Castellani 1939) in the mycological collection of the Laboratory of Forest Pathology at UFLA.

2.2. DNA extraction, PCR amplification and Sequencing

Genomic DNA was extracted from all the *Calonectria* isolates obtained from leaves and soil samples. The partial gene regions actin (*act*), calmodulin (*cmdA*), histone H3 (*his3*), RNA polymerase II (*rpb2*), translation elongation factor 1-alpha (*tef1*), and β-tubulin (*tub2*) were used to identify *Calonectria* species based on previous studies (Liu and Chen 2017; Liu et al. 2020). The DNA extraction and PCR amplification were performed following the procedures indicated in our previous study (Sanchez-Gonzalez et al. 2022). The successful PCR products were sent to Macrogen Inc. (Macrogen, Seoul, Korea) for purification and sequencing in forward and reverse directions, using the same primer pairs used for PCR. All the sequences obtained were edited with Chromas v. 2.6.6 (Technelysium Pty Ltd, South Brisbane, QLD, Australia) software, and assembled with SeqAssem software v. 07/2008 (Hepperle 2004).

2.3. Multi-locus Phylogenetic Analyses

Genotypes based on the sequences of the six gene regions for all the isolates obtained in this study and isolates obtained in our previous study (Sanchez-Gonzalez et al. 2022) were determined with the DnaSP v. 5.10 software (Librado and Rozas 2009). One representative isolate per each genotype was selected for phylogenetic analyses. The sequences of *act*, *cmdA*, *his3*, *rpb2*, *tef1* and *tub2* gene regions were used for standard nucleotide BLAST search, and sequences of closely related *Calonectria* species, including the ex-type isolates were obtained from GenBank when available. Sequence alignments were conducted following

the alignment strategy FFT-NS-i (Slow; interactive refinement method) in the online interface of MAFFT v. 7.0 (Katoh et al. 2019; http://mafft.cbrc.jp/alignment/server) and manually corrected using MEGA7 (Kumar et al. 2016). All the sequences generated in this study and used in the phylogenetic analyses were deposited in the GenBank database (http://www.ncbi.nlm.nih.gov).

Maximum Likelihood (ML) and Bayesian Inference (BI) analyses were conducted for each individual gene region and their concatenated dataset. The individual and partitioned ML analyses were performed with IQ-TREE (Nguyen et al. 2015) in the IQ-TREE web server (Chernomor et al. 2016; Trifinopoulos et al. 2016; http://iqtree.cibiv.univie.ac.at). The best nucleotide substitution models for ML analyses were obtained using ModelFinder (Kalyaanamoorthy et al. 2017) according to the Bayesian Information Criterion (BIC). The ML models used were K2P+I+G4 (act), TIM3e+G4 (cmdA), TIM3+F+I+G4 (his3), K2P+G4 (rpb2), TVMe+I+G4 (tef1) and K2P+G4 (tub2). Branch support values were calculated based on ultrafast bootstrapping (UFBoot2) with 10,000 replicates (Hoang et al. 2018). The individual and partitioned BI analyses were performed by the methods described in our previous study (Sanchez-Gonzalez et al. 2022) on XSEDE at the CIPRES Science Gateway v.3.3 (http://www.phylo.org/, accessed on 29 December 2022) with MrBayes v.3.2.7a (Ronquist et al. 2012). The BI models used were K80+I+G (act), SYM+G (cmdA), GTR+I+G (his3), SYM+I+G (rpb2), GTR+I+G (tef1) and HKY+I+G (tub2). In all the phylogenetic analyses, sequences of two isolates of *Calonectria gracilipes* (CBS 115674 and CBS 111141) were used as the outgroup taxa. The phylogenetic trees from ML and BI analyses were visualized with FigTree v. 1.4.4 (Rambaut 2009) and edited with Inkscape v. 1.0 (https://inkscape.org).

2.4. Species Diversity, Genotyping, and Distribution of *Calonectria* species

The species diversity per plantation and overall were calculated after all the *Calonectria* isolates were identified, and the number of isolates per species was recorded. The genotype diversity within each *Calonectria* species was determined based on the sequences of *act*, *cmdA*, *his3*, *rpb2*, *tef1*, and *tub2*, and the number of isolates for each genotype was registered.

2.5. Mating Type Identification by PCR

In order to know if genetic recombination through sexual reproduction could be possible in the populations of heterothallic species of *Calonectria*, the idiomorph of all isolates within each species was determined by PCR using the primer pairs Cal_MAT111_F/Cal_MAT111_R and Cal_MAT121_F/Cal_MAT121_R, which amplify the MAT1-1-1 and MAT1-2-1 genes, respectively, using the protocol described by Li et al. (2020). Additionally, four representative isolates of the *Calonectria* species considered homothallic were used for PCR amplification, to confirm their homothallic status.

2.6. Morphology

Three representative isolates for each *Calonectria* species were selected based on phylogenetic analyses for morphology comparison. The asexual characteristics commonly used for morphological comparison among *Calonectria* species are the size of macroconidia, macroconidia septation and the width of the vesicles (Liu et al. 2021; Wu and Chen 2021). For each isolate, the induction of asexual structures and its characterization

were performed as described by Liu and Chen (2017). Thirty replicate measurements of each morphological structure were made. The growth of each isolate was measured by incubating at 25°C on MEA plates in the dark (three replicates per isolate) after seven days.

3. Results

3.1. Sample Collection and *Calonectria* Isolation

A total of 500 leaf samples and 250 soil samples were collected randomly from the *Eucalyptus* plantations. From these, 197 *Calonectria*-like fungi were isolated, 160 isolated from the leaves and 37 isolated from the soil samples (Table 1). The total number of *Calonectria* isolates per plantation ranged from 1 to 51. For *Calonectria* isolated from leaves, no isolates were obtained from the plantation AN, while the plantations SM and AR presented the highest number of isolates, with 46 and 38, respectively. For *Calonectria* isolated from soil, only the samples from plantations AN, J, AR, P, SM and MA yield *Calonectria* isolates, while no isolates were obtained from plantations VA, PR, I, and BF (Table 1).

3.2. Multi-locus Phylogenetic Analyses

A total of 56 representative isolates for all the genotypes determined based on the six gene sequences were used for phylogenetic analyses (Table 2). Results of the BLAST search performed with *act*, *cmdA*, *his3*, *rpb2*, *tef1*, and *tub2* sequences showed that the isolates belonged to five species complexes of *Calonectria*, including *C. brassicae* species complex, *C. candelabrum* species complex, *C. cylindrospora* species complex, *C. pteridis* species complex, and *C. spathiphylli* species complex. Sequences of 64 *Calonectria* species closely related to the isolates from this study were downloaded from GenBank and used for phylogenetics analyses (Table 3).

Table 2 Representative *Calonectria* isolates used for phylogenetics analyses.

Species	Isolate code[a]	Genotype	Host/substrate	Country	Genbank accession numbers[b]					
					act	*cmdA*	*his3*	*rpb2*	*tef1*	*tub2*
C. amazonica	45BFB	AAAAAA	*E. urophylla*	Brazil:Cidelandia,MA	OQ261791	OQ262019	OQ262166	OQ262357	OQ262502	OQ262689
C. amazonica	AR42	AAABAB	*E. urophylla*	Brazil:Dom Eliseu,PA	OQ261821	OQ261989	OQ262196	OQ262381	OQ262531	OQ262719
C. amazonica	28PC	AAAAAC	*E. urophylla*	Brazil:Itinga do Maranhao,MA	OQ261776	OQ262008	OQ262151	OQ262342	OQ262487	OQ262675
C. amazonica	30PB	AAABBB	*E. urophylla*	Brazil:Itinga do Maranhao,MA	OQ261777	OQ262010	OQ262152	OQ262343	OQ262488	OQ262676
C. amazonica	J4	AAABAA	*E. urophylla*	Brazil:Microregion of Paragominas,MA	OQ261866	OQ262052	OQ262243	OQ262411	OQ262576	OQ262766
C. brasiliensis	SM28	ABABAA	*E. urophylla*	Brazil:Açailandia,MA	OQ261925	OQ262119	OQ262303	OQ262451	OQ262635	OQ262825
C. brasiliensis	MA33	AABACA	Soil	Brazil:Cidelandia,MA	OQ261883	OQ262073	OQ262260	OQ262419	OQ262593	OQ262783
C. brasiliensis	MA27	AAB-CB	Soil	Brazil:Cidelandia,MA	OQ261881	OQ262071	OQ262258	NA	OQ262591	OQ262781
C. brasiliensis	AR11	AAA-BA	*E. urophylla*	Brazil:Dom Eliseu,PA	OQ261806	OQ261978	OQ262181	NA	OQ262516	OQ262704
C. brasiliensis	AR67	ACAA-A	Soil	Brazil:Dom Eliseu,PA	OQ261837	OQ262003	OQ262213	OQ262391	NA	OQ262736
C. brasiliensis	J6	BDACAA	Soil	Brazil:Microregion of Paragominas,MA	OQ261868	OQ262054	OQ262245	OQ262413	OQ262578	OQ262768
C. brasiliensis	J7	ABADAA	Soil	Brazil:Microregion of Paragominas,MA	OQ261869	OQ262055	OQ262246	OQ262414	OQ262579	OQ262769
C. brasiliensis	J8	ACCEAA	Soil	Brazil:Microregion of Paragominas,MA	OQ261870	OQ262056	OQ262247	OQ262415	OQ262580	OQ262770
C. brasiliensis	J9	AEAAAA	Soil	Brazil:Microregion of Paragominas,MA	OQ261871	OQ262057	OQ262248	OQ262416	OQ262581	OQ262771
C. brasiliensis	P19	AAAFCB	*E. urophylla*	Brazil:Itinga do Maranhao,MA	OQ261898	OQ262093	OQ262275	OQ262428	OQ262608	OQ262798
C. imperata	AR20	AAAAAA	*E. urophylla*	Brazil:Dom Eliseu,PA	OQ261812	OQ261982	OQ262187	OQ262376	OQ262522	OQ262710
C. imperata	SM60	BAAAAA	Soil	Brazil:Açailandia,MA	OQ261952	OQ262141	OQ262329	OQ262476	OQ262662	OQ262852
C. imperata	P12	ABAAAA	*E. urophylla*	Brazil:Itinga do Maranhao,MA	OQ261891	OQ262086	OQ262268	OQ262424	OQ262601	OQ262791
C. imperata	I2	AAAABA	*E. urophylla*	Brazil:Imperatriz,MA	OQ261854	OQ262032	OQ262231	OQ262400	OQ262564	OQ262754
C. imperata	AR64	AAAAAB	*E. urophylla*	Brazil:Dom Eliseu,PA	OQ261834	OQ262000	OQ262210	OQ262389	OQ262543	OQ262733
C. imperata	I4	BAAAAB	*E. urophylla*	Brazil:Imperatriz,MA	OQ261856	OQ262034	OQ262233	OQ262402	OQ262566	OQ262756
C. imperata	I7	AAAABC	*E. urophylla*	Brazil:Imperatriz,MA	OQ261859	OQ262037	OQ262236	OQ262405	OQ262569	OQ262759
C. imperata	AR10	ABAAAD	*E. urophylla*	Brazil:Dom Eliseu,PA	OQ261805	OQ261977	OQ262180	OQ262371	OQ262515	OQ262703
C. imperata	AR62	BBAAAA	*E. urophylla*	Brazil:Dom Eliseu,PA	OQ261832	OQ261999	OQ262208	OQ262387	OQ262541	OQ262731
C. imperata	SM3	BAAABA	*E. urophylla*	Brazil:Açailandia,MA	OQ261927	OQ262100	OQ262305	OQ262453	OQ262637	OQ262827
C. imperata	P13	BAAAAE	*E. urophylla*	Brazil:Itinga do Maranhao,MA	OQ261892	OQ262087	OQ262269	OQ262425	OQ262602	OQ262792
C. imperata	AR39	ABAABC	*E. urophylla*	Brazil:Dom Eliseu,PA	OQ261819	OQ261988	OQ262194	OQ262380	OQ262529	OQ262717

C. imperata	MA19	AAA-AC	*E. urophylla*	Brazil:Cidelandia,MA	OQ261877	OQ262067	OQ262254	NA	OQ262587	OQ262777
C. imperata	SM63	CAA-AC	Soil	Brazil:Açailandia,MA	OQ261955	OQ262144	OQ262332	NA	OQ262665	OQ262855
C. imperata	AR68	AAA-AE	Soil	Brazil:Dom Eliseu,PA	OQ261838	OQ262004	OQ262214	NA	OQ262546	OQ262737
C. imperata	I14	BAAAAF	*E. urophylla*	Brazil:Imperatriz,MA	OQ261848	OQ262044	OQ262225	OQ262397	OQ262558	OQ262749
C. imperata	SM13	ABAAAB	*E. urophylla*	Brazil:Açailandia,MA	OQ261913	OQ262108	OQ262291	OQ262439	OQ262623	OQ262814
C. maranhensis	MA29	AAAAAA	Soil	Brazil:Cidelandia,MA	OQ261882	OQ262072	OQ262259	OQ262418	OQ262592	OQ262782
C. maranhensis	SM27	ABAAAA	*E. urophylla*	Brazil:Açailandia,MA	OQ261924	OQ262118	OQ262302	OQ262450	OQ262634	OQ262824
C. ovata	40AVA	AAAAAA	*E. grandis x E. brassiana*	Brazil:Microregion of Paragominas,MA	OQ261787	OQ262017	OQ262162	OQ262353	OQ262498	OQ262685
C. ovata	10VA	AAABAA	*E. grandis x E. brassiana*	Brazil:Microregion of Paragominas,MA	OQ261772	OQ262016	OQ262147	OQ262338	OQ262483	OQ262671
C. ovata	44VAB	ABAAAA	*E. grandis x E. brassiana*	Brazil:Microregion of Paragominas,MA	OQ261790	OQ262011	OQ262165	OQ262356	OQ262501	OQ262688
C. ovata	7FVA	AAAAAB	*E. grandis x E. brassiana*	Brazil:Microregion of Paragominas,MA	OQ261795	OQ262015	OQ262170	OQ262361	OQ262505	OQ262693
C. ovata	SM22	AAABA-	*E. urophylla*	Brazil:Açailandia,MA	OQ261920	OQ262114	OQ262298	OQ262446	OQ262630	NA
C. ovata	32AVA2	AAACAA	*E. grandis x E. brassiana*	Brazil:Microregion of Paragominas,MA	OQ261780	OQ262023	OQ262155	OQ262346	OQ262491	OQ262679
C. ovata	AN3	AAADAA	Soil	Brazil:Microregion of Paragominas,MA	OQ261798	OQ261962	OQ262173	OQ262364	OQ262508	OQ262696
C. ovata	AN7	AAAEAB	Soil	Brazil:Microregion of Paragominas,MA	OQ261802	OQ261966	OQ262177	OQ262368	OQ262512	OQ262700
C. paragominensis	PFC2	AAAACA	*E. grandis* × *E. brassiana*	Brazil:Microregion of Paragominas,MA	ON009347	OM974326	OM974335	OM974344	OM974353	OM974362
C. paragominensis	PFC3	AAAABB	*E. grandis* × *E. brassiana*	Brazil:Microregion of Paragominas,MA	ON009348	OM974327	OM974336	OM974345	OM974354	OM974363
C. paragominensis	PFC4	ABAABA	*E. grandis* × *E. brassiana*	Brazil:Microregion of Paragominas,MA	ON009349	OM974328	OM974337	OM974346	OM974355	OM974364
C. paragominensis	PFC5	AABAAA	*E. grandis* × *E. brassiana*	Brazil:Microregion of Paragominas,MA	ON009350	OM974329	OM974338	OM974347	OM974356	OM974365
C. quinqueramosa	SM61	ABB-BA	Soil	Brazil:Açailandia,MA	OQ261953	OQ262142	OQ262330	NA	OQ262663	OQ262853
C. quinqueramosa	AR66	AAA-AC	Soil	Brazil:Dom Eliseu,PA	OQ261836	OQ262002	OQ262212	NA	OQ262545	OQ262735
C. quinqueramosa	AN4	AAABAB	Soil	Brazil:Microregion of Paragominas,MA	OQ261799	OQ261963	OQ262174	OQ262365	OQ262509	OQ262697
C. quinqueramosa	AN8	AAADAB	Soil	Brazil:Microregion of Paragominas,MA	OQ261803	OQ261967	OQ262178	OQ262369	OQ262513	OQ262701
C. quinqueramosa	AN6	BAACAB	Soil	Brazil:Microregion of Paragominas,MA	OQ261801	OQ261965	OQ262176	OQ262367	OQ262511	OQ262699
C. quinqueramosa	J10	AAC-AC	Soil	Brazil:Microregion of Paragominas,MA	OQ261863	OQ262058	OQ262240	NA	OQ262573	OQ262763

C. quinqueramosa	AN5	ABDACD	Soil	Brazil:Microregion of Paragominas,MA	OQ261800	OQ261964	OQ262175	OQ262366	OQ262510	OQ262698
C. variabilis	26BVA	CAAAAA	*E. grandis x E. brassiana*	Brazil:Microregion of Paragominas,MA	OQ261775	OQ262018	OQ262150	OQ262341	OQ262486	OQ262674
C. variabilis	37DVA	BAAAAA	*E. grandis x E. brassiana*	Brazil:Microregion of Paragominas,MA	OQ261786	OQ262026	OQ262161	OQ262352	OQ262497	NA
C. variabilis	SM2	AAAAAA	*E. urophylla*	Brazil:Açailandia,MA	OQ261917	OQ262099	OQ262295	OQ262443	OQ262627	OQ262818

[a] Laboratorio de Patologia Florestal, Universidade Federal de Lavras, Lavras, Brazil.

[b] *act*: actin; *cmdA*: calmodulin; *his3*: histone H3; *rpb2*: RNA polymerase II; *tef1*: translation elongation factor 1-alpha; *tub2*: β-tubulin. N/A = Not available.

Table 3 *Calonectria* species and GenBank accession numbers of DNA sequences used in this study.

Species complex	***Species***	**Isolate representing the species**[a,b]	**Other isolate numbers**	***Host/ Substrate***	**Country**	**Genbank accession numbers**[c]					
						act	***cmdA***	***his3***	***rpb2***	***tef1***	***tub2***
Calonectria spathiphylli species complex	*C. densa*	**CMW 31182**		Soil	Ecuador	GQ280525	GQ267444	GQ267281	N/A	GQ267352	GQ267232
		CMW 31184		Soil	Ecuador	GQ280523	GQ267442	GQ267279	N/A	GQ267350	GQ267230
		CMW 31185		Soil	Ecuador	GQ280524	GQ267443	GQ267280	N/A	GQ267351	GQ267231
	C. humicola	**CMW 31183**		Soil	Ecuador	GQ280526	GQ267445	GQ267282	N/A	GQ267353	GQ267233
		CMW 31186		Soil	Ecuador	GQ280527	GQ267446	GQ267283	N/A	GQ267354	GQ267234
		CMW 31187		Soil	Ecuador	GQ280528	GQ267447	GQ267284	N/A	GQ267355	GQ267235
	C. paragominensis	**CCDCA 11648**		*E. grandis* × *E. brassiana*	Brazil	ON009346	OM974325	OM974334	OM974343	OM974352	OM974361
		PFC5		*E. grandis* × *E. brassiana*	Brazil	ON009350	OM974329	OM974338	OM974347	OM974356	OM974365
	C. pseudospathiphylli	**CBS 109165**	CPC 1623	Soil	Ecuador	GQ280493	GQ267412	AF348241	KY653435	FJ918562	AF348225
		CPC 1641		Soil	Ecuador	N/A	N/A	AF348233	N/A	N/A	AF348217
	C. spathiphylli	**CBS 114540**	ATCC44730, CSF11330	*Spathiphyllum sp.*	USA	GQ280505	GQ267424	AF348230	MT412666	GQ267330	AF348214
		CBS 116168	CSF 11401	*Spathiphyllum sp.*	Switzerland	GQ280506	GQ267425	FJ918530	MT412667	FJ918561	FJ918512
Calonectria candelabrum species complex	*C. brasiliana*	**CBS 111484**	CSF 11249	Soil	Brazil	MT334968	MT335198	MT335438	MT412502	MT412729	MT412951
		CBS 111485	CSF 11250	Soil	Brazil	MT334969	MT335199	MT335439	MT412503	MT412730	MT412952
	C. brassiana	**CBS 134855**		Soil	Brazil	N/A	KM396056	KM396139	N/A	KM395882	KM395969
		CBS 134856		Soil	Brazil	N/A	KM396057	KM396140	N/A	KM395883	KM395970
	C. brevistipitata	**CBS 115671**	CSF 11288	Soil	Mexico	MT334973	MT335203	MT335443	MT412507	MT412734	MT412956
		CBS 110928	CSF 11235	Soil	Mexico	MT334974	MT335204	MT335444	MT412508	MT412735	MT412957
	C. candelabrum	CMW 31000	CSF 11404	*Eucalyptus sp.*	Brazil	MT334977	MT335207	MT335447	MT412511	MT412738	MT412959
		CMW 31001	CSF 11405	*Eucalyptus sp.*	Brazil	MT334978	MT335208	MT335448	MT412512	MT412739	MT412960

C. colombiana	**CBS 115127**		Soil	Colombia	GQ280538	GQ267455	FJ972442	N/A	FJ972492	FJ972423
	CBS 115638		Soil	Colombia	GQ280539	GQ267456	FJ972441	N/A	FJ972491	FJ972422
C. eucalypticola	**CBS 134847**		*Eucalyptus sp.*	Brazil	N/A	KM396051	KM396134	N/A	KM395877	KM395964
	CBS 134846		*Eucalyptus sp.*	Brazil	N/A	KM396050	KM396133	N/A	KM395876	KM395963
C. exiguispora	**CMW 49752**		Soil	Colombia	OP796405	OP822275	OP822382	OP822489	OP822168	OP822596
	CMW 49753		Soil	Colombia	OP796406	OP822276	OP822383	OP822490	OP822169	OP822597
C. fragariae	**CBS 133607**		*Fragaria × ananassa*	Brazil	N/A	KM998966	KM998964	N/A	KM998963	KM998965
	LPF 141.1		*Fragaria × ananassa*	Brazil	N/A	KX500191	KX500194	N/A	KX500197	KX500195
C. glaebicola	**CBS 134852**		Soil	Brazil	N/A	KM396053	KM396136	N/A	KM395879	KM395966
	CBS 134853		*Eucalyptus sp.*	Brazil	N/A	KM396054	KM396137	N/A	KM395880	KM395967
C. hemileiae	**COAD 2544**		*Hemileia vastatrix*	Brazil	N/A	MK037392	MK006026	N/A	MK006027	MK037391
C. imperata	**CCDCA 11649**		*E. urophylla*	Brazil	ON009351	OM974330	OM974339	OM974348	OM974357	OM974366
	PFC9		*E. urophylla*	Brazil	ON009354	OM974333	OM974342	OM974351	OM974360	OM974369
C. matogrossensis	**GFP 006**		*E. urophylla*	Brazil	N/A	MH837653	MH837648	N/A	MH837659	MH837664
	GFP 018		*E. urophylla*	Brazil	N/A	MH837657	MH837652	N/A	MH837663	MH837668
C. metrosideri	**CBS 133603**		*Metrosideros polymorpha*	Brazil	N/A	KC294304	KC294307	N/A	KC294310	KC294313
	CBS 133604	CSF 11309	*M. polymorpha*	Brazil	MT335056	MT335288	MT335528	MT412585	MT412819	MT413033
C. nemoricola	**CBS 134837**		Soil	Brazil	N/A	KM396066	KM396149	N/A	KM395892	KM395979
	CBS 134838		Soil	Brazil	N/A	KM396067	KM396150	N/A	KM395893	KM395980
C. pauciramosa	**CBS 138824**	CSF 16461	Soil	South Africa	MT335093	MT335325	MT335565	MT412618	MT412856	MT413068
	CMW 31474	CSF 11422	*E. urophylla × E. grandis*	China	MT335104	MT335336	MT335576	MT412629	MT412867	MT413079
C. piauiensis	**CBS 134850**		Soil	Brazil	N/A	KM396060	KM396143	N/A	KM395886	KM395973
	CBS 134851		Soil	Brazil	N/A	KM396061	KM396144	N/A	KM395887	KM395974
C. pseudometrosideri	**CBS 134845**		Soil	Brazil	N/A	KM395995	KM396083	N/A	KM395821	KM395909

		CBS 134843		*M. polymorpha*	Brazil	N/A	KM395993	KM396081	N/A	KM395819	KM395907
	C. pseudospathulata	**CBS 134841**		Soil	Brazil	N/A	KM396070	KM396153	N/A	KM395896	KM395983
		CBS 134840		Soil	Brazil	N/A	KM396069	KM396152	N/A	KM395895	KM395982
	C. putriramosa	**CBS 111449**	CSF 11246	*Eucalyptus cutting*	Brazil	MT335129	MT335364	MT335604	MT412657	MT412895	MT413105
		CBS 111470	CSF 11247	Soil	Brazil	MT335130	MT335365	MT335605	MT412658	MT412896	MT413106
	C. silvicola	**CBS 135237**	LPF081	Soil	Brazil	N/A	KM396065	KM396148	N/A	KM395891	KM395978
		CBS 134836		Soil	Brazil	N/A	KM396062	KM396145	N/A	KM395888	KM395975
	C. spathulata	**CMW 16744**	CSF 11331	*E. viminalis*	Brazil	MT335139	MT335376	MT335616	MT412668	MT412907	MT413117
		CBS 112513	CSF 11259	*Eucalyptus sp.*	Colombia	MT335140	MT335377	MT335617	MT412669	MT412908	MT413118
	C. venezuelana	**CBS 111052**	CSF 11238	Soil	Venezuela	MT335155	MT335394	MT335634	MT412685	MT412925	MT413132
Calonectria brassicae species complex	*C. brachiatica*	**CMW 25298**	CSF11364	*Pinus maximinoi*	Colombia	N/A	MT335195	MT335435	MT412499	MT412726	MT412948
		CMW 25302	CSF11365	*P. tecunumanii*	Colombia	N/A	MT335196	MT335436	MT412500	MT412727	MT412949
	C. brassicae	**CBS 111869**	CSF11255	*Argyreia splendens*	Indonesia	MT334972	MT335202	MT335442	MT412506	MT412733	MT412955
	C. clavata	**CMW 23690**	CSF11353	*Callistemon viminalis*	USA	MT334993	MT335223	MT335463	MT412527	MT412754	MT412975
		CMW 30994	CSF11400	*Root debris in peat*	USA	MT334994	MT335224	MT335464	MT412528	MT412755	MT412976
	C. duoramosa	**CBS 134656**		Soil	Brazil	N/A	KM396027	KM396110	N/A	KM395853	KM395940
		LPF453		Soil	Brazil	N/A	KM396028	KM396111	N/A	KM395854	KM395941
	C. ecuadorae	**CMW 23677**	CSF11344	Soil	Ecuador	MT335012	MT335242	MT335482	MT412544	MT412773	MT412991
		CBS 111706	CSF16433	Soil	Ecuador	MT335010	MT335240	MT335480	MT412542	MT412771	MT412989
	C. gracilis	**CBS 111807**	AR2677	*Manilkara zapota*	Brazil	GQ280488	GQ267407	DQ190646	KY653390	GQ267323	AF232858
		CBS 111284		Soil	Brazil	GQ280489	GQ267408	DQ190647	KY653389	GQ267324	DQ190567
	C. octoramosa	**CBS 111423**	CSF16431	Soil	Ecuador	MT335071	MT335303	MT335543	MT412600	MT412834	MT413048
	C. orientalis	**CMW 20291**	CSF11336	Soil	Indonesia	MT335072	MT335304	MT335544	MT412601	MT412835	MT413049
		CMW 20273	CSF11335	Soil	Indonesia	MT335073	MT335305	MT335545	MT412602	MT412836	MT413050

	C. paraensis	**CBS 134669**		Soil	Brazil	N/A	KM396011	KM396094	N/A	KM395837	KM395924
		LPF429		Soil	Brazil	N/A	KM396015	KM396098	N/A	KM395841	KM395928
	C. parvispora	**CBS 111465**	CSF16432	Soil	Brazil	MT335082	MT335314	MT335554	MT412607	MT412845	MT413057
		CMW 30981	CSF11388	Soil	Brazil	MT335081	MT335313	MT335553	MT412606	MT412844	MT413056
	C. pauciphialidica	**CMW 30980**	CSF11387	Soil	Ecuador	MT335083	MT335315	MT335555	MT412608	MT412846	MT413058
	C. pini	**CMW 31209**	CSF11410	*P. patula*	Colombia	MT335107	MT335339	MT335579	MT412632	MT412870	MT413082
		CMW 31210		*P. patula*	Colombia	GQ280518	GQ267437	GQ267274	N/A	GQ267345	GQ267225
	C. pseudobrassicae	**CBS 134662**		Soil	Brazil	N/A	KM396023	KM396106	N/A	KM395849	KM395936
		CBS 134661		Soil	Brazil	N/A	KM396022	KM396105	N/A	KM395848	KM395935
	C. pseudoecuadoriae	**CBS 111402**		Soil	Ecuador	N/A	KX784589	N/A	KY653432	KX784723	KX784652
	C. quinqueramosa	**CBS 134654**		Soil	Brazil	N/A	KM396029	KM396112	N/A	KM395855	KM395942
		CBS 134655		Soil	Brazil	N/A	KM396030	KM396113	N/A	KM395856	KM395943
	C. robigophila	**CBS 134652**		*Eucalyptus sp.*	Brazil	N/A	KM396024	KM396107	N/A	KM395850	KM395937
		CBS 134653		*Eucalyptus sp.*	Brazil	N/A	KM396025	KM396108	N/A	KM395851	KM395938
Calonectria cylindrospora species complex	*C. auriculiformis*	**CMW 47178**	CSF11445	Soil	Vietnam	MT334964	MT335190	MT335430	MT412494	MT412721	MT412944
		CMW 47179	CSF11446	Soil	Vietnam	N/A	MT335191	MT335431	MT412495	MT412722	MT412945
	C. brasiliensis	**CBS 230.51**	CSF11225	*Eucalyptus sp.*	Brazil	MT334970	MT335200	MT335440	MT412504	MT412731	MT412953
		CMW 32949	CSF11426	*Eucalyptus sp.*	Brazil	MT334971	MT335201	MT335441	MT412505	MT412732	MT412954
	C. cerciana	**CMW 25309**	CSF11367	*E. urophylla* × *E. grandis*	China	MT334981	MT335211	MT335451	MT412515	MT412742	MT412963
		CMW 25290	CSF11362	*E. urophylla* × *E. grandis*	China	MT334982	MT335212	MT335452	MT412516	MT412743	MT412964
	C. cylindrospora	CBS 119670	CSF11299	*Pistacia lentiscus*	Italy	MT335006	MT335236	MT335476	MT412540	MT412767	MT412985
		CMW 30978	CSF11385	*Ilex vomitoria*	USA	MT335007	MT335237	MT335477	MT412541	MT412768	MT412986
	C. hawksworthii	**CBS 111870**	CSF11256	*Nelumbo nucifera*	Mauritius	MT335024	MT335254	MT335494	MT412556	MT412785	MT413003
		CMW 14878	CSF11321	*Eucalyptus sp.*	Indonesia	MT335141	MT335378	MT335618	MT412670	MT412909	MT413119
	C. insularis	**CMW 30991**	CSF11397	Soil	Madagascar	N/A	MT335269	MT335509	MT412567	MT412800	MT413017

		CMW 30992	CSF11398	Soil	Mexico	N/A	MT335270	MT335510	MT412568	MT412801	MT413018
	C. lageniformis	**CBS 111324**		*Eucalyptus sp.*	,Mauritius	N/A	KX784574	N/A	KY653400	KX784702	KX784632
	C. maranhensis	**CBS 134811**		*Eucalyptus sp.*	Brazil	N/A	KM396035	KM396118	N/A	KM395861	KM395948
		CBS 134812		*Eucalyptus sp.*	Brazil	N/A	KM396036	KM396119	N/A	KM395862	KM395949
	C. plurilateralis	**CBS 111401**		Soil	Ecuador	N/A	MT335340	MT335580	KY653430	KX784719	KX784648
		CSF 11243		Soil	Ecuador	N/A	N/A	N/A	MT412633	MT412871	MT413083
	C. propaginicola	**CBS 134815**		*Eucalyptus sp.*	Brazil	N/A	KM396040	KM396123	N/A	KM395866	KM395953
		CBS 134816		*Eucalyptus sp.*	Brazil	N/A	KM396041	KM396124	N/A	KM395867	KM395954
	C. tonkinensis	**CMW 47430**		Soil	Vietnam	MT335147	MT335384	MT335624	N/A	MH119225	MH119291
		CSF 11452		Soil	Vietnam	N/A	N/A	N/A	MT412676	MT412915	MT413122
	C. variabilis	**CMW 3187**	CSF11312	*Schefflera morototoni*	Brazil	N/A	MT335392	MT335632	MT412683	MT412923	MT413130
		CMW 2914	CSF11311	*Theobroma grandiflorum*	Brazil	N/A	MT335393	MT335633	MT412684	MT412924	MT413131
Calonectria pteridis species complex	*C. amazonica*	**CBS116250**	CSF11296	*E. tereticornis*	Brazil	MT334955	MT335182	MT335421	MT412488	MT412712	MT412935
		CBS 115486	CSF11285	*E. tereticornis*	Brazil	MT334956	MT335183	MT335422	MT412489	MT412713	MT412936
	C. gordoniae	**CMW 23694**	CSF11356	*Gordonia lasianthus*	USA	MT335021	MT335251	MT335491	MT412553	MT412782	MT413000
		CBS 112142	CBS 112142, ATCC 201837			GQ280453	GQ267381	DQ190708	KY653386	GQ267309	AF449449
	C. guahibo	**CMW 49791**		Soil	Colombia	OP796480	OP822350	OP822457	OP822564	OP822243	OP822671
		CMW 49790		Soil	Colombia	OP796479	OP822349	OP822456	OP822563	OP822242	OP822670
	C. ovata	**CMW 16724**	CSF11327	*E. urophylla*	Brazil	MT335075	MT335307	MT335547	N/A	MT412838	MT413052
		CMW 30979	CSF11386	*E. tereticornis*	Brazil	MT335076	MT335308	MT335548	N/A	MT412839	MT413053
	C. pseudopteridis	**CBS 163.28**	CSF11224	*Washingtonia robusta*	USA	MT335112	MT335347	MT335587	MT412640	MT412878	N/A
	C. pseudovata	**CBS 134674**		Soil	Brazil	N/A	KM396032	KM396115	N/A	KM395858	KM395945
		CBS 134675		Soil	Brazil	N/A	KM396033	KM396116	N/A	KM395859	KM395946
	C. pteridis	**CBS 111793**		*Arachniodes adiantiformis*	USA	GQ280494	GQ267413	DQ190679	KY653438	FJ918563	DQ190578

		CBS 111871				GQ280495	GQ267414	DQ190681	KY653439	FJ918564	DQ190580
	C. terricola	**CBS 116247**		Soil	Brazil	N/A	N/A	N/A	N/A	KX784738	KX784665
		CBS 116248		Soil	Brazil	N/A	N/A	N/A	N/A	KX784739	KX784666
Calonectria gracilipes species complex	*C. gracilipes*	**CBS 115674**	CSF 11289	Soil	Colombia	MT335022	MT335252	MT335492	MT412554	MT412783	MT413001
		CBS 111141	CSF11239	Soil	Colombia	MT335023	MT335253	MT335493	MT412555	MT412784	MT413002

[a] Ex-type isolates are marked in bold.

[b] ATCC: American Type Culture Collection, Virginia, USA; CBS: Westerdijk Fungal Biodiversity Institute, Utrecht, The Netherlands; CCDCA: Coleção de Culturas de Microrganismos do Departamento de Ciência dos Alimentos/UFLA, Lavras, Brazil; CMW: Culture collection of the Forestry and Agricultural Biotechnology Institute (FABI), University of Pretoria, Pretoria, South Africa; COAD: Coleção Octávio de Almeida Drumond, Universidade Federal de Viçosa, Viçosa, Brazil; CPC: Pedro Crous working collection housed at Westerdijk Fungal Biodiversity Institute; CSF: Culture Collection located at China Eucalypt Research Centre (CERC), Chinese Academy of Forestry, ZhanJiang, GuangDong Province, China; GFP: Universidade Federal de Brasilia, Brasilia, Brazil; LPF: Laboratorio de Patologia Florestal, Universidade Federal de Viçosa, Viçosa, Brazil; PFC: Laboratorio de Patologia Florestal, Universidade Federal de Lavras, Lavras, Brazil.

[c] *act*: actin; *cmdA*: calmodulin; *his3*: histone H3; *rpb2*: RNA polymerase II; *tef1*: translation elongation factor 1-alpha; *tub2*: β-tubulin. N/A = Not available.

The alignments, including gaps were as follows: *act* (124 taxa, 256 bp), *cmdA* (172 taxa, 627 bp), *his3* (171 taxa, 437 bp), *rpb2* (116 taxa, 863 bp), *tef1* (175 taxa, 511 bp), *tub2* (175 taxa, 523 bp) and concatenated (177 taxa, 3217 bp). The concatenated dataset had 871 parsimony-informative characters, 107 parsimony-uninformative characters, and 2239 constant characters. For the individual and partitioned BI analyses, the convergence of the chains was confirmed by an effective sampling site (ESS) > 200, a potential scale reduction factor (PSRF) = 1, and an average standard deviation of split frequencies (ASDSF) ≤ 0.01.

Topologies of the phylogenetic trees derived from the ML and BI analyses were similar. Well-supported lineages were formed in the tree from the concatenated dataset, in both ML and BI analyses. Thus, only ML trees are presented in this study (Fig. 2, Supplementary Figs. S1–S6) with the UFBoot2 support values and posterior probabilities (PP) showed at the nodes (ML/BI). For the 56 representative isolates included in the phylogenetic analyses, 17 isolates resided in the *C. candelabrum* species complex, 15 in the *C. cylindrospora* species complex, 13 in the *C. pteridis* species complex, seven in the *C. brassicae* species complex and four in the *C. spathiphylli* species complex.

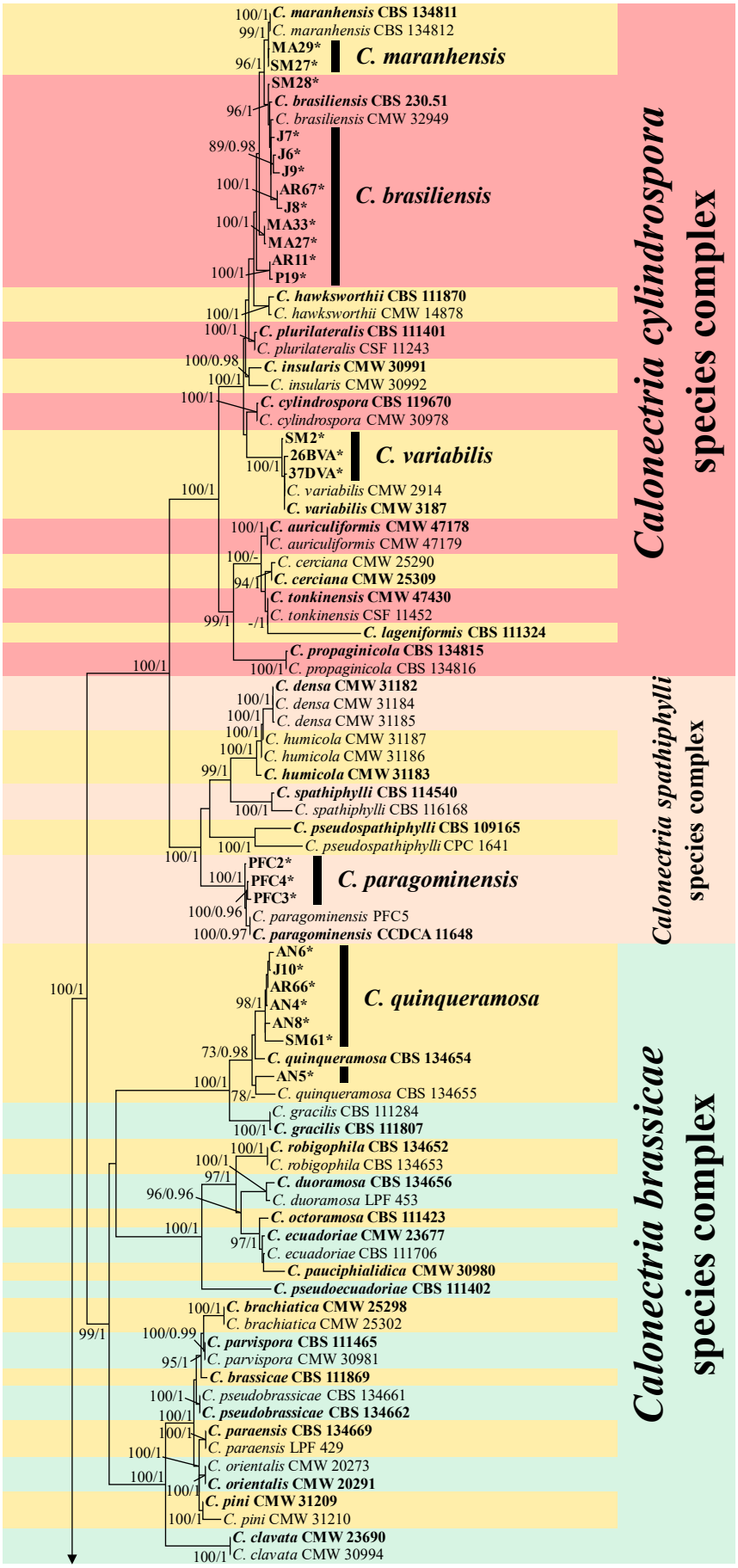
C. maranhensis CBS 134811
C. maranhensis CBS 134812
MA29*
SM27*
C. maranhensis
SM28*
C. brasiliensis CBS 230.51
C. brasiliensis CMW 32949
J7*
J6*
J9*
AR67*
J8*
MA33*
MA27*
AR11*
P19*
C. brasiliensis
C. hawksworthii CBS 111870
C. hawksworthii CMW 14878
C. plurilateralis CBS 111401
C. plurilateralis CSF 11243
C. insularis CMW 30991
C. insularis CMW 30992
C. cylindrospora CBS 119670
C. cylindrospora CMW 30978
SM2*
26BVA*
37DVA*
C. variabilis
C. variabilis CMW 2914
C. variabilis CMW 3187
C. auriculiformis CMW 47178
C. auriculiformis CMW 47179
C. cerciana CMW 25290
C. cerciana CMW 25309
C. tonkinensis CMW 47430
C. tonkinensis CSF 11452
C. lageniformis CBS 111324
C. propaginicola CBS 134815
C. propaginicola CBS 134816
Calonectria cylindrospora species complex
C. densa CMW 31182
C. densa CMW 31184
C. densa CMW 31185
C. humicola CMW 31187
C. humicola CMW 31186
C. humicola CMW 31183
C. spathiphylli CBS 114540
C. spathiphylli CBS 116168
C. pseudospathiphylli CBS 109165
C. pseudospathiphylli CPC 1641
PFC2*
PFC4*
PFC3*
C. paragominensis
C. paragominensis PFC5
C. paragominensis CCDCA 11648
Calonectria spathiphylli species complex
AN6*
J10*
AR66*
AN4*
AN8*
SM61*
C. quinqueramosa
C. quinqueramosa CBS 134654
AN5*
C. quinqueramosa CBS 134655
C. gracilis CBS 111284
C. gracilis CBS 111807
C. robigophila CBS 134652
C. robigophila CBS 134653
C. duoramosa CBS 134656
C. duoramosa LPF 453
C. octoramosa CBS 111423
C. ecuadoriae CMW 23677
C. ecuadoriae CBS 111706
C. pauciphialidica CMW 30980
C. pseudoecuadoriae CBS 111402
C. brachiatica CMW 25298
C. brachiatica CMW 25302
C. parvispora CBS 111465
C. parvispora CMW 30981
C. brassicae CBS 111869
C. pseudobrassicae CBS 134661
C. pseudobrassicae CBS 134662
C. paraensis CBS 134669
C. paraensis LPF 429
C. orientalis CMW 20273
C. orientalis CMW 20291
C. pini CMW 31209
C. pini CMW 31210
C. clavata CMW 23690
C. clavata CMW 30994
Calonectria brassicae species complex

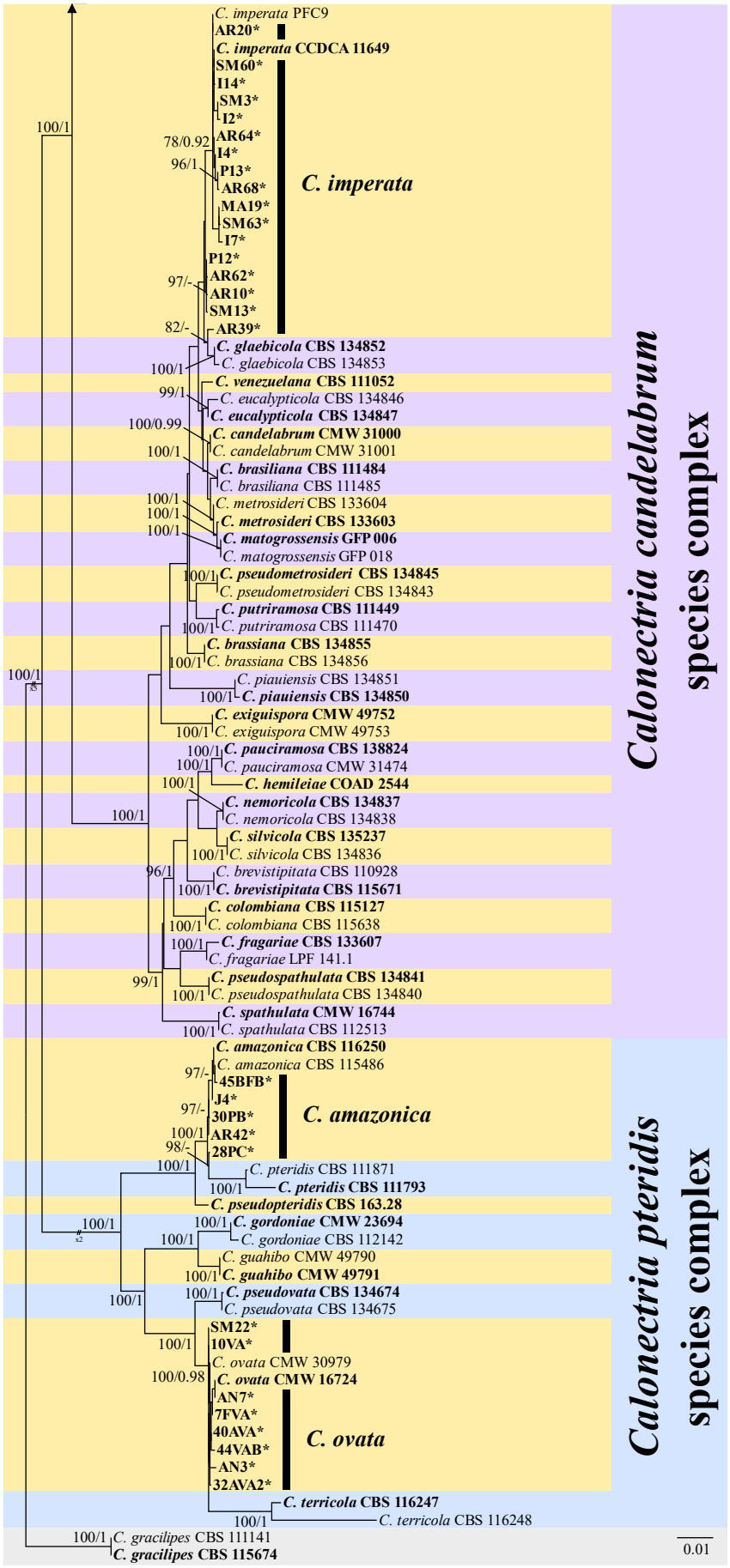
C. imperata PFC9
AR20*
C. imperata CCDCA 11649
SM60*
I14*
SM3*
I2*
AR64*
I4*
P13*
AR68*
MA19*
SM63*
I7*
P12*
AR62*
AR10*
SM13*
AR39*
C. imperata
C. glaebicola CBS 134852
C. glaebicola CBS 134853
C. venezuelana CBS 111052
C. eucalypticola CBS 134846
C. eucalypticola CBS 134847
C. candelabrum CMW 31000
C. candelabrum CMW 31001
C. brasiliana CBS 111484
C. brasiliana CBS 111485
C. metrosideri CBS 133604
C. metrosideri CBS 133603
C. matogrossensis GFP 006
C. matogrossensis GFP 018
C. pseudometrosideri CBS 134845
C. pseudometrosideri CBS 134843
C. putriramosa CBS 111449
C. putriramosa CBS 111470
C. brassiana CBS 134855
C. brassiana CBS 134856
C. piauiensis CBS 134851
C. piauiensis CBS 134850
C. exiguispora CMW 49752
C. exiguispora CMW 49753
C. pauciramosa CBS 138824
C. pauciramosa CMW 31474
C. hemileiae COAD 2544
C. nemoricola CBS 134837
C. nemoricola CBS 134838
C. silvicola CBS 135237
C. silvicola CBS 134836
C. brevistipitata CBS 110928
C. brevistipitata CBS 115671
C. colombiana CBS 115127
C. colombiana CBS 115638
C. fragariae CBS 133607
C. fragariae LPF 141.1
C. pseudospathulata CBS 134841
C. pseudospathulata CBS 134840
C. spathulata CMW 16744
C. spathulata CBS 112513
Calonectria candelabrum species complex
C. amazonica CBS 116250
C. amazonica CBS 115486
45BFB*
J4*
30PB*
AR42*
28PC*
C. amazonica
C. pteridis CBS 111871
C. pteridis CBS 111793
C. pseudopteridis CBS 163.28
C. gordoniae CMW 23694
C. gordoniae CBS 112142
C. guahibo CMW 49790
C. guahibo CMW 49791
C. pseudovata CBS 134674
C. pseudovata CBS 134675
SM22*
10VA*
C. ovata CMW 30979
C. ovata CMW 16724
AN7*
7FVA*
40AVA*
44VAB*
AN3*
32AVA2*
C. ovata
C. terricola CBS 116247
C. terricola CBS 116248
C. gracilipes CBS 111141
C. gracilipes CBS 115674
Calonectria pteridis species complex
0.01

Fig. 2 Phylogenetic tree of *Calonectria* species based on concatenated *act*, *cmdA*, *his3*, *rpb2*, *tef1*, and *tub2* gene regions. Numbers at the nodes represent support values of UFBoot2 (≥ 70%) and PP (≥ 0.90) (ML/BI). Values below 70% (UFBoot2) and 0.90 (PP) are marked with "-". Ex-type isolates are highlighted in bold, and "*" indicates isolates sequenced in this study. The taxa used as outgroup is *C. gracilipes*. The scale bar represents the number of nucleotide substitutions per site

3.3. Species within each *Calonectria* species complex

In the *C. candelabrum* species complex, 17 isolates (AR10, AR20, AR39, AR62, AR64, AR68, I14, I2, I4, I7, MA19, P12, P13, SM13, SM3, SM60, and SM63) representing 17 genotypes were grouped with *C. imperata* (Fig. 2). Some isolates formed three distinct subclades, subclade 1 (P12, AR62, AR10 and SM13), subclade 2 (MA19, SM63 and I7), and subclade 3 (P13 and AR68). However, fixed single nucleotide polymorphisms (SNP) were identified, and the SNP differences between the isolates of each subclade and the ex-type isolate (CCDCA 11649) of *C. imperata* in the concatenated dataset were six (P12, AR62, AR10 and SM13), five (MA19, SM63 and I7) and three (P13 and AR68). Consequently, all 17 isolates were identified as *C. imperata*.

In the *C. cylindrospora* species complex, ten isolates (AR11, AR67, J6, J7, J8, J9, MA27, MA33, P19 and SM28) representing 10 genotypes were closely related to *C. brasiliensis* (Fig. 2). Some isolates formed four subclades, subclade 1 (J6 and J9), subclade 2 (AR67 and J8), subclade 3 (MA33 and MA27), and subclade 4 (AR11 and P19). Fixed SNP were identified, and the SNP differences between each subclade and the ex-type isolate (CBS 230.51) of *C. brasiliensis* were two (J6 and J9), four (AR67 and J8), seven (MA33 and MA27) and 11 (AR11 and P19). Thus, based on the phylogenetic analyses, these isolates were identified as *C. brasiliensis.* Three isolates (SM2, 26BVA and 37DVA) representing three genotypes were grouped with *C. variabilis* (Fig. 2). Only the isolate SM2 presented a single SNP difference with the ex-type isolate (CMW 3187) of *C. variabilis*. They identified as *C. variabilis*. Two isolates (MA29 and SM27) representing two genotypes were grouped with *C. maranhensis* (Fig. 2). Both isolates presented a single SNP difference with the ex-type isolate (CBS 134811) of *C. maranhensis*, consequently, they were identified as *C. maranhensis*.

In the *C. pteridis* species complex, eight isolates (AN3, AN7, 7FVA, 10VA, 40AVA, 44VAB, SM22, and 32AVA2) representing eight genotypes were grouped with *C. ovata*. The SNP differences between these isolates and the ex-type isolate (CMW 16724) of *C. ovata* were one (40AVA and 7FVA), and four (44VAB). These eight isolates were identified as *C. ovata.* Five isolates (AR42, 45BFB, 28PC, 30PB and J4) representing five genotypes were grouped with *C. amazonica*. The SNP differences between these isolates and the ex-type isolate (CBS 116250) of *C. amazonica* were one (J4), three (30PB and 45BFB), four (AR42) and six (28PC). The five isolates were identified as *C. amazonica*.

In the *C. brassicae* species complex, seven isolates (AN4, AN5, AN6, AN8, AR66, J10 and SM61) representing seven genotypes were grouped with *C. quinqueramosa*. The isolates AN4, AN6, AN8, AR66, J10 and SM61 formed a distinct subclade. However, fixed SNP were identified, and the SNP differences

between these isolates and the ex-type isolate (CBS 134654) of *C. quinqueramosa* were only 11 bases. Thus, the seven isolates were identified as *C. quinqueramosa*.

In the *C. spathiphylli* species complex, the isolates PFC2, PFC3, PFC4, PFC5 representing four genotypes were grouped with *C. paragominensis*, as originally reported in our previous study (Sanchez-Gonzalez et al. 2022). These isolates were included in this study to show the species diversity in the sampled plantation and the genotypic diversity within the species. The SNP differences between these isolates and the ex-type isolate (CCDCA 11648) of *C. paragominensis* were five (PFC2 and PFC4) and seven (PFC3). The sequence data of PFC5 is 100% identical to the ex-type isolate.

3.4. Species diversity, genotyping, and distribution of *Calonectria* species

Fifty-six isolates representing 56 genotypes of 197 *Calonectria* isolates were identified at species level based on phylogenetic analyses of six gene regions. In accordance with this species identification, we identified the remaining 141 isolates based on the DNA sequences of *act*, *cmdA*, *his3*, *rpb2*, *tef1*, and *tub2* when available. Thus, the species composition of the complete collection was *C. imperata* (96 isolates), *C. amazonica* (49 isolates), *C. ovata* (18 isolates), *C. brasiliensis* (12 isolates), *C. variabilis* (eight isolates), *C. quinqueramosa* (seven isolates), *C. paragominensis* (four isolates), and *C. maranhensis* (three isolates). Regarding the substrate, the species *C. amazonica, C. brasiliensis, C. imperata, C. maranhensis* and *C. ovata* were isolated from diseased leaves and soil, *C. paragominensis* and *C. variabilis* were only isolated from diseased leaves, and *C. quinqueramosa* was isolated only from soil (Table 2, Supplementary Table S1).

With respect to the *Eucalyptus* genotype, the species *C. amazonica*, *C. brasiliensis*, *C. imperata* and *C. maranhensis* were isolated only from diseased leaves of *E. urophylla* genotype, *C. ovata* and *C. variabilis* were isolated from diseased leaves of both *E. urophylla* and *E. grandis* x *E. brassiana* hybrid genotype, and *C. paragominensis* was isolated only from diseased leaves of *E. grandis* x *E. brassiana* hybrid genotype. No *Calonectria* isolates were obtained from diseased leaves of the *E. grandis* x *E. urophylla* hybrid genotype (Table 2, Supplementary Table S1).

The genotypes within each *Calonectria* species were determined based on sequences of *act*, *cmdA*, *his3*, *rpb2*, *tef1*, and *tub2* when available (Table 4). Thus, the number of genotypes per *Calonectria* species were as follows: *C. imperata* (17), *C. brasiliensis* (10), *C. ovata* (8), *C. quinqueramosa* (7), *C. amazonica* (5), *C. paragominensis* (4), *C. variabilis* (3), and *C. maranhensis* (2).

Table 4 Details of genotypes and number of isolates within each *Calonectria* species.

***Calonectria* species**	**Number of isolates per *Calonectria* species**	**Number of genotypes based on six gene sequences**	**Genotypes[a]**	**Number of isolates per genotype**
C. imperata	96	17	BAAAAA	26
			AAAAAA	17
			ABAAAA	15
			AAAABA	8
			AAAAAB	6
			BAAAAB	5
			AAAABC	4
			ABAAAD	3
			BBAAAA	2
			BAAABA	2
			BAAAAE	2
			ABAABC	1
			AAA-AC	1
			CAA-AC	1
			AAA-AE	1
			BAAAAF	1
			ABAAAB	1
C. brasiliensis	12	10	ABABAA	2
			AABACA	1
			AAB-CB	1
			AAA-BA	2
			ACAA-A	1
			BDACAA	1
			ABADAA	1
			ACCEAA	1
			AEAAAA	1
			AAAFBC	1
C. ovata	18	8	AAAAAA	6
			AAABAA	6
			ABAAAA	1
			AAAAAB	1
			AAABA-	1
			AAACAA	1
			AAADAA	1
			AAAEAB	1
C. quinqueramosa	7	7	ABB-BA	1
			AAA-AC	1
			AAABAB	1
			AAADAB	1
			BAACAB	1
			AAC-AC	1
			ABDACD	1
C. amazonica	49	5	AAAAAA	37
			AAABAB	8
			AAAAAC	2
			AAABBB	1
			AAABAA	1
C. paragominensis	4	4	AABAAA	1
			AAAABB	1
			ABAABA	1
			AAAACA	1
C. variabilis	8	3	AAAAAA	4
			BAAAAA	3
			CAAAAA	1
C. maranhensis	3	2	AAAAAA	2
			ABAAAA	1

[a] "-" = Not available.

In relation to the total number of species found, the most abundant species was *C. imperata* with 48.7% of all the isolates, followed by *C. amazonica* (24.9%), *C. ovata* (9.1%), *C. brasiliensis* (6.1%), *C. variabilis* (4.1%), *C. quinqueramosa* (3.6%), *C. paragominensis* (2%), and *C. maranhensis* (1.5%). With respect to the prevalence, *C. amazonica* was the most prevalent, found in seven of ten plantations, followed by *C. imperata* and *C. brasiliensis,* found in six and five plantations, respectively. The remaining *Calonectria* species were found in one to four plantations. The *Eucalyptus* plantation with the highest species diversity of *Calonectria* was SM with seven species, followed by AR with five species, in the remaining plantations one to three species were identified (Table 5).

Table 5 Number of isolates and *Calonectria* species identified from ten *Eucalyptus* plantations.

Plantation code	***C. variabilis***	***C. brasiliensis***	***C. maranhensis***	***C. paragominensis***	***C. quinqueramosa***	***C. imperata***	***C. amazonica***	***C. ovata***	**Number of *Calonectria* species per plantation**
AN	0	0	0	0	4	0	1	3	3
J	0	4	0	0	1	0	5	0	3
VA	7	0	0	4	0	0	0	12	3
AR	0	3	0	0	1	34	3	1	5
PR	0	0	0	0	0	0	1	0	1
P	0	1	0	0	0	16	8	0	3
SM	1	2	1	0	1	15	29	2	7
MA	0	2	2	0	0	12	0	0	3
I	0	0	0	0	0	19	0	0	1
BF	0	0	0	0	0	0	2	0	1
Total	8	12	3	4	7	96	49	18	8

3.5. Mating Type Identification by PCR

For heterothallic species, only the MAT1-1-1 gene was amplified for all 49 isolates of *C. amazonica*, only the MAT1-2-1 gene was amplified for the three isolates of *C. maranhensis*. In *C. ovata*, the MAT1-1-1 and MAT1-2-1 genes were amplified in nine different isolates each one. In *C. brasiliensis*, the MAT1-1-1 and MAT1-2-1 genes were amplified in seven and five different isolates, respectively. The MAT1-1-1 and MAT1-2-1 genes were successfully amplified in the four representative isolates of *C. imperata*, *C. paragominensis*, *C. quinqueramosa,* and *C. variabilis*, confirming their homothallic nature.

3.6. Morphology

Twenty-four isolates representing the eight *Calonectria* species identified in this study were selected based on the phylogenetic analyses for morphological comparison with respect to macroconidia and vesicles. Three isolates per *Calonectria* species were used. Based on the vesicles shape, the isolates of *C. amazonica* and *C. quinqueramosa* produced clavate to narrowly clavate vesicles; the isolates of *C. brasiliensis, C. imperata*, *C. maranhensis,* and *C. ovata* produced ellipsoidal to ovoid or obpyriform vesicles, and the

isolates of *C. paragominensis* and *C. variabilis* produce globoid to sphaeropedunculate vesicles. Regarding the vesicle shape and macroconidia septation, most of the isolates were consistent with the originally described for each species (Table 6), with exception of the isolate AN2 of *C. ovata* that lost the ability to produce vesicles in culture media.

The isolates of *C. amazonica*, *C. imperata* and *C. quinqueramosa* presented overlapping dimensions about the vesicle width with the originally described for each species, while the isolates of *C. brasiliensis* and *C. ovata* presented narrowed vesicles in comparison with the originally described for each species (Table 5). In case of *C. maranhensis, C. paragominensis,* and *C. variabilis,* some isolates within each species presented narrowed or similar vesicle width with respect to the originally described for each species (Table 5).

Measurements of macroconidia size showed that variations among the isolates within each *Calonectria* species exist. For example, the isolates of *C. amazonica*, *C. brasiliensis*, and *C. imperata* were longer than the originally described for each species, while the isolates of *C. maranhensis* and *C. ovata* were shorter than the originally described for each species (Table 5). In case of *C. paragominensis*, the isolates presented similar size to the ex-type isolate (CCDCA 11648). For *C. quinqueramosa*, the isolate SM61 presented on average similar length to the ex-type isolate (CBS 134654) while the isolates AR66 and J10 were shorter. In *C. variabilis*, the isolates 37DVA and 26BVA were shorter than the ex-type isolate (CMW 3187) while the isolate SM2 was similar.

Table 6 Morphology of *Calonectria* species and isolates obtained in this study.

Species	Isolate Code[a]	Macroconidia Size (L × W)[b,c,d]	Macroconidia Average (L × W)[b,c,d]	Macroconidia Septation	Vesicle Width[b,d]	Colony diameter on MEA (mm)	References
C. amazonica	**CBS 116250**	(68–)74–84(–88) × (4−)4.5−5.5(−6)	79 × 5	1(−3)	5–6	40−65	Lombard et al. 2016
	45BFB	(73–)78–95(–106) × (3.6–)3.9–4.5(–4.7)	86 × 4.2	1	3–5	54±3.6	This study
	30PB	(84–)93–104(–107) × (3.7–)4.0–4.6(–4.9)	98 × 4.3	1	4–6	55±5.0	This study
	SM55	(31–)78–109(–115) × (2.4–)3.5–4.3(–4.8)	94 × 3.9	1	3–6	48±3.8	This study
C. brasiliensis	**CBS 230.51**	(35–)36–40(–41) × 3–5	38 × 3.5	1	7–11	30–45	Lombard et al. 2010b
	AR5	(49–)51–56(–58) × (3–)3.3–3.7(–3.9)	54 × 3.5	1	4–6	48±2.9	This study
	SM28	(36–)39–47(–50) × (2.5–)2.8–3.3(–3.5)	43 × 3.1	1	2–6	50±13.7	This study
	MA33	(45–)49–56(–59) × (2.9–)3–3.8(–4.5)	53 × 3.4	1	5–8	60±2.5	This study
C. imperata	**CCDCA 11649**	(38–)43–49(–52) × (2–)2.7–3.2(–4)	46 × 3	(–1)	3–6	44.5	Sanchez-Gonzalez et al. 2022
	AR39	(45–)47–53(–56) × (2.6–)2.9–3.5(–3.8)	50 × 3.2	1	3–7	43±0.6	This study
	MA23	(53–)58–64(–67) × (3.7–)3.8–4.5(–4.6)	61 × 4.2	1	3–7	49±12	This study
	I12	(42–)50–61(–66) × (3.2–)3.6–4.5(–5)	55 × 4.1	1	5–6	51±3.2	This study
C. maranhensis	**CBS 134811**	(50–)56–58(–65) × (3–)5(–6)	57 × 5	1	7–11	50–55	Alfenas et al., 2015
	MA25	(30–)33–41(–48) × (2.3–)2.5–3.1(–3.7)	37 × 2.8	1	2–5	51±3.8	This study
	MA29	(40–)45–52(–54) × (2.9–)3.2–3.9(–4.3)	49 × 3.6	1	5–14	50±5.5	This study
	SM27	(44–)46–53(–58) × (2.8–)3–3.6(–3.9)	50 × 3.3	1	4–8	52±7.6	This study
C. ovata	**CMW 16724**	(50–)65–80(–110) × 4–6	70 × 5	1(–3)	8–14	N/A	El-Gholl et al. 1993; Crous 2002; Alfenas et al. 2015
	7FVA	(43–)51–65(–69) × (3.8–)4.1–4.9(–5.4)	58 × 4.5	1	6–8	39±2.1	This study
	10VA	(53–)59–70(–77) × (3.5–)3.7–4.4(–4.8)	64 × 4.1	1	5–9	59±13.4	This study
	AN2	(40–)44–56(–59) × (2.8–)3.3–4(–4.4)	50 × 3.7	1	N/A	42±1.5	This study
C. paragominensis	**CCDCA 11648**	(47–)56–66(–71) × (4–)4.8–5.9(–7)	61 × 5	1(–3)	8–12	36.1	Sanchez-Gonzalez et al. 2022
	PFC2	(49–)54–65(–70) × (3.9–)4.1–4.8(–5.1)	60 × 4.5	(–2)	7–12	46±2.1	Sanchez-Gonzalez et al. 2022
	PFC3	(41–)50–71(–79) × (3.6–)4–5.3(–5.8)	60 × 4.6	(–3)	5–8	30±10.0	Sanchez-Gonzalez et al. 2022
	PFC4	(39–)51–69(–76) × (3.6–)4.3–5.4(–5.9)	60 × 4.8	(–3)	3–6	50±3.1	Sanchez-Gonzalez et al. 2022
C. quinqueramosa	**CBS 134654**	(45–)57–61(–70) × 4–6	59 × 5	1	3–5	57–70	Alfenas et al. 2015
	AR66	(38–)42–48(–50) × (2.7–)2.9–3.4(–3.6)	50 × 3.1	1	3–7	36±3.1	This study
	J10	(41–)45–50(–52) × (2.8–)3–3.5(–3.9)	47 × 3.3	1	2–5	46±1.2	This study
	SM61	(31–)56–71(–72) × (2.1–)3.3–4.1(–4.6)	63 × 3.7	1	3–4	39±4.0	This study
C. variabilis	**CMW 3187**	(48–)68–77(–85) × 4–5(–7)	73 × 5	(1–)3(–4)	6–11	N/A	Crous 2002; Alfenas et al. 2015
	37DVA	(31–)35–47(–54) × (3–)3.1–3.6(–3.9)	41 × 3.4	(–3)	N/A	46±7.6	This study
	26BVA	(26–)31–44(–51) × (2–)2.7–4.2(–4.8)	37 × 3.4	(–2)	4–6	38±1.0	This study
	SM2	(53–)62–73(–78) × (4.4–)4.6–5.6(–6)	67 × 5	(–3)	5–14	46±5.6	This study

[a] Ex-type isolate is marked in bold; [b] All measurements are in µm (n = 30). [c] L × W = length × width. [d] Measurements are presented in the format [(minimum–) (mean – standard deviation) – (mean + standard deviation) (–maximum)]. N/A = Not available.

4. Discussion

A total of 197 *Calonectria* isolates were obtained from diseased leaves and soil samples of ten *Eucalyptus* plantations located in the states of Pará and Maranhão, Brazil. These isolates were identified at species level through multi-locus phylogenetic analyses and DNA sequence comparisons of six gene regions. Eight *Calonectria* species belonging to five species complexes were recognized, which are: *C. imperata* in the *C. candelabrum* species complex, *C. brasiliensis*, *C. variabilis* and *C. maranhensis* in the *C. cylindrospora* species complex, *C. amazonica* and *C. ovata* in the *C. pteridis* species complex, *C. quinqueramosa* in the *C. brassicae* species complex and *C. paragominensis* in the *C. spathiphylli* species complex.

The most dominant species was *C. imperata* (48.7% of the isolates) followed by *C. amazonica* (24.9% of the isolates). *Calonectria imperata* has been recently included in *C. candelabrum* species complex, it was isolated from diseased leaves of *E. urophylla* (Sanchez-Gonzalez et al. 2022), and for first time, it was isolated from soil associated to *Eucalyptus* plantation. *Calonectria amazonica* has been reported to cause CLB in *E. tereticornis* (Lombard et al. 2016), and to our knowledge, this is the first record of *C. amazonica* causing CLB in *E. urophylla* in Brazil. *Calonectria ovata* has been reported to cause CLB in *E. urophylla* and cutting rot in Brazilian nurseries, and its pathogenicity to *E. grandis*, *E. robusta*, *E. tereticornis*, *E. torelliana* and other *Eucalyptus* species has been demonstrated (Blum et al. 1992; El-Gholl et al. 1993; Crous et al. 1998). Here, *C. ovata* was isolated only from diseased leaves of *E. urophylla* and the *E. grandis* x *E. brassiana* hybrid genotype.

Calonectria maranhensis originally was isolated from soil and *Eucalyptus* sp. leaves with CLB from commercial plantations in the Maranhão state, Brazil (Alfenas et al. 2015), and in this study was isolated from *E. urophylla* leaf and soil samples. *Calonectria brasiliensis* have been reported to cause damping-off in *E. urophylla* seedlings after being artificially inoculated, and necrotic leaf blight and cutting rot in seedlings of *Anadenanthera peregrina*, *Azadirachta indica* and *Piptadenia gonoacantha* (Aparecido et al. 2008; Lombard et al. 2010b; Alfenas et al. 2013). However, in this study *C. brasiliensis* was found causing CLB in *E. urophylla* trees and was isolated from leaf and soil samples. *Calonectria variabilis* previously was reported as pathogenic to *Schefflera morototoni*, *Theobroma grandiflorum*, and *Eucalyptus* sp. (Liu et al. 2020; Crous et al. 1993), here, *C. variabilis* was found causing CLB in *E. urophylla* and in the *E. grandis x E. brassiana* hybrid genotype.

Calonectria quinqueramosa has been previously found in soils of *Eucalyptus* plantations in the state of Pará (Alfenas et al. 2015). In this study, was isolated from soil samples of *E. urophylla* and *E. grandis x E. urophylla* plantations in the states of Pará and Maranhão, Brazil, and future studies regarding its pathogenicity to *Eucalyptus* need to be addressed. *Calonectria paragominensis* was recently included in the *C. spathiphylli* species complex and have been reported to cause CLB to *E. grandis* × *E. brassiana* in Brazil (Sanchez-Gonzalez et al. 2022).

Based on sequences of *act*, *cmdA*, *his3*, *rpb2*, *tef1*, and *tub2* the genotypes within each *Calonectria* species were determined. *Calonectria imperata* presented the highest number of genotypes, 17 genotypes in 96

isolates, followed by *C. brasiliensis* with 10 genotypes in 12 isolates and *C. ovata* with 8 genotypes in 18 isolates. Although *C. amazonica* was the second dominant species identified, with 49 isolates, only five genotypes were determined for this species.

The sexual thallism for the eight *Calonectria* species was detected by the amplification of the MAT1-1-1 and MAT1-2-1 genes. The thallism detected for *C. amazonica, C. brasiliensis, C. imperata, C. ovata, C. paragominensis, C. quinqueramosa* and *C. variabilis* by MAT genes amplification are consistent with previous studies (Crous 2002; Alfenas et al. 2015; Li et al. 2020;Sanchez-Gonzalez et al. 2022). Although the sexual thallism of *C. maranhensis* has not been reported (Alfenas et al. 2015), only the MAT1-2-1 gene was amplified for the three isolates of *C. maranhensis* obtained in this study, indicating that this species as putatively heterothallic. The MAT1-1-1 gene was amplified for all 49 isolates of *C. amazonica*, indicating that the asexual cycle is its main reproductive mode, which could explain the low number of genotypes found.

The morphological comparison showed that the vesicle shape and macroconidia septation is conserved among the isolates of the same *Calonectria* species, and that variations in macroconidia size and vesicle width among the isolates within each *Calonectria* species exist. These results are consistent with previous studies, where differences in macroconidia size and vesicle width have been indicated for the isolates within other *Calonectria* species (Liu et al. 2021; Wu and Chen 2021). Furthermore, these results confirmed the importance of multi-locus phylogeny for proper identification of *Calonectria* species, since it is not possible to discriminate between different *Calonectria* species based solely on morphological characteristics.

This study increase our knowledge about the species and genetic diversity, distribution, mating strategy and morphological characteristics of *Calonectria* in ten commercial *Eucalyptus* plantations located in the Brazilian states of Pará and Maranhão. Eight *Calonectria* species were isolated form diseased leaves of *Eucalyptus* and soil samples. Most of these species, with the exception of *C. quinqueramosa*, have been reported as pathogenic to *Eucalyptus* in earlier studies (Crous et al. 1993; El-Gholl et al. 1993; Crous et al. 1998; Aparecido et al. 2008; Alfenas et al. 2015; Lombard et al. 2016; Sanchez-Gonzalez et al. 2022). This information could help build an efficient management plan for CLB in *Eucalyptus* plantations and the development of resistant *Eucalyptus* clones.

Supplementary Information The online version contains supplementary material available at:

Acknowledgements The first author thanks the “Coordenação de Aperfeiçoamento de Pessoal de Nível Superior (CAPES)” for providing a doctorate scholarship through Brazil's PAEC OAS-GCUB Scholarships Program. We thank Heitor S. Dallapiccola and Francisco J. A. Gomes for their assistance with sample collection. We thank the facilities provided by the Molecular Biology and Electron Microscopy and Ultrastructural Analysis Laboratories at Universidade Federal de Lavras (UFLA) for the completion of this study.

Author Contributions EISG, TGZ, RGM, and MAF contributed to the study conceptualization, experimentation, and design. EISG contributed to the data analysis. EAVZ, TGZ, and RGM contributed to the project administration and resources. All authors contributed to the draft manuscript, its review and editing. All authors read and approved the final version of the manuscript, and to be accountable for all aspects of the work.

Funding This research was financed by Suzano Papel e Celulose S. A.

Declarations

Competing interests The authors declare no competing interests.

Conflicts of interest The authors declare no conflict of interest.

References

Alfenas AC, Zauza EAV, Mafia RG, de Assis TF (2009) Clonagem e doenças do eucalipto. Editora UFV, Brazil

Alfenas RF, Pereira OL, Jorge VL, Crous PW, Alfenas AC (2013) A new species of *Calonectria* causing leaf blight and cutting rot of three forest tree species in Brazil. Trop Plant Pathol 38:513–521. https://doi.org/10.1590/S1982-56762013000600007

Alfenas RF, Lombard L, Pereira OL, Alfenas AC, Crous PW (2015) Diversity and potential impact of *Calonectria* species in *Eucalyptus* plantations in Brazil. Stud Mycol 80:89–130. https://doi.org/10.1016/j.simyco.2014.11.002

Aparecido CC, Furtado EL, Figueiredo MB (2008) Caracterização morfofisiológica de isolados do gênero *Cylindrocladium*. Summa Phytopathologica 34:38–47. https://doi.org/10.1590/S0100-54052008000100008

Blum LEB, Dianese JC, Costa CL (1992) Comparative pathology of *Cylindrocladium clavatum* and *C. scoparium* on *Eucalyptus* spp. and screening of *Eucalyptus* provenances for resistance to *Cylindrocladium* damping-off. Int J Pest Manage 38:155–159. https://doi.org/10.1080/09670879209371674

Castellani A (1939) Viability of some pathogenic fungi in distilled water. J Trop Med Hyg 42:225–226.

Chernomor O, von Haeseler A, Minh BQ (2016) Terrace aware data structure for phylogenomic inference from supermatrices. Syst Biol 65:997–1008. https://doi.org/10.1093/sysbio/syw037

Crous PW, Janse BJH, Victor D, Marais GF, Alfenas AC (1993) Characterization of some *Cylindrocladium* species with three-septate conidia using morphology, isozyme banding patterns and DNA polymorphisms. Syst Appl Microbiol 16:266–273. https://doi.org/10.1016/S0723-2020(11)80479-0

Crous PW, Alfenas AC, Junghans TG (1998) Variability within *Calonectria* ovata and its anamorph *Cylindrocladium ovatum* from Brazil. Sydowia 50:1–13.

Crous PW (2002) Taxonomy and pathology of Cylindrocladium (Calonectria) and allied genera. The American Phytopathological Society: St. Paul, MN, USA.

Crous PW, Luangsa-Ard JJ, Wingfield MJ, Carnegie AJ, Hernández-Restrepo M et al (2018) Fungal Planet description sheets: 785–867. Persoonia 41:238–417. https://doi.org/10.3767/persoonia.2018.41.12

Crous PW, Carnegie AJ, Wingfield MJ, Sharma R, Mughini G et al (2019) Fungal Planet description sheets: 868–950. Persoonia 42:291–473. https://doi.org/10.3767/persoonia.2019.42.11

Crous PW, Hernández-Restrepo M, Schumacher RK, Cowan DA, Maggs-Kölling G et al (2021a) New and interesting fungi. 4. Fung Syst Evol 7:255. https://doi.org/10.3114/fuse.2021.07.13

Crous PW, Cowan DA, Maggs-Kölling G, Yilmaz N, Thangavel R et al (2021b) Fungal Planet description sheets: 1182–1283. Persoonia 46:313. https://doi.org/10.3767/persoonia.2021.46.11

El-Gholl NE, Alfenas AC, Crous PW, Schubert TS (1993) Description and pathogenicity of *Cylindrocladium ovatum* sp. nov. Can J Bot 71:466–470. https://doi.org/10.1139/b93-051

Graça RN, Alfenas AC, Maffia LA, Titon M, Alfenas RF, Lau D, Rocabado JMA (2009) Factors influencing infection of eucalypts by *Cylindrocladium pteridis*. Plant Pathol 58:971–981. https://doi.org/10.1111/j.1365-3059.2009.02094.x

Hepperle D (2004) SeqAssem. Win32–Version. A sequence analysis tool contig assembler and trace data visualization tool for molecular sequences. Win32-Version. Distributed by the author via: http://www.sequentix.de. Accessed 24 july 2022

Hoang DT, Chernomor O, von Haeseler A, Minh BQ, Vinh LS (2018) UFBoot2: Improving the ultrafast bootstrap approximation. Mol Biol Evol 35:518–522. https://doi.org/10.1093/molbev/msx281

IBÁ (2022) IBÁ–Indústria Brasileira de Árvores. Relatório 2021. https://iba.org/datafiles/publicacoes/relatorios/relatorio-anual-iba2022-compactado.pdf

Kalyaanamoorthy S, Minh BQ, Wong TK, von Haeseler A, Jermiin LS (2017) ModelFinder: fast model selection for accurate phylogenetic estimates. Nat Methods 14:587–589. https://doi.org/10.1038/nmeth.4285

Katoh K, Rozewicki J, Yamada KD (2019) MAFFT online service: Multiple sequence alignment, interactive sequence choice and visualization. Brief Bioinf 201160–1166. https://doi.org/10.1093/bib/bbx108

Kumar S, Stecher G, Tamura K (2016) MEGA7: Molecular evolutionary genetics analysis version 7.0 for bigger datasets. Mol Biol Evol 33:1870–1874. https://doi.org/10.1093/molbev/msw054

Li J, Wingfield BD, Wingfield MJ, Barnes I, Fourie A, Crous PW, Chen SF (2020) Mating genes in *Calonectria* and evidence for a heterothallic ancestral state. Persoonia 45:163–176. https://doi.org/10.3767/persoonia.2020.45.06

Librado P, Rozas J (2009) DnaSP v5: a software for comprehensive analysis of DNA polymorphism data. Bioinformatics 25:1451–1452. https://doi.org/10.1093/bioinformatics/btp187

Liu Q, Chen, S (2017) Two novel species of *Calonectria* isolated from soil in a natural forest in China. MycoKeys 26:25–60. https://doi.org/10.3897/mycokeys.26.14688

Liu QL, Li J, Wingfield MJ, Duong TA, Wingfield BD, Crous PW, Chen SF (2020) Reconsideration of species boundaries and proposed DNA barcodes for *Calonectria*. Stud Mycol 97:100095–100095. https://doi.org/10.1016/j.simyco.2020.08.001

Liu L, Wu W, Chen S (2021) Species Diversity and Distribution Characteristics of *Calonectria* in Five Soil Layers in a *Eucalyptus* Plantation. *J Fung* 7:857. https://doi.org/10.3390/jof7100857

Liu Q, Wingfield MJ, Duong TA, Wingfield BD, Chen S (2022) Diversity and Distribution of *Calonectria* Species from Plantation and Forest Soils in Fujian Province, China. J Fung 8:811. https://doi.org/10.3390/jof8080811

Lombard L, Wingfield MJ, Alfenas AC, Crous PW (2016) The forgotten *Calonectria* collection: pouring old wine into new bags. Stud Mycol 85:35–64. https://doi.org/10.1016/j.simyco.2016.11.004

Lombard L, Crous PW, Wingfield BD, Wingfield MJ (2010a) Phylogeny and systematics of the genus *Calonectria*. Stud Mycol 66:31–69. https://doi.org/10.3114/sim.2010.66.03

Lombard L, Crous PW, Wingfield BD, Wingfield MJ (2010b) Multigene phylogeny and mating tests reveal three cryptic species related to *Calonectria pauciramosa*. Stud Mycol 66:15–30. https://doi.org/10.3114/sim.2010.66.02

Mohali SR, Stewart JE (2021) *Calonectria vigiensis* sp. nov. (Hypocreales, Nectriaceae) associated with dieback and sudden-death symptoms of *Theobroma cacao* from Mérida state, Venezuela. Botany 99:683–693. https://doi.org/10.1139/cjb-2021-0050

Nguyen LT, Schmidt HA, von Haeseler A, Minh BQ (2015) IQ-TREE: A fast and effective stochastic algorithm for estimating maximum-likelihood phylogenies. Mol Biol Evol 32:268–274. https://doi.org/10.1093/molbev/msu300

Pham NQ, Marincowitz S, Chen S, Rodas CA, Wingfield MJ (2022a) Soil-borne *Calonectria* (Hypocreales, Nectriaceae) associated with *Eucalyptus* plantations in Colombia. MycoKeys, 94:17–35. https://doi.org/10.3897/mycokeys.94.96301

Pham NQ, Marincowitz S, Chen S, Yaparudin Y, Wingfield MJ (2022b) *Calonectria* species, including four novel taxa, associated with *Eucalyptus* in Malaysia. Mycol Prog 21:181–197. https://doi.org/10.1007/s11557-021-01768-8

Rambaut A (2009) FigTree, a graphical viewer of phylogenetic trees. Available online http://tree.bio.ed.ac.uk/software/figtree/. Accessed 29 July 2020

Ronquist F, Teslenko M, van Der Mark P, Ayres DL, Darling A, Höhna S, Larget B, Liu L, Suchard MA, Huelsenbeck JP (2012) MrBayes 3.2: Efficient Bayesian phylogenetic inference and model choice across a large model space. Syst Biol 61:539–542. https://doi.org/10.1093/sysbio/sys029

Sanchez-Gonzalez EI, Soares TDPF, Zarpelon TG, Zauza EAV, Mafia RG, Ferreira MA (2022) Two new species of *Calonectria* (Hypocreales, Nectriaceae) causing *Eucalyptus* leaf blight in Brazil. MycoKeys 91:169–197. https://doi.org/10.3897/mycokeys.91.84896

Trifinopoulos J, Nguyen LT, von Haeseler A, Minh BQ (2016) W-IQ-TREE: A fast online phylogenetic tool for maximum likelihood analysis. Nucl Acid Res 44:W232–W235. https://doi.org/10.1093/nar/gkw256

Wang Q, Liu Q, Chen S (2019) Novel species of *Calonectria* isolated from soil near *Eucalyptus* plantations in southern China. Mycologia, 111:1028–1040. https://doi.org/10.1080/00275514.2019.1666597

Wu W, Chen S (2021) Species Diversity, Mating Strategy and Pathogenicity of *Calonectria* Species from Diseased Leaves and Soils in the *Eucalyptus* Plantation in Southern China. J Fung 7:73. https://doi.org/10.3390/jof7020073

Zhang Y, Chen C, Chen C, Chen J, Xiang M et al (2022). Identification and Characterization of *Calonectria* Species Associated with Plant Diseases in Southern China. *Journal of Fungi*, *8*(7), 719. https://doi.org/10.3390/jof8070719

European Journal of Forest Research

Supplementary information

Calonectria species associated with *Eucalyptus* plantations in northeastern Brazil: phylogeny, morphology, and mating strategy

Enrique Ignacio Sánchez-González[1], Thaissa de Paula Farias Soares[2], Talyta Galafassi Zarpelon[2], Edival Angelo Valverde Zauza[2], Reginaldo Gonçalves Mafia[2], Maria Alves Ferreira[1]

[1] Universidade Federal de Lavras, Departamento de Fitopatologia, Lavras, MG, 37200-900, Brasil
[2] Suzano Papel e Celulose S. A. Centro de Tecnologia, Aracruz, ES, 29197-900, Brasil

Correspondence
Maria Alves Ferreira, Universidade Federal de Lavras, Departamento de Fitopatologia, Laboratorio de Patologia Florestal, Lavras, MG, 37200-900, Brasil.
Email: mariaferreira@ufla.br; Tel: +55 (35) 3829-1799

List of Content

Table S1. *Calonectria* isolates obtained in this study.

Species	Isolate code[a]	Genotype	Host	Country	Genbank accession numbers[b]					
					act	***cmdA***	***his3***	***rpb2***	***tef1***	***tub2***
C. amazonica	48BFA	AAAAAA	*E. urophylla*	Brazil:Cidelandia,MA	OQ261792	OQ262014	OQ262167	OQ262358	OQ262503	OQ262690
C. amazonica	4PRB	AAAA_C	*E. urophylla*	Brazil:Dom Eliseu,PA	OQ261794	OQ262022	OQ262169	OQ262360	NA	OQ262692
C. amazonica	AN1	AAAAAA	*E. grandis x E. urophylla*	Brazil:Microregion of Paragominas,MA	OQ261796	OQ261960	OQ262171	OQ262362	OQ262506	OQ262694
C. amazonica	AR12	A_A_AA	*E. urophylla*	Brazil:Dom Eliseu,PA	OQ261807	NA	OQ262182	NA	OQ262517	OQ262705
C. amazonica	AR6	AAAAAA	*E. urophylla*	Brazil:Dom Eliseu,PA	OQ261830	OQ261973	OQ262206	OQ262385	OQ262540	OQ262729
C. amazonica	J1	AAAAAA	*E. urophylla*	Brazil:Microregion of Paragominas,MA	OQ261862	OQ262049	OQ262239	OQ262408	OQ262572	OQ262762
C. amazonica	J2	AAABAB	*E. urophylla*	Brazil:Microregion of Paragominas,MA	OQ261864	OQ262050	OQ262241	OQ262409	OQ262574	OQ262764
C. amazonica	J3	AAAAAA	*E. urophylla*	Brazil:Microregion of Paragominas,MA	OQ261865	OQ262051	OQ262242	OQ262410	OQ262575	OQ262765
C. amazonica	J5	AAAAAA	*E. urophylla*	Brazil:Microregion of Paragominas,MA	OQ261867	OQ262053	OQ262244	OQ262412	OQ262577	OQ262767
C. amazonica	P1	AAAAAA	*E. urophylla*	Brazil:Itinga do Maranhao,MA	OQ261888	OQ262075	OQ262265	OQ262421	OQ262598	OQ262788
C. amazonica	P10	AAABAB	*E. urophylla*	Brazil:Itinga do Maranhao,MA	OQ261889	OQ262084	OQ262266	OQ262422	OQ262599	OQ262789
C. amazonica	P2	AAAAAA	*E. urophylla*	Brazil:Itinga do Maranhao,MA	OQ261899	OQ262076	OQ262276	OQ262429	OQ262609	OQ262799
C. amazonica	P5	AAABAB	*E. urophylla*	Brazil:Itinga do Maranhao,MA	OQ261905	OQ262079	OQ262283	OQ262433	OQ262615	OQ262806
C. amazonica	P6	AAAAAA	*E. urophylla*	Brazil:Itinga do Maranhao,MA	OQ261906	OQ262080	OQ262284	OQ262434	OQ262616	OQ262807
C. amazonica	P8	AAABAB	*E. urophylla*	Brazil:Itinga do Maranhao,MA	OQ261908	OQ262082	OQ262286	OQ262435	OQ262618	OQ262809
C. amazonica	SM1	AAAAAA	*E. urophylla*	Brazil:Açailandia,MA	OQ261910	OQ262098	OQ262288	OQ262436	OQ262620	OQ262811
C. amazonica	SM11	AAAAAA	*E. urophylla*	Brazil:Açailandia,MA	OQ261912	OQ262107	OQ262290	OQ262438	OQ262622	OQ262813
C. amazonica	SM15	AAAAAA	*E. urophylla*	Brazil:Açailandia,MA	OQ261914	OQ262109	OQ262292	OQ262440	OQ262624	OQ262815
C. amazonica	SM19	AAAAAA	*E. urophylla*	Brazil:Açailandia,MA	OQ261916	OQ262111	OQ262294	OQ262442	OQ262626	OQ262817
C. amazonica	SM20	AAAAAA	*E. urophylla*	Brazil:Açailandia,MA	OQ261918	OQ262112	OQ262296	OQ262444	OQ262628	OQ262819
C. amazonica	SM25	AAAAAA	*E. urophylla*	Brazil:Açailandia,MA	OQ261922	OQ262116	OQ262300	OQ262448	OQ262632	OQ262822
C. amazonica	SM26	AAAAAA	*E. urophylla*	Brazil:Açailandia,MA	OQ261923	OQ262117	OQ262301	OQ262449	OQ262633	OQ262823
C. amazonica	SM29	AAABAB	*E. urophylla*	Brazil:Açailandia,MA	OQ261926	OQ262120	OQ262304	OQ262452	OQ262636	OQ262826
C. amazonica	SM30	AAAAAA	*E. urophylla*	Brazil:Açailandia,MA	OQ261928	OQ262121	OQ262306	OQ262454	OQ262638	OQ262828
C. amazonica	SM31	AAAAAA	*E. urophylla*	Brazil:Açailandia,MA	OQ261929	OQ262122	OQ262307	OQ262455	OQ262639	OQ262829
C. amazonica	SM32	AAABAB	*E. urophylla*	Brazil:Açailandia,MA	OQ261930	OQ262123	OQ262308	OQ262456	OQ262640	OQ262830
C. amazonica	SM36	AAAAAA	*E. urophylla*	Brazil:Açailandia,MA	OQ261931	OQ262124	OQ262309	OQ262457	OQ262641	OQ262831
C. amazonica	SM38	AAAAAA	*E. urophylla*	Brazil:Açailandia,MA	OQ261933	OQ262126	OQ262311	OQ262459	OQ262643	OQ262833
C. amazonica	SM39	AAAAAA	*E. urophylla*	Brazil:Açailandia,MA	OQ261934	OQ262127	OQ262312	OQ262460	OQ262644	OQ262834
C. amazonica	SM44	A_ABAB	*E. urophylla*	Brazil:Açailandia,MA	OQ261938	NA	OQ262316	OQ262463	OQ262648	OQ262838
C. amazonica	SM46	AAAAAA	*E. urophylla*	Brazil:Açailandia,MA	OQ261939	OQ262130	OQ262317	OQ262464	OQ262649	OQ262839
C. amazonica	SM5	AAAAAA	*E. urophylla*	Brazil:Açailandia,MA	OQ261941	OQ262101	OQ262319	OQ262465	OQ262651	OQ262841
C. amazonica	SM50	AAAAAA	*E. urophylla*	Brazil:Açailandia,MA	OQ261942	OQ262132	OQ262320	OQ262466	OQ262652	OQ262842
C. amazonica	SM51	AAAAAA	*E. urophylla*	Brazil:Açailandia,MA	OQ261943	OQ262133	OQ262321	OQ262467	OQ262653	OQ262843
C. amazonica	SM52	AAAAAA	*E. urophylla*	Brazil:Açailandia,MA	OQ261944	OQ262134	OQ262322	OQ262468	OQ262654	OQ262844
C. amazonica	SM53	AAAAAA	*E. urophylla*	Brazil:Açailandia,MA	OQ261945	OQ262135	OQ262323	OQ262469	OQ262655	OQ262845
C. amazonica	SM54	AA_AAA	*E. urophylla*	Brazil:Açailandia,MA	OQ261946	OQ262136	NA	OQ262470	OQ262656	OQ262846
C. amazonica	SM55	AAAAAA	*E. urophylla*	Brazil:Açailandia,MA	OQ261947	OQ262137	OQ262324	OQ262471	OQ262657	OQ262847
C. amazonica	SM57	AAAAAA	*E. urophylla*	Brazil:Açailandia,MA	OQ261949	OQ262139	OQ262326	OQ262473	OQ262659	OQ262849
C. amazonica	SM6	AAAAAA	*E. urophylla*	Brazil:Açailandia,MA	OQ261951	OQ262102	OQ262328	OQ262475	OQ262661	OQ262851
C. amazonica	SM65	AAAAAA	*E. urophylla*	Brazil:Açailandia,MA	OQ261956	OQ262145	OQ262333	OQ262478	OQ262666	OQ262856
C. amazonica	SM66	AAAAAA	*E. urophylla*	Brazil:Açailandia,MA	OQ261957	OQ262146	OQ262334	OQ262479	OQ262667	OQ262857
C. amazonica	SM8	AAAAAA	*E. urophylla*	Brazil:Açailandia,MA	OQ261958	OQ262104	OQ262336	OQ262481	OQ262669	OQ262859
C. amazonica	SM9	AAAAAA	*E. urophylla*	Brazil:Açailandia,MA	OQ261959	OQ262105	OQ262337	OQ262482	OQ262670	OQ262860
C. brasiliensis	AR5	_AA_BA	*E. urophylla*	Brazil:Dom Eliseu,PA	NA	OQ261972	OQ262200	NA	OQ262534	OQ262723
C. brasiliensis	SM16	ABABAA	*E. urophylla*	Brazil:Açailandia,MA	OQ261915	OQ262110	OQ262293	OQ262441	OQ262625	OQ262816
C. imperata	AR1	BAAAAA	*E. urophylla*	Brazil:Dom Eliseu,PA	OQ261804	OQ261968	OQ262179	OQ262370	OQ262514	OQ262702
C. imperata	AR13	AAAAAA	*E. urophylla*	Brazil:Dom Eliseu,PA	OQ261808	OQ261979	OQ262183	OQ262372	OQ262518	OQ262706
C. imperata	AR14	ABAAAA	*E. urophylla*	Brazil:Dom Eliseu,PA	OQ261809	OQ261980	OQ262184	OQ262373	OQ262519	OQ262707
C. imperata	AR16	AAAAAA	*E. urophylla*	Brazil:Dom Eliseu,PA	OQ261810	OQ261981	OQ262185	OQ262374	OQ262520	OQ262708
C. imperata	AR2	BAAAAA	*E. urophylla*	Brazil:Dom Eliseu,PA	OQ261811	OQ261969	OQ262186	OQ262375	OQ262521	OQ262709
C. imperata	AR24	AAA_BC	*E. urophylla*	Brazil:Dom Eliseu,PA	OQ261813	OQ261983	OQ262188	NA	OQ262523	OQ262711
C. imperata	AR28	BAA_AA	*E. urophylla*	Brazil:Dom Eliseu,PA	OQ261814	OQ261984	OQ262189	NA	OQ262524	OQ262712
C. imperata	AR3	ABAAAD	*E. urophylla*	Brazil:Dom Eliseu,PA	OQ261815	OQ261970	OQ262190	OQ262377	OQ262525	OQ262713
C. imperata	AR30	BAAAAA	*E. urophylla*	Brazil:Dom Eliseu,PA	OQ261816	OQ261985	OQ262191	OQ262378	OQ262526	OQ262714
C. imperata	AR32	BAAAAA	*E. urophylla*	Brazil:Dom Eliseu,PA	OQ261817	OQ261986	OQ262192	OQ262379	OQ262527	OQ262715
C. imperata	AR37	BAA_AA	*E. urophylla*	Brazil:Dom Eliseu,PA	OQ261818	OQ261987	OQ262193	NA	OQ262528	OQ262716
C. imperata	AR4	ABA_AD	*E. urophylla*	Brazil:Dom Eliseu,PA	OQ261820	OQ261971	OQ262195	NA	OQ262530	OQ262718
C. imperata	AR43	BAA_AA	*E. urophylla*	Brazil:Dom Eliseu,PA	OQ261822	OQ261990	OQ262197	NA	OQ262532	OQ262720
C. imperata	AR47	AAA__A	*E. urophylla*	Brazil:Dom Eliseu,PA	OQ261823	OQ261991	OQ262198	NA	NA	OQ262721
C. imperata	AR48	BAAAAA	*E. urophylla*	Brazil:Dom Eliseu,PA	OQ261824	OQ261992	OQ262199	OQ262382	OQ262533	OQ262722
C. imperata	AR51	BAA_AA	*E. urophylla*	Brazil:Dom Eliseu,PA	OQ261825	OQ261993	OQ262201	NA	OQ262535	OQ262724
C. imperata	AR53	AAA_AA	*E. urophylla*	Brazil:Dom Eliseu,PA	OQ261826	OQ261994	OQ262202	NA	OQ262536	OQ262725
C. imperata	AR56	BAAAAA	*E. urophylla*	Brazil:Dom Eliseu,PA	OQ261827	OQ261995	OQ262203	OQ262383	OQ262537	OQ262726
C. imperata	AR57	BAAAAA	*E. urophylla*	Brazil:Dom Eliseu,PA	OQ261828	OQ261996	OQ262204	OQ262384	OQ262538	OQ262727

C. imperata	AR58	AAA_BA	*E. urophylla*	Brazil:Dom Eliseu,PA	OQ261829	OQ261997	OQ262205	NA	OQ262539	OQ262728
C. imperata	AR61	BAAA_A	*E. urophylla*	Brazil:Dom Eliseu,PA	OQ261831	OQ261998	OQ262207	OQ262386	NA	OQ262730
C. imperata	AR65	AAAAAA	*E. urophylla*	Brazil:Dom Eliseu,PA	OQ261835	OQ262001	OQ262211	OQ262390	OQ262544	OQ262734
C. imperata	AR69	ABA_AA	*E. urophylla*	Brazil:Dom Eliseu,PA	OQ261839	OQ262005	OQ262215	NA	OQ262547	OQ262738
C. imperata	AR7	BAA_AA	*E. urophylla*	Brazil:Dom Eliseu,PA	OQ261840	OQ261974	OQ262216	OQ262392	OQ262548	OQ262739
C. imperata	AR71	ABAAAA	*E. urophylla*	Brazil:Dom Eliseu,PA	OQ261841	OQ262006	OQ262217	OQ262393	OQ262549	OQ262740
C. imperata	AR72	AA_AAA	*E. urophylla*	Brazil:Dom Eliseu,PA	OQ261842	OQ262007	NA	NA	OQ262550	OQ262741
C. imperata	AR8	_AA_AA	*E. urophylla*	Brazil:Dom Eliseu,PA	NA	OQ261975	OQ262218	NA	OQ262551	OQ262742
C. imperata	AR9	BAAAAA	*E. urophylla*	Brazil:Dom Eliseu,PA	OQ261843	OQ261976	OQ262219	OQ262394	OQ262552	OQ262743
C. imperata	I1	AAA_BA	*E. urophylla*	Brazil:Imperatriz,MA	OQ261844	OQ262031	OQ262220	NA	OQ262553	OQ262744
C. imperata	I10	_AAABA	*E. urophylla*	Brazil:Imperatriz,MA	NA	OQ262040	OQ262221	OQ262395	OQ262554	OQ262745
C. imperata	I11	AAA_BC	*E. urophylla*	Brazil:Imperatriz,MA	OQ261845	OQ262041	OQ262222	NA	OQ262555	OQ262746
C. imperata	I12	AAA_BA	*E. urophylla*	Brazil:Imperatriz,MA	OQ261846	OQ262042	OQ262223	NA	OQ262556	OQ262747
C. imperata	I13	BAAAAA	*E. urophylla*	Brazil:Imperatriz,MA	OQ261847	OQ262043	OQ262224	OQ262396	OQ262557	OQ262748
C. imperata	I15	AAA_B_	*E. urophylla*	Brazil:Imperatriz,MA	OQ261849	OQ262045	OQ262226	NA	OQ262559	NA
C. imperata	I16	B_A_AA	*E. urophylla*	Brazil:Imperatriz,MA	OQ261850	NA	OQ262227	NA	OQ262560	OQ262750
C. imperata	I17	AAAABA	*E. urophylla*	Brazil:Imperatriz,MA	OQ261851	OQ262046	OQ262228	OQ262398	OQ262561	OQ262751
C. imperata	I18	BAA_AB	*E. urophylla*	Brazil:Imperatriz,MA	OQ261852	OQ262047	OQ262229	NA	OQ262562	OQ262752
C. imperata	I19	BAAAAB	*E. urophylla*	Brazil:Imperatriz,MA	OQ261853	OQ262048	OQ262230	OQ262399	OQ262563	OQ262753
C. imperata	I3	BAAAAB	*E. urophylla*	Brazil:Imperatriz,MA	OQ261855	OQ262033	OQ262232	OQ262401	OQ262565	OQ262755
C. imperata	I5	BAAAAA	*E. urophylla*	Brazil:Imperatriz,MA	OQ261857	OQ262035	OQ262234	OQ262403	OQ262567	OQ262757
C. imperata	I6	BAAAAA	*E. urophylla*	Brazil:Imperatriz,MA	OQ261858	OQ262036	OQ262235	OQ262404	OQ262568	OQ262758
C. imperata	I8	BAAAAA	*E. urophylla*	Brazil:Imperatriz,MA	OQ261860	OQ262038	OQ262237	OQ262406	OQ262570	OQ262760
C. imperata	I9	BAAAAA	*E. urophylla*	Brazil:Imperatriz,MA	OQ261861	OQ262039	OQ262238	OQ262407	OQ262571	OQ262761
C. imperata	MA10	BAA_AA	*E. urophylla*	Brazil:Cidelandia,MA	OQ261872	OQ262062	OQ262249	NA	OQ262582	OQ262772
C. imperata	MA11	BAAAAA	*E. urophylla*	Brazil:Cidelandia,MA	OQ261873	OQ262063	OQ262250	OQ262417	OQ262583	OQ262773
C. imperata	MA13	AAA_AB	*E. urophylla*	Brazil:Cidelandia,MA	OQ261874	OQ262064	OQ262251	NA	OQ262584	OQ262774
C. imperata	MA14	ABA_AA	*E. urophylla*	Brazil:Cidelandia,MA	OQ261875	OQ262065	OQ262252	NA	OQ262585	OQ262775
C. imperata	MA16	AAA_AB	*E. urophylla*	Brazil:Cidelandia,MA	OQ261876	OQ262066	OQ262253	NA	OQ262586	OQ262776
C. imperata	MA21	AAA_BC	*E. urophylla*	Brazil:Cidelandia,MA	OQ261878	OQ262068	OQ262255	NA	OQ262588	OQ262778
C. imperata	MA23	ABA_AA	*E. urophylla*	Brazil:Cidelandia,MA	OQ261879	OQ262069	OQ262256	NA	OQ262589	OQ262779
C. imperata	MA5	ABAAAA	*E. urophylla*	Brazil:Cidelandia,MA	OQ261884	OQ262074	OQ262261	OQ262420	OQ262594	OQ262784
C. imperata	MA7	AAA_AA	*E. urophylla*	Brazil:Cidelandia,MA	OQ261885	OQ262059	OQ262262	NA	OQ262595	OQ262785
C. imperata	MA8	AAA_AA	*E. urophylla*	Brazil:Cidelandia,MA	OQ261886	OQ262060	OQ262263	NA	OQ262596	OQ262786
C. imperata	MA9	ABA_AA	*E. urophylla*	Brazil:Cidelandia,MA	OQ261887	OQ262061	OQ262264	NA	OQ262597	OQ262787
C. imperata	P11	ABAAAA	*E. urophylla*	Brazil:Itinga do Maranhao,MA	OQ261890	OQ262085	OQ262267	OQ262423	OQ262600	OQ262790
C. imperata	P14	ABAAAA	*E. urophylla*	Brazil:Itinga do Maranhao,MA	OQ261893	OQ262088	OQ262270	OQ262426	OQ262603	OQ262793
C. imperata	P15	ABA_AA	*E. urophylla*	Brazil:Itinga do Maranhao,MA	OQ261894	OQ262089	OQ262271	NA	OQ262604	OQ262794
C. imperata	P16	AAA_AA	*E. urophylla*	Brazil:Itinga do Maranhao,MA	OQ261895	OQ262090	OQ262272	NA	OQ262605	OQ262795
C. imperata	P17	BAAAAA	*E. urophylla*	Brazil:Itinga do Maranhao,MA	OQ261896	OQ262091	OQ262273	OQ262427	OQ262606	OQ262796
C. imperata	P18	AAA_AA	*E. urophylla*	Brazil:Itinga do Maranhao,MA	OQ261897	OQ262092	OQ262274	NA	OQ262607	OQ262797
C. imperata	P20	_AAAAB	*E. urophylla*	Brazil:Itinga do Maranhao,MA	NA	OQ262094	OQ262277	OQ262430	OQ262610	OQ262800
C. imperata	P21	BAAAAA	*E. urophylla*	Brazil:Itinga do Maranhao,MA	OQ261900	OQ262095	OQ262278	OQ262431	OQ262611	OQ262801
C. imperata	P22	BBA_AA	*E. urophylla*	Brazil:Itinga do Maranhao,MA	OQ261901	OQ262096	OQ262279	NA	OQ262612	OQ262802
C. imperata	P23	AAA__B	*E. urophylla*	Brazil:Itinga do Maranhao,MA	OQ261902	OQ262097	OQ262280	NA	NA	OQ262803
C. imperata	P3	ABAAAA	*E. urophylla*	Brazil:Itinga do Maranhao,MA	OQ261903	OQ262077	OQ262281	OQ262432	OQ262613	OQ262804
C. imperata	P4	ABA_AA	*E. urophylla*	Brazil:Itinga do Maranhao,MA	OQ261904	OQ262078	OQ262282	NA	OQ262614	OQ262805
C. imperata	P7	BAA_AB	*E. urophylla*	Brazil:Itinga do Maranhao,MA	OQ261907	OQ262081	OQ262285	NA	OQ262617	OQ262808
C. imperata	P9	ABA_AA	*E. urophylla*	Brazil:Itinga do Maranhao,MA	OQ261909	OQ262083	OQ262287	NA	OQ262619	OQ262810
C. imperata	SM10	AAAAAA	*E. urophylla*	Brazil:Açailandia,MA	OQ261911	OQ262106	OQ262289	OQ262437	OQ262621	OQ262812
C. imperata	SM23	AAAAAA	*E. urophylla*	Brazil:Açailandia,MA	OQ261921	OQ262115	OQ262299	OQ262447	OQ262631	OQ262821
C. imperata	SM37	AAAAAA	*E. urophylla*	Brazil:Açailandia,MA	OQ261932	OQ262125	OQ262310	OQ262458	OQ262642	OQ262832
C. imperata	SM4	B_AAAE	*E. urophylla*	Brazil:Açailandia,MA	OQ261935	NA	OQ262313	OQ262461	OQ262645	OQ262835
C. imperata	SM42	AAA_AB	*E. urophylla*	Brazil:Açailandia,MA	OQ261936	OQ262128	OQ262314	NA	OQ262646	OQ262836
C. imperata	SM43	AAAAAA	*E. urophylla*	Brazil:Açailandia,MA	OQ261937	OQ262129	OQ262315	OQ262462	OQ262647	OQ262837
C. imperata	SM47	ABA_AA	*E. urophylla*	Brazil:Açailandia,MA	OQ261940	OQ262131	OQ262318	NA	OQ262650	OQ262840
C. imperata	SM56	BAAABA	*E. urophylla*	Brazil:Açailandia,MA	OQ261948	OQ262138	OQ262325	OQ262472	OQ262658	OQ262848
C. imperata	SM59	BAAAAA	*E. urophylla*	Brazil:Açailandia,MA	OQ261950	OQ262140	OQ262327	OQ262474	OQ262660	OQ262850
C. imperata	SM62	AAAABA	*E. urophylla*	Brazil:Açailandia,MA	OQ261954	OQ262143	OQ262331	OQ262477	OQ262664	OQ262854
C. imperata	SM7	_AAAAA	*E. urophylla*	Brazil:Açailandia,MA	NA	OQ262103	OQ262335	OQ262480	OQ262668	OQ262858
C. maranhensis	MA25	AAA_AA	*E. urophylla*	Brazil:Cidelandia,MA	OQ261880	OQ262070	OQ262257	NA	OQ262590	OQ262780
C. ovata	32AVA1	AAAAAA	*E. grandis x E. brassiana*	Brazil:Microregion of Paragominas,MA	OQ261779	OQ262024	OQ262154	OQ262345	OQ262490	OQ262678
C. ovata	36AVA	AAABAA	*E. grandis x E. brassiana*	Brazil:Microregion of Paragominas,MA	OQ261781	OQ262009	OQ262156	OQ262347	OQ262492	OQ262680
C. ovata	36AVAA	AAABAA	*E. grandis x E. brassiana*	Brazil:Microregion of Paragominas,MA	OQ261782	OQ262020	OQ262157	OQ262348	OQ262493	OQ262681
C. ovata	36VAB	AAABAA	*E. grandis x E. brassiana*	Brazil:Microregion of Paragominas,MA	OQ261783	OQ262013	OQ262158	OQ262349	OQ262494	OQ262682
C. ovata	40BVA	AAAAAA	*E. grandis x E. brassiana*	Brazil:Microregion of Paragominas,MA	OQ261788	OQ262012	OQ262163	OQ262354	OQ262499	OQ262686

C. ovata	44VAA	AAAAAA	*E. grandis x E. brassiana*	Brazil:Microregion of Paragominas,MA	OQ261789	OQ262029	OQ262164	OQ262355	OQ262500	OQ262687
C. ovata	49VA	AAAAAA	*E. grandis x E. brassiana*	Brazil:Microregion of Paragominas,MA	OQ261793	OQ262028	OQ262168	OQ262359	OQ262504	OQ262691
C. ovata	AN2	AAABAA	*E. grandis x E. urophylla*	Brazil:Microregion of Paragominas,MA	OQ261797	OQ261961	OQ262172	OQ262363	OQ262507	OQ262695
C. ovata	AR63	A_AAAA	*E. urophylla*	Brazil:Dom Eliseu,PA	OQ261833	NA	OQ262209	OQ262388	OQ262542	OQ262732
C. ovata	SM21	AAABAA	*E. urophylla*	Brazil:Açailandia,MA	OQ261919	OQ262113	OQ262297	OQ262445	OQ262629	OQ262820
C. variabilis	24VAA	AAAAAA	*E. grandis x E. brassiana*	Brazil:Microregion of Paragominas,MA	OQ261773	OQ262030	OQ262148	OQ262339	OQ262484	OQ262672
C. variabilis	26BVAA	A_AAAA	*E. grandis x E. brassiana*	Brazil:Microregion of Paragominas,MA	OQ261774	NA	OQ262149	OQ262340	OQ262485	OQ262673
C. variabilis	31AVA	AAAAAA	*E. grandis x E. brassiana*	Brazil:Microregion of Paragominas,MA	OQ261778	OQ262027	OQ262153	OQ262344	OQ262489	OQ262677
C. variabilis	37DAB	BAAAAA	*E. grandis x E. brassiana*	Brazil:Microregion of Paragominas,MA	OQ261784	OQ262021	OQ262159	OQ262350	OQ262495	OQ262683
C. variabilis	37DVAA	BAAAAA	*E. grandis x E. brassiana*	Brazil:Microregion of Paragominas,MA	OQ261785	OQ262025	OQ262160	OQ262351	OQ262496	OQ262684

[a]Laboratorio de Patologia Florestal, Universidade Federal de Lavras, Lavras, Brazil.
[b] *act*: actin; *cmdA*: calmodulin; *his3*: histone H3; *rpb2*: RNA polymerase II; *tef1*: translation elongation factor 1-alpha; *tub2*: β-tubulin.

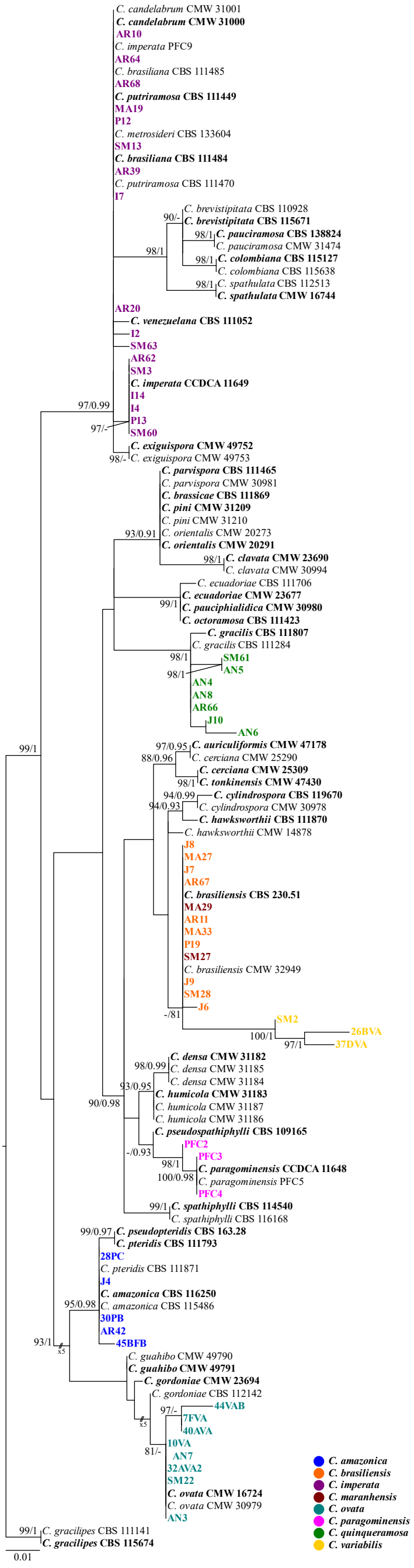

Fig. 1S Phylogenetic tree of *Calonectria* species based on *act* gene region. Numbers at the nodes represent support values of UFBoot2 (≥ 80%) and PP (≥ 0.90) (ML/BI). Values below 80% (UFBoot2) and 0.90 (PP) are marked with "-". Ex-type isolates are highlighted in bold. The taxa used as outgroup is *C. gracilipes*. The scale bar represents the number of nucleotide substitutions per site.

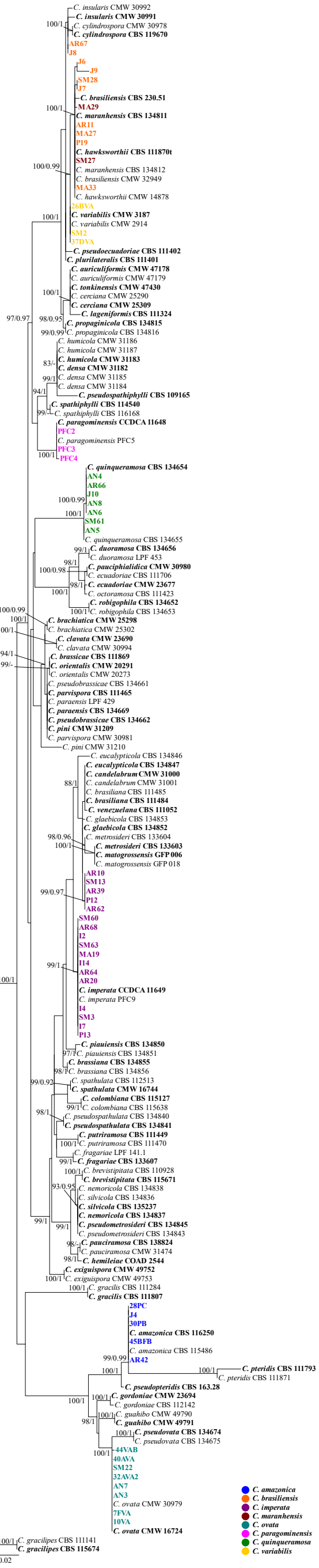

Fig. 2S Phylogenetic tree of *Calonectria* species based on *cmdA* gene region. Numbers at the nodes represent support values of UFBoot2 (≥ 80%) and PP (≥ 0.90) (ML/BI). Values below 80% (UFBoot2) and 0.90 (PP) are marked with "-". Ex-type isolates are highlighted in bold. The taxa used as outgroup is *C. gracilipes*. The scale bar represents the number of nucleotide substitutions per site.

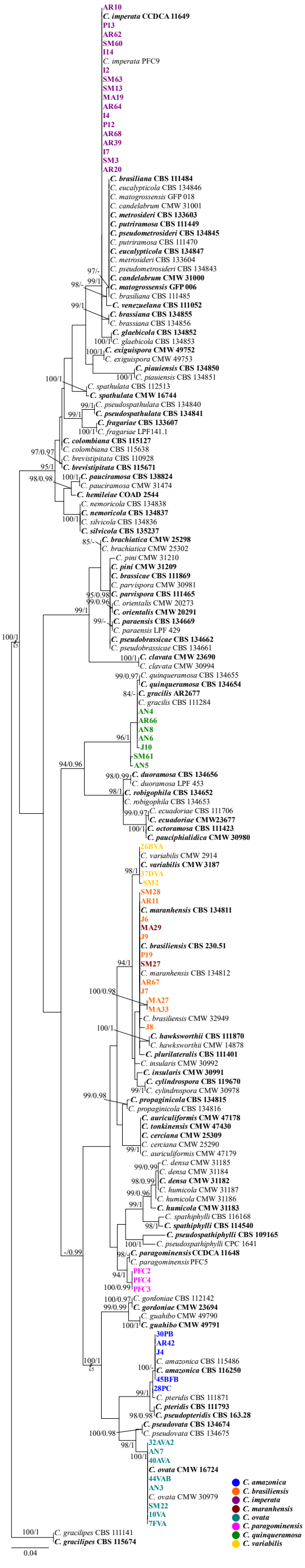

Fig. 3S Phylogenetic tree of *Calonectria* species based on *his3* gene region. Numbers at the nodes represent support values of UFBoot2 (≥ 80%) and PP (≥ 0.90) (ML/BI). Values below 80% (UFBoot2) and 0.90 (PP) are marked with "-". Ex-type isolates are highlighted in bold. The taxa used as outgroup is *C. gracilipes*. The scale bar represents the number of nucleotide substitutions per site.

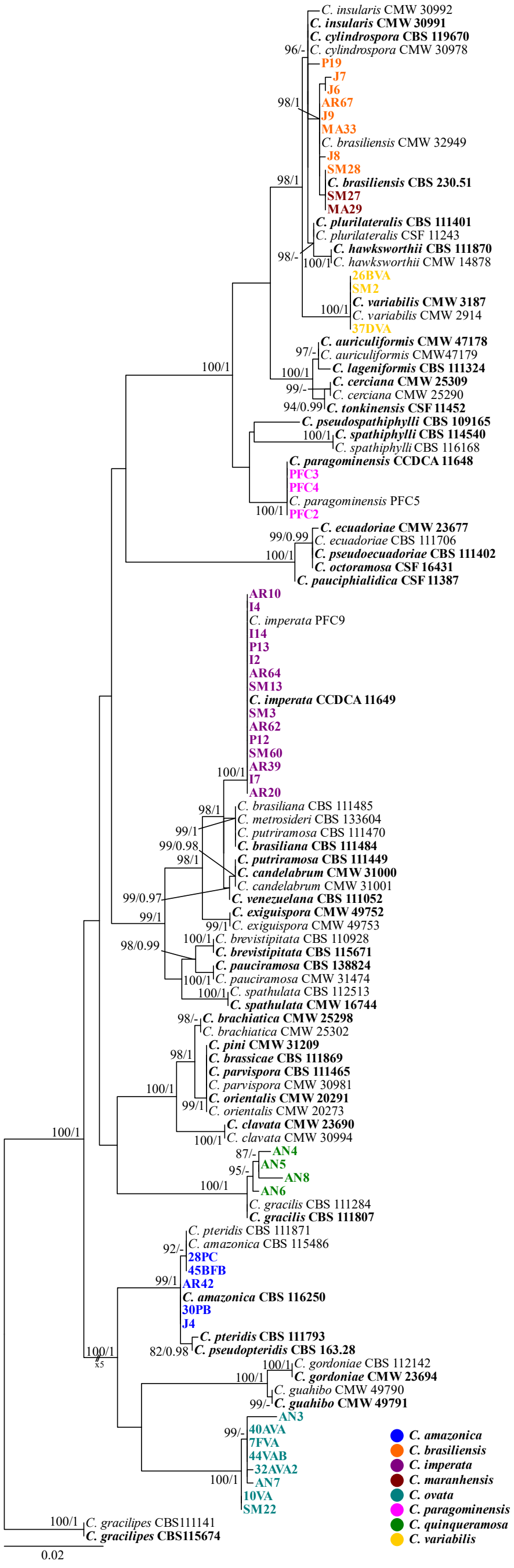

Fig. 4S Phylogenetic tree of *Calonectria* species based on *rpb2* gene region. Numbers at the nodes represent support values of UFBoot2 (≥ 80%) and PP (≥ 0.90) (ML/BI). Values below 80% (UFBoot2) and 0.90 (PP) are marked with "-". Ex-type isolates are highlighted in bold. The taxa used as outgroup is *C. gracilipes*. The scale bar represents the number of nucleotide substitutions per site.

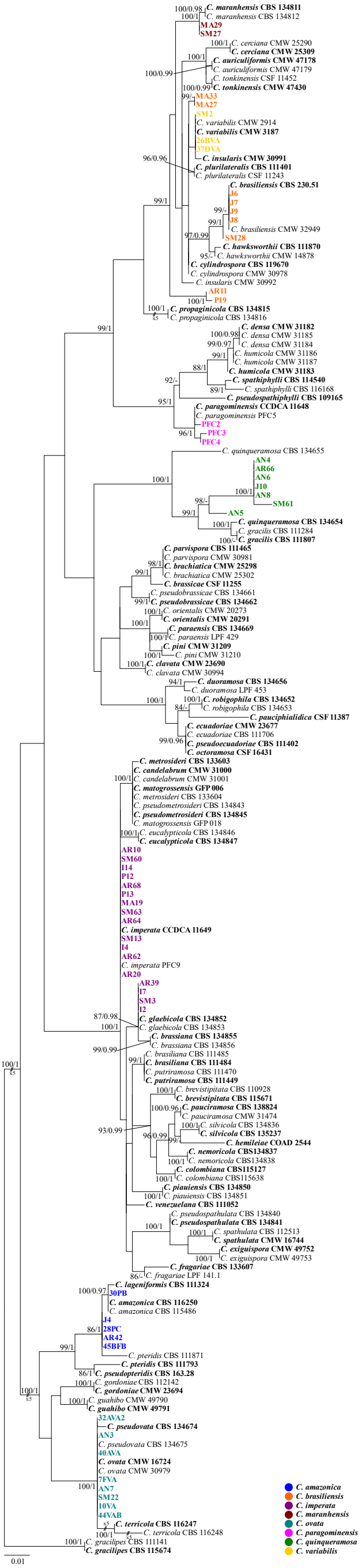

Fig. 5S Phylogenetic tree of *Calonectria* species based on *tef1* gene region. Numbers at the nodes represent support values of UFBoot2 (≥ 80%) and PP (≥ 0.90) (ML/BI). Values below 80% (UFBoot2) and 0.90 (PP) are marked with "-". Ex-type isolates are highlighted in bold. The taxa used as outgroup is *C. gracilipes*. The scale bar represents the number of nucleotide substitutions per site.

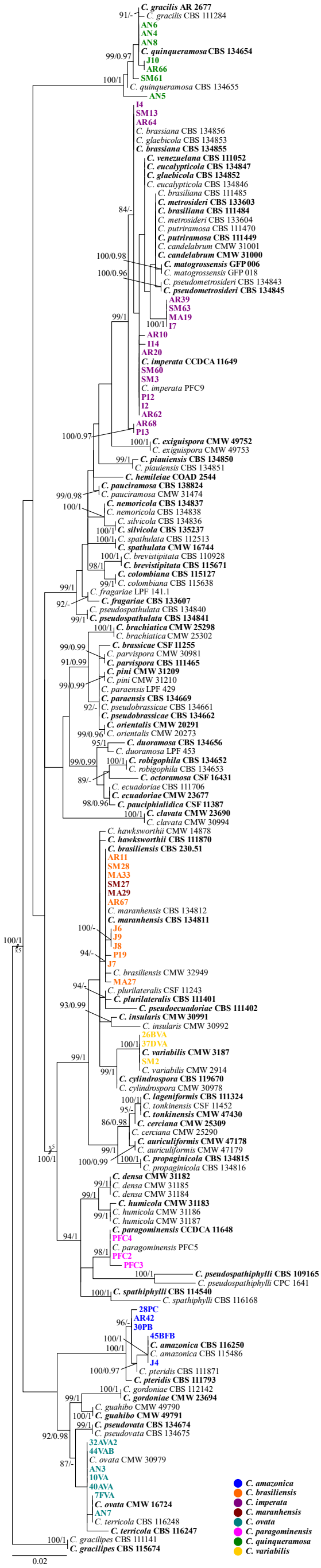

Fig. 6S Phylogenetic tree of *Calonectria* species based on *tub2* gene region. Numbers at the nodes represent support values of UFBoot2 (≥ 80%) and PP (≥ 0.90) (ML/BI). Values below 80% (UFBoot2) and 0.90 (PP) are marked with "-". Ex-type isolates are highlighted in bold. The taxa used as outgroup is *C. gracilipes*. The scale bar represents the number of nucleotide substitutions per site.